



**HAL**  
open science

# Molecular chaperones, proteases, and unfolded protein responses

Michael Schroda, Catherine Devitry

► **To cite this version:**

Michael Schroda, Catherine Devitry. Molecular chaperones, proteases, and unfolded protein responses. Academic Press. The Chlamydomonas Sourcebook: Introduction to Chlamydomonas and Its Laboratory Use (Grossman, A. R. and Wollman, F.-A., eds.), Organellar and Metabolic Processes, vol. 2. Elsevier, Amsterdam, 3rd edition., 2, Elsevier, In press, 9780128214305. hal-03995015

**HAL Id: hal-03995015**

**<https://hal.science/hal-03995015>**

Submitted on 17 Feb 2023

**HAL** is a multi-disciplinary open access archive for the deposit and dissemination of scientific research documents, whether they are published or not. The documents may come from teaching and research institutions in France or abroad, or from public or private research centers.

L'archive ouverte pluridisciplinaire **HAL**, est destinée au dépôt et à la diffusion de documents scientifiques de niveau recherche, publiés ou non, émanant des établissements d'enseignement et de recherche français ou étrangers, des laboratoires publics ou privés.

## Chapter 20

### Molecular chaperones, proteases, and unfolded protein responses

Michael Schroda<sup>1</sup> and Catherine deVitry<sup>2</sup>

<sup>1</sup> Molekulare Biotechnologie & Systembiologie, TU Kaiserslautern, Paul-Ehrlich Straße 23, D-67663 Kaiserslautern, Germany

<sup>2</sup> Biologie du Chloroplaste et Perception de la Lumière chez les Microalgues, Institut de Biologie Physico-Chimique, UMR CNRS/UPMC 7141, Paris, France

#### Abstract

Cells must ensure protein homeostasis to live and sustain growth. Important players for achieving this are molecular chaperones and proteases. In this chapter we describe our current knowledge of small heat shock proteins, chaperonins and cochaperonins, HSP70 and its cochaperones, HSP90 and its cochaperones, HSP100/ClpB, as well as of the protease systems ClpP, FtsH and Deg in *Chlamydomonas reinhardtii*. Moreover, we elaborate on how imbalances of protein homeostasis in different compartments of a *Chlamydomonas* cell are sensed to trigger compartment-specific unfolded protein responses.

**Key Words:** protein homeostasis, HSP100, HSP90, HSP70, HSP60, small HSP, heat shock, unfolded protein response, HSF1, VIPP1, VIPP2, FtsH, ClpP, Deg

## Introduction

Living organisms are open systems that must be kept in equilibrium. Homeostasis refers to any self-regulating process that maintains equilibrium through various sensing, feedback, and control mechanisms (Cannon 1929). When homeostasis is successful, life continues; when it is not successful, death occurs. Cellular protein homeostasis is brought about by ribosomes that drive protein biosynthesis, molecular chaperones and compatible solutes that support protein folding and prevent protein unfolding, and proteases that process proteins to a mature form or remove proteins that are no longer needed or cannot be folded. Cellular protein homeostasis is ensured when the rate of protein synthesis matches the capacity of protein folding and protein depletion through growth or degradation (Balchin et al. 2016).

The protein folding capacity of cells growing under optimal conditions is largely determined by ATP-dependent molecular chaperones of the HSP90, HSP70, and HSP60 classes and their cochaperones (Balchin et al. 2016). Abiotic stresses such as heat or oxidative stress, which increase the rate of protein unfolding, challenge cellular protein homeostasis because the folding capacity is no longer sufficient to maintain optimal cellular function. Unfolded proteins aggregate and, if left uncontrolled, the accumulating aggregates can become toxic, presumably due to their exposed hydrophobic surfaces (Bolognesi et al. 2010). Responses to avoid this include rapid increases in the levels of heat shock proteins (HSPs), including components of the general folding machinery (HSP90, HSP70, and HSP60 systems), components of the CLPB/HSP100 and small HSP (sHSP) families, and certain proteases.

In this chapter we review the current knowledge on molecular chaperones and proteases in *Chlamydomonas* with an emphasis on their roles in maintaining chloroplast function. Specifically, we focus on the ATP-independent sHSPs, on ATP-dependent HSP100s, HSP90s, HSP70s and HSP60s, including most of their cochaperones, and on the ClpP, FtsH and Deg proteases. We do not discuss the large families of protein disulfide isomerases and immunophilins as well as specialized systems like trigger factor, HSP33, or prefoldin, although they do have roles in protein folding. We also leave out the proteasome, autophagy, and intraorganellar proteases, including N- and C-terminal processing peptidases, presequence proteases, lon proteases and intramembrane proteases (for reviews on these systems, see (Adam 2015; van Wijk 2015; Zou and Bozhkov 2021)). After introducing the chaperone and protease systems, we detail recent findings in *Chlamydomonas* on the regulation of unfolded protein responses in the cytosol, the chloroplast, and the ER.

## Small Heat Shock Proteins (sHSPs)

*General structure* – Small heat shock proteins (sHSPs) are ancient proteins that all share an  $\alpha$ -crystallin domain of about 90 amino acids. The  $\alpha$ -crystallin core is flanked by an N-terminal domain of variable length and sequence and a short C-terminal extension (Haslbeck and Vierling 2015). Under ambient conditions, sHSPs assemble into barrel-like structures of 12 to more than 32 subunits (Kim et al. 1998; van Montfort et al. 2001; Fleckenstein et al. 2015).

*Molecular mechanism underlying sHSP function* – Under conditions that promote protein unfolding, sHSP dimers liberated from barrel-like assemblies or synthesized *de novo*, bind unfolded proteins and intercalate into the forming aggregates in an ATP-independent process (Santhanagopalan et al. 2018). Aggregates containing sHSPs facilitate the access of HSP70 and ClpB/HSP104 chaperones, which in ATP-dependent reactions disentangle individual proteins from the aggregates and assist in refolding them to their native state (Mogk et al. 2003; Cashikar et al. 2005). In *Synechocystis*, a sHSPs has been shown to associate with membranes, increasing the molecular order of their fluid-like state and thereby preserving membrane integrity at elevated temperatures (Tsvetkova et al. 2002).

*Chlamydomonas sHSP members and phylogeny* – The *Chlamydomonas* genome encodes eight sHSPs (termed HSP22A-H, Table 1) while there are 19 sHSPs encoded on the *Arabidopsis* genome (Scharf et al. 2001; Schroda and Vallon 2009). In *Arabidopsis*, sHSPs are targeted to the cytosol, chloroplasts, mitochondria, ER, peroxisomes and nucleus, while in *Chlamydomonas* as well as in *Volvox* and *Gonium*, sHSPs appear to be targeted only to the cytosol (HSP22A, B, and H), chloroplast (HSP22C-F), and mitochondria (HSP22G) (Table 1) (Rütgers et al. 2017a; Waters and Vierling 2020). However, experimental proof for the localizations in *Chlamydomonas* exists only for chloroplast HSP22E/F (Rütgers et al. 2017a), while for all other algal sHSPs localizations are based on prediction programs. Note that HSP22A was mis-localized to the chloroplast (Grimm et al. 1989; Eisenberg-Domovich et al. 1994).

*sHSP gene families in green algae and land plants* have expanded from a common ancestor gene (encoding a cytosolic sHSP) after the two lineages diverged (Waters and Vierling 2020). Hence, in contrast to organelle-targeted HSP70s and HSP60s, organelle-targeted sHSPs in land plants and green algae are not derived from the endosymbiont ancestor of chloroplasts and are not orthologous (Schroda 2004). The expansion of the gene families in both lineages has not occurred in a burst, but rather in a step-wise fashion (Waters and Vierling 2020). Gene expansion in green algae is still ongoing, as indicated by apparent recent gene duplication events in *Chlamydomonas* and *Volvox*: *Chlamydomonas* genes *HSP22E* and *HSP22F* and *Volvox* genes *HSP22A* and *HSP22B* share 98% sequence identity in their coding regions and are arranged head-to-head with ~368 bp and ~111 kbp between their transcriptional start sites, respectively (Rütgers et al. 2017a). The *Chlamydomonas HSP22A* and *HSP22B* genes are also arranged head-to head with only ~200 bp between their transcriptional start sites and ~72% identical residues in their amino acid sequences. The *HSP22H* and *HSP22A* genes are located on the same chromosome and only separated by ~25 kb.

*Functions of Chlamydomonas sHSPs* – Their role in coping with protein aggregates explains why sHSPs are strongly expressed under conditions that cause proteotoxic stress, including heat (Grimm et al. 1989; Tanaka et al. 2000; Mühlhaus et al. 2011; Hemme et al. 2014; Rütgers et al. 2017a; Rütgers et al. 2017b), high light exposure or other treatments leading to ROS accumulation (Fischer et al. 2005; Mettler et al. 2014; Blaby et al. 2015; Heredia-Martínez et al. 2018; Perlaza et al. 2019; Theis et al. 2020), heavy metals (Blaby-Haas et al. 2016), or the downregulation of protein quality control components like chloroplast ClpP1 (Ramundo et al. 2014). Several *sHSP* genes were also induced under nutrient stress conditions, including N-, S-, and P-starvation (Zhang et al. 2004; Moseley

et al. 2006; Schmollinger et al. 2014), presumably because starvation entails large changes in the cellular proteome.

The amount of sHSPs accumulating under severe stress can be substantial. For example, HSP22A was not detected under non-stress conditions but became the 7<sup>th</sup> most abundant soluble protein after 24 h of heat stress (Hemme et al. 2014; Schroda et al. 2015) (Table 1). Nevertheless, HSP22A, HSP22C and HSP22E/F were among the few proteins whose abundances declined by active degradation during long-term heat stress (Mühlhaus et al. 2011; Hemme et al. 2014), indicating that sHSP levels are tightly controlled. While HSP22A, HSP22C, and HSP22E/F are frequently detected by mass spectrometry in proteomic analyses, HSP22B is rarely detected and HSP22D, HSP22G, and HSP22H never (Table 1). It is possible that HSP22D, HSP22G, and HSP22H accumulate only under very specific conditions such as gametogenesis, zygote formation or zygote germination.

Despite their strong accumulation under various conditions, there are only few functional studies on sHSPs in *Chlamydomonas*. An early study has shown that cytosolic HSP22A reversibly interacts with the chloroplast envelope under heat stress conditions (Eisenberg-Domovich et al. 1994). Dissociation of membrane bound HSP22A occurred only at 25 to 38°C and reassociation only at 38 to 42°C, the temperatures at which HSP22A expression is induced. Whether HSP22A interacts directly with the membrane or with denatured membrane proteins is not clear.

Chloroplast HSP22E/F also have been shown to bind to chloroplast membranes after prolonged exposure of cells to H<sub>2</sub>O<sub>2</sub> (Theis et al. 2020). Such oxidative stress may lead to lipid oxidation and the accumulation of oxidized, misfolded/misassembled membrane proteins. Here, HSP22E/F might aid in coping with such problems and serve to maintain membrane integrity (see section on compartment-specific UPRs).

39 high-confidence interactors with chloroplast HSP22E/F in soluble extracts from heat stressed cells were identified by immunoprecipitation/mass spectrometry (Rütgers et al. 2017a). Among them were the ATP-dependent chloroplast chaperones HSP70B and CPN60A/B, which most likely are not direct interaction partners of HSP22E/F but act on protein aggregates into which HSP22E/F had intercalated and assist in their refolding to the native state. Other HSP22E/F interactors appear to be thermolabile substrate proteins. They were characterized by a lower helicity and lower pI than bulk chloroplast proteins. A bias towards lower pI was also observed for substrates of sHSPs from *C. elegans* (Fleckenstein et al. 2015). Several of these apparently thermolabile proteins are involved in energy-requiring anabolic reactions, including chlorophyll biosynthesis, CO<sub>2</sub>-fixation, starch synthesis, sulfur and nitrogen assimilation, and protein biosynthesis. It was proposed that their thermolability might be a desired trait to allow for a rapid ratcheting down of these pathways upon heat stress. The ATP and reducing equivalents saved when these proteins are no longer functioning would become available for the *de novo* synthesis and fueling of molecular chaperones and the synthesis of saturated fatty acids to restore membrane viscosity (Hemme et al. 2014; Schroda et al. 2015; Rütgers et al. 2017a).

## Chaperonins

*General structure* – Chaperonins were first described in plastids where they were shown to interact with the newly synthesized large subunit of Rubisco (Barraclough and Ellis 1980). Chaperonins consist of two stacked rings formed by subunits of ~60 kDa yielding a

barrel-shaped architecture (Horwich et al. 2007; Balchin et al. 2016; Hayer-Hartl et al. 2016; Gestaut et al. 2019). Each subunit contains three distinct domains: an equatorial domain harboring ATPase activity; an apical domain that binds nonnative substrate proteins; and a hinge-like intermediate domain that connects the above two domains and transmits the allosteric signal triggered by nucleotide binding and hydrolysis within the individual subunit (Figure 1A).

Two groups of chaperonins can be distinguished: group I chaperonins are found in eubacteria (GroEL), plastids (Cpn60), and mitochondria (Hsp60). They assemble into heptameric rings that stack back-to-back (Figure 1B). Each side of the tetradecameric double ring alternately interacts via the apical domains with an oligomeric cochaperonin that forms a lid to encapsulate substrates within a central cavity. This cochaperonin is called GroES in bacteria, Hsp10 in mitochondria, and Cpn10/20 in plastids. While bacterial and mitochondrial chaperonins and their cochaperonins are homo-oligomers, their counterparts in chloroplasts are hetero-oligomers (Trösch et al. 2015; Zhao and Liu 2017). The subunits of chloroplast chaperonins are divided into alpha and beta forms that share only ~50% sequence identity and for which further sub-forms exist (Hill and Hemmingsen 2001; Schroda 2004). The same is true for the cochaperonin, which is composed of subunits of ~10 kDa (Cpn10) and ~20 kDa (Cpn20); the latter represents a head-to-tail fusion of 10-kDa subunits connected by a short linker (Weiss et al. 2009).

Group II chaperonins are found in archaea (thermosome) and the eukaryotic cytosol where they form a T-complex protein Ring Complex (TRiC), also called Chaperonin Containing TCP-1 (CCT), and are essential for cell viability. The complex is composed of two stacked, octameric rings that in eukaryotes consist of eight paralogous subunits sharing only 27-39% sequence identity (Gestaut et al. 2019; Grantham 2020). The subunit order in the octameric ring is fixed (CCT 2-4-1-3-6-8-7-5) as is the relative positioning of the two rings which are stacked back-to-back, with CCT2 and CCT6 facing each other. Group II chaperonins do not require a cochaperonin. Instead, helical protrusions of each subunit contribute to an in-built lid that substitutes for the function of GroES/Hsp10/Cpn10-20.

*Molecular mechanism underlying chaperonin function* – The mechanism by which group I chaperonins assist in protein folding has been elucidated in detail for the bacterial GroEL/ES system, in which the two GroEL heptameric rings act in an asymmetric and anti-cooperative behavior termed “two-stroke engine” (Horwich et al. 2007; Hayer-Hartl et al. 2016). Unfolded substrate proteins bind to a hydrophobic cleft formed between helices H and I that are exposed in the apical domain of GroEL subunits of the *cis* ring (Figure 1, yellow helices). Subsequent binding first of ATP and then of GroES to the *cis* ring induces conformational changes of GroEL that enlarge the cavity ~2-fold and changes the wall surface from hydrophobic to highly hydrophilic, net negative (Figure 1C). This transition is thought to promote the formation of the hydrophobic core of the substrate protein and thus its folding to the native state. Subsequent ATP hydrolysis by GroEL takes about 10 seconds during which substrate folding can take place. Binding of a new substrate and ATP to the opposite ring promotes GroES dissociation and subsequent release of the folded protein and ADP.

In the absence of nucleotides (ATP), TRiC/CCT chaperonins are in an open state with the apical domains of the eight subunits exhibiting various conformations and motifs that allow an engagement with various substrate proteins (Gestaut et al. 2019). The binding

of ATP to the equatorial domains leads to the formation of apical domain contacts, generating a more compact open conformation resembling a tetramer of dimers. ATP hydrolysis induces a conformational rotation of the apical domains resulting in lid closure and release of the bound substrate into the central chamber, which adopts a highly polar/charged environment that facilitates folding. The ATPase cycle of TRiC/CCT chaperonins is highly asymmetric and this is achieved by very different affinities for ATP in the eight paralogous subunits. This asymmetric ATP utilization has led to the idea of a sequential closure that initiates on the high affinity hemisphere and progresses through the other subunits.

*Chlamydomonas chaperonin and cochaperonin members* – *Chlamydomonas* encodes four group I chaperonin subunits and four cochaperonin subunits, which are targeted to the chloroplast (CPN60A, CPN60B1, CPN60B2, CPN23, CPN20, CPN11) and mitochondria (CPN60C and CPN10) (Schroda 2004) (Table 2). They are orthologs of the respective proteins in chloroplasts and mitochondria of land plants and therefore were derived from the endosymbiotic bacteria that evolved into mitochondria and chloroplasts.

Each of the eight subunits of the CCT/TRiC complex (group II chaperonins, Table 2) encoded by *Chlamydomonas* is orthologous to the respective subunit in other eukaryotes. Hence, the gene duplication events giving rise to the eight paralogous subunits must have occurred early in the evolution of eukaryotes.

*Structure-function relationship of Chlamydomonas group I chaperonins* – The presence of only a single mitochondrial chaperonin subunit (CPN60C) implies that the mitochondrial chaperonin is a homo-oligomer, just like bacterial GroEL (Figure 1B). This is different for the chloroplast chaperonin: chaperonin complexes isolated from stromal extracts of cells grown under ambient conditions contained all three subunits at a stoichiometry somewhere between 5:3:6 and 6:2:6 for CPN60A:CPN60B1:CPN60B2 (Zhao et al. 2019). When all three subunits were co-expressed in *E. coli*, the stoichiometry was 5:6:3 and when the recombinantly produced subunits were mixed it was 4:7:3, suggesting that the stoichiometry of the three subunits might be flexible (Bai et al. 2015; Zhao et al. 2019). Unfortunately, a cryo-EM structure of the native chaperonin at 4.06 Å did not allow the subunit types to be distinguished and a crystal structure at 3.8 Å could only be obtained for the CPN60B1 homo-oligomer (Zhang et al. 2016a; Zhao et al. 2019). However, since the number of CPN60A subunits was always below seven, the *Chlamydomonas* chaperonin cannot consist of two homo-oligomeric rings of CPN60A and CPN60B subunits, as suggested previously for the chaperonin in *Arabidopsis* (Vitlin Gruber et al. 2013). Moreover, expression of CPN60A subunits alone in *E. coli* did not yield tetradecamers, while expression of CPN60B1 and CPN60B2 alone did. The co-expression of CPN60A with one B-type subunit reduced the yield of tetradecamers and this was relieved by co-expressing all three subunits (Bai et al. 2015). These findings indicate that CPN60 hetero-oligomers represent the functional complex *in vivo* and that its composition may be dynamically altered, e.g., by changes in environmental conditions. The composition of the chaperonin might be kept dynamic by its partial disassembly upon ATP hydrolysis (Bai et al. 2015; Guo et al. 2015).

Homo-oligomers of CPN60B1 or CPN60B2 could not efficiently support folding of *Rhodospirillum rubrum* Rubisco with GroES *in vitro*, while hetero-oligomers of all three

subunits could. Moreover, only if at least one CPN60B subunit was co-expressed with CPN60A, was the growth defect of an *E. coli* mutant lacking GroEL (but containing GroES) fully restored (*i.e.*, also at 42°C) (Bai et al. 2015; Guo et al. 2015; Zhang et al. 2016a). Here, the folding of obligate GroEL substrates *in vitro* depended on the CPN60 subunit composition of the chaperonin, further supporting the idea that a variable chaperonin composition expands the substrate spectrum.

Domain swapping experiments revealed that, within CPN60A, only the apical domain and one part of the intermediate domain can be replaced by CPN60B1 sequences without abolishing its functional cooperation with CPN60B1. The dispensability of the CPN60A apical domain was confirmed by domain swapping experiments with *E. coli* GroEL, whose functionality was only impaired when its apical domain was replaced by that from CPN60A and not by exchanges with apical domains from CPN60B1 or B2 (Zhang et al. 2016b). Crystal structures of the apical domains from CPN60A and B1 solved at 1.75 Å revealed that the hydrophobic surface in the substrate binding groove formed by helices H and I of CPN60B1 was wider and shorter than that of CPN60A, with the groove in CPN60A being more similar to that of GroEL than the groove in CPN60B1. Two hydrophobic amino acids in the apical domain of CPN60B1 mediate its interaction with the cochaperonin. These amino acids are hydrophilic in CPN60A and their replacement by the hydrophobic ones from CPN60B1 restored functionality of the CPN60A apical domain in GroEL. *Vice versa*, CPN60A/B1/B2 could not complement the lack of GroEL in *E. coli* if the two hydrophobic amino acids in the apical domains of B1 and B2 were replaced by the hydrophilic ones from CPN60A (Zhang et al. 2016b).

If these hydrophilic residues in the CPN60A apical domain abolish the interaction with the co-chaperonin, what are they good for? It turned out that they are important for a more efficient capturing of the major substrate of the chaperonin, the Rubisco large subunit (Zhang et al. 2016b). Hence, the different apical domains provided by CPN60A and B subunits in the chaperonin complex promote efficient substrate binding and cochaperonin interaction. The hetero-oligomeric nature of the chaperonin also leads to an asymmetrical distribution of amino acid hydrophobicity and electrostatic potential in the inner chamber, while it is symmetrical in GroEL (Zhao et al. 2019). Support for the idea that individual chaperonin subunits exhibit higher specificity for distinct substrates comes from studies on *Arabidopsis* knock-out lines of individual chaperonin subunits: here, Cpn60β4 was shown to provide specificity for the folding of NdhH, and Cpn60α2 for the folding of KASI, a protein important for the formation of the heart-shaped *Arabidopsis* embryo (Peng et al. 2011; Ke et al. 2017).

*Structure-function relationship of Chlamydomonas cochaperonins* – There is only a single subunit of the mitochondrial cochaperonin (CPN10), indicating that, like its chaperonin partner, the mitochondrial cochaperonin is a homo-oligomer. In contrast, the chloroplast cochaperonin complex, immunoprecipitated from stromal extracts, contained all three cochaperonin subunits, suggesting the occurrence of hetero-oligomers (Zhao et al. 2019). Of the recombinantly produced subunits, only CPN20 formed tetramers, while CPN11 and CPN23 remained monomeric; all three mixed together gave rise to a hetero-oligomer consisting of 2 x CPN20, 1 x CPN23, and 1 x CPN11, *i.e.*, seven 10-kDa domains (Tsai et al. 2012). None of the cochaperonins alone could support bacterial GroEL in the folding of *R. rubrum* Rubisco, but all combinations of CPN20 and CPN23 with CPN11 could (Tsai

et al. 2012; Guo et al. 2015; Zhao et al. 2019). However, CPN20 alone was able to support Rubisco refolding by CPN60A/B1/B2, suggesting that a symmetrical match between chaperonin and cochaperonin is not strictly required for chaperonin function (Guo et al. 2015). Moreover, CPN20, like the combination of two or all three cochaperonins, complemented the lack of GroES in *E. coli* at 37°C and 42°C, and with CPN60A/B1/B2 also the lack of GroEL/ES (Guo et al. 2015; Zhao et al. 2019). Since growth of *E. coli* lacking GroEL/ES at 45°C could be complemented only by the expression of GroEL/ES or of CPN60A/B1/B2-CPN23/20/11, and these systems mediated Rubisco refolding with highest efficiency, it seems clear that the native chloroplast chaperonins and cochaperonins are hetero-oligomers of three subunits each (Zhao et al. 2019).

Single-particle cryo-EM analysis of the native CPN60A/B1/B2 complex mixed with all three recombinantly produced cochaperonins resulted in a 3.82 Å structure (Zhao et al. 2019). Here, each of the seven 10-kDa cochaperonin domains interacted via a  $\beta$ -hairpin loop with a CPN60 subunit. Hence, hetero-oligomerization of the cochaperonin results in a 7-fold symmetry that matches the 7-fold symmetry of the chaperonin. The N-terminal 10-kDa domain of CPN20 lacks the sequence that forms a roof-like  $\beta$ -hairpin in the dome-shaped cochaperonin complex. This sequence is present in CPN11 and both 10-kDa domains of CPN23 (Tsai et al. 2012; Zhao et al. 2019). In *Arabidopsis*, this structure is missing in the Cpn10 subunit. Individual subunits also are predicted to have different affinities for CPN60 (higher for CPN11 and CPN23, lower for CPN20) (Tsai et al. 2012). Hence, different roofs and different affinities for CPN60 resulting from different combinations of cochaperonin subunits may help to expand the substrate spectrum of the (co)chaperonin complex.

*In vivo functions of Chlamydomonas chaperonins* – In line with the essential role of CPN60A for the functionality of the CPN60 tetradecamer, amiRNA-mediated downregulation of CPN60A resulted in impaired growth of *Chlamydomonas* cells under mixotrophic conditions, and abolished growth under photoautotrophic conditions and after heat stress (Bai et al. 2015). CPN60 subunits were pulled down with HSP22E/F from lysates of heat-stressed cells, pointing to a potential role of the chaperonin in the refolding of denatured proteins in HSP22E/F-containing aggregates (Rütgers et al. 2017a). This is supported by the strong accumulation of all chaperonin and cochaperonin subunits (including the mitochondrial ones) upon heat stress (Thompson et al. 1995; Tanaka et al. 2000; Mühlhaus et al. 2011; Hemme et al. 2014) (Table 2). A moonlighting function of CPN60A was observed in *Chlamydomonas*, where it was found to specifically interact with group II intron RNA, suggesting a specialized role as a general organellar RNA splicing factor (Balczun et al. 2006).

There are no studies on the functions of group II chaperonins in *Chlamydomonas*. As judged from their ranks in proteomics analyses, the eight CCT subunits are of rather low abundance under non-stress conditions, but their levels increase by ~30% (median) after 24 h of heat stress (Hemme et al. 2014) (Table 2), implying a function also of group II chaperonins in coping with heat stress. Actin and tubulin are considered as obligate folding substrates of TRiC/CCT, but studies on human cells revealed a larger substrate spectrum of TRiC including folding intermediates of structurally and functionally diverse polypeptides (Yam et al. 2008). These substrates tend to be topologically complex with aggregation prone  $\beta$ -sheets. Both properties often cause slow folding kinetics and render

the proteins prone to aggregation. TRiC has been shown to play a role in suppressing the formation of huntingtin aggregates (protein aggregates found in people with Huntington's disease) (Tam et al. 2006).

## HSP70s

*General structure of HSP70s and their cochaperones* – HSP70s are highly conserved proteins of ~70 kDa consisting of an N-terminal 45-kDa nucleotide binding domain (NBD), a 15-kDa substrate binding domain (SBD $\beta$ ), a 10-kDa  $\alpha$ -helical lid domain (SBD $\alpha$ ), and a disordered C-terminal tail (Mayer and Bukau 2005; Rosenzweig et al. 2019) (Figure 2). The NBD consists of four subdomains, IA, IB, IIA and IIB, that form two lobes separated by a deep cleft with a catalytic center at the bottom for ATP binding and hydrolysis. A conserved flexible interdomain linker connects the NBD with SBD $\beta$ , which is made up of an eight-stranded  $\beta$ -sandwich with a central hydrophobic pocket. Cytosolic HSP70s contain a highly conserved MEEVD motif at their C-termini, which is important for binding cochaperones.

HSP70s work in concert with specific cochaperones. The J-domain proteins (JDPs) represent the largest family of HSP70 cochaperones. All members harbor a J domain of ~70 amino acids, which consists of four  $\alpha$ -helices. Helices II and III form a hairpin with a conserved histidine-proline-aspartate (HPD) motif in the connecting loop that is essential for stimulating ATP hydrolysis in their HSP70 partner (Kelley 1998) (Figure 2). JDPs are divided into three groups (Cheetham and Caplan 1998): type I JDPs contain the J domain, the Gly/Phe-rich region, the Cys-rich zinc-finger domain, and the DnaJ C-terminal domain that is required for dimerization. Type II JDPs contain a J domain, the Gly/Phe-rich region, and the C-terminal domain. Most JDPs belong to type III and contain a J domain and a large variety of specialized other domains.

Nucleotide exchange factors (NEFs) are another important group of HSP70 cochaperones (Bracher and Verghese 2015; Rosenzweig et al. 2019). They promote the replacement of HSP70-bound ADP with ATP. Four types exist that are structurally quite diverse: 1. GrpE-type NEFs operate on HSP70s in bacteria (GrpE), chloroplasts (CGE), and mitochondria (MGE). They form dimers and consist of four domains: two unstructured N-termini, two long paired  $\alpha$ -helices, a four-helix bundle, and two  $\beta$ -sheet domains (Harrison et al. 1997) (Figure 2). Hsp110-type NEFs operate on HSP70s in the cytosol (Hsp110) and the ER (Grp170). They share a similar domain architecture with canonical HSP70s, *i.e.*, NBD, SBD $\beta$ , and SBD $\alpha$ , but have long insertions and C-terminal extensions (Bracher and Verghese 2015). 3. HspBP1 and Sil1 act on HSP70s in the cytosol and the ER, respectively, and share an Armadillo repeat architecture. 4. BAG-domain proteins act on cytosolic HSP70s. They are characterized by a diversity of  $\alpha$ -helix bundle architectures, but all share a conserved sequence signature that targets subdomain IIB of the HSP70 partner.

Organellar HSP70s depend on HSP70 escort proteins (HEPs) for their de novo folding (Sichting et al. 2005; Blamowska et al. 2012). HEPs are small L-shaped proteins. One leg of the "L" consists of two two-stranded, antiparallel  $\beta$ -sheets, each harboring a CXXC motif at the connecting loop via which a Zn<sup>2+</sup> ion is coordinated. Two short  $\alpha$ -helices constitute the other leg (Momose et al. 2007).

*Molecular mechanism underlying HSP70 function* – ATP binding to the catalytic center of the NBD induces rotation of the NBD lobes, through which a crevice at the bottom of the NBD opens for the binding of the interdomain linker and the docking of SBD $\alpha$  and SBD $\beta$  to the NBD (Kityk et al. 2015; Rosenzweig et al. 2019) (Figure 2). This interaction enables the SBD $\beta$  to bind substrate. Moreover, the docking of SBD $\beta$  to the NBD locks the NBD lobes in a conformation preventing ATP hydrolysis. The binding of a polypeptide substrate into the hydrophobic pocket of SBD $\beta$  triggers the release of SBD $\beta$  and SBD $\alpha$  from the NBD and the back-rotation of the NBD lobes into a position suitable for ATP hydrolysis. However, this is often accompanied by slipping of the interdomain linker out of the crevice at the bottom of the NBD, which alters the position of the NBD lobes such that ATP hydrolysis is not supported. Slipping out of the interdomain linker is prevented by the binding of the J domain from a J-domain cochaperone that, at the same time, transfers a substrate into the binding pocket of SBD $\beta$ . Other than the mere binding of a substrate, this combined action leads to very efficient ATP hydrolysis and substrate delivery (Liberek et al. 1991; Han and Christen 2003). Upon ATP hydrolysis, the SBD $\alpha$  lid docks onto the substrate binding pocket of SBD $\beta$  preventing substrate dissociation. Moreover, the crevice at the bottom of the NBD closes, leaving the SBD and the NBD largely independent of one another and connected only by the interdomain linker. Release of ADP to allow for the rebinding of ATP is facilitated by NEFs. These factors have a common function in that they open the nucleotide binding cleft by targeting subdomain IIB (Bracher and Verghese 2015). Moreover, they may also prevent the unproductive rebinding of the released substrate by blocking the HSP70 substrate binding pocket. Upon ATP binding, SBD $\alpha$  and SBD $\beta$  separate from each other and SBD $\beta$  interacts with the NBD. This interaction induces a shearing movement in the  $\beta$ - sandwich to open the substrate binding pocket, facilitating substrate release.

Substrate proteins recognized by HSP70s expose hydrophobic amino acids flanked by basic residues (Rüdiger et al. 1997), a characteristic feature of non-native proteins, but also of native HSP70 substrates. Binding of HSP70 prevents the formation of aggregates (holdase activity). In addition, the ATP-driven unfolding activity of HSP70s may introduce local conformational changes that allow non-native substrate proteins to assume the native state (Sharma et al. 2009). Thus, HSP70s play a major role in the folding of nascent chains and in the renaturation of non-native proteins that have accumulated during stress. However, they are also involved in many highly specialized functions like the regulation of the general stress response in bacteria (Tomoyasu et al. 1998), the uncoating of clathrin-coated vesicles (Ungewickell et al. 1995), the delivery of precursors to translocons at the cytosolic side of compartment membranes and their pulling through the translocons at the compartment side (Craig 2018). HSP70 systems often cooperate with other cellular chaperone systems, including HSP100/ClpB, in protein disaggregation and refolding (Haslberger et al. 2007), chaperonins in general protein folding (Langer et al. 1992), the proteasome in quality control (Ballinger et al. 1999), and the HSP90 system in protein folding and signal transduction (Pratt and Toft 2003; Schopf et al. 2017).

*Chlamydomonas HSP70 chaperone and cochaperone members* – *Chlamydomonas* encodes five canonical HSP70 proteins that are targeted to the cytosol (HSP70A), ER (BIP1 and BIP2), chloroplast (HSP70B), and mitochondria (HSP70C) (Schroda 2004) (Table 3). While the localization of HSP70A and HSP70B to cytosol and chloroplast were verified

experimentally (Drzymalla et al. 1996; Schroda et al. 2001b; Shapiro et al. 2005; Willmund et al. 2008a; Muranaka et al. 2016; Rütgers et al. 2017a), the localization of BIP1 and HSP70C to the ER and mitochondria can be inferred from the correct targeting of fluorescent reporter proteins to these compartments when they are fused to the N-terminal targeting peptides of HSP70C and BIP1 (Mackinder et al. 2017; Niemeyer et al. 2021). BIP2's localization to the ER is based on the presence of an HDEL motif at its C-terminus. ER-localization of the BIPs was also demonstrated by immunofluorescence (Diaz-Troya et al. 2008; Diaz-Troya et al. 2011). The amino acid sequences of BIP1 and BIP2 are 92% identical, suggesting that their genes were duplicated recently. Accordingly, both genes are located in a cluster of genes encoding ER-targeted chaperones that also includes the *HSP90B* gene (Schroda 2004; Schroda and Vallon 2009). Two genes encode non-canonical, C-terminally truncated HSP70s termed HSP70D and HSP70F. They are similar to HSP70s from cyanobacteria and chloroplasts and have N-terminal extensions that might be organellar targeting signals (Schroda and Vallon 2009) (Table 3). Orthologs, in particular of HSP70D, exist in other algae but not in land plants. *Arabidopsis* encodes 12 canonical HSP70s, with five targeted to the cytosol, three to the ER, and two each to mitochondria and chloroplasts (Lin et al. 2001; Sung et al. 2001). Hence, *Chlamydomonas* harbors a minimal set of canonical HSP70s.

In contrast, *Chlamydomonas* encodes many HSP70 cochaperones. With at least 63 members, the largest component of this suite of proteins is the JDPs (Nordhues et al. 2010). Only three of them are type I JDPs, with likely roles in protein folding, *i.e.*, they contain a Gly/Phe-rich region, a Cys-rich zinc-finger domain, and the DnaJ C-terminal domain. These are DNJ1, MDJ1 and CDJ1, which are predicted to be targeted to the cytosol, mitochondria, and chloroplast, respectively (Willmund et al. 2008a). Most of the other JDPs are predicted to be cytosolic and therefore tailor specific functions of HSP70A. Only six J-domain proteins appear to be targeted to the chloroplast in *Chlamydomonas*, while this is the case for at least 19 in *Arabidopsis* (Table 3) (Chiu et al. 2013; Trösch et al. 2015). The HSP110 family members HSP70E and HSP70G most likely are nucleotide exchange factors for HSP70A and BIP1/2, respectively. Other apparent cochaperones of HSP70A are HSPBP1 and BAG6. In contrast to *Arabidopsis* with seven BAG-domain cochaperones, *Chlamydomonas* appears to encode only one, BAG6 (Kabbage and Dickman 2008). Moreover, HSP70A appears to share cochaperones CHIP, HOP, and TPR2 with HSP90A that bind to the MEEVD motif present at the C-termini of both chaperones (see Table 4 and section on HSP90s). In addition to specific JDPs, chloroplast HSP70B and mitochondrial HSP70C have GrpE-type NEFs termed CGE1/2 and MGE1, respectively (Schroda et al. 2001b; Willmund et al. 2007). Moreover, both chaperones require escort proteins termed HEP2 and HEP1, respectively (Willmund et al. 2008b).

*Functions of Chlamydomonas HSP70s* – All five canonical *Chlamydomonas* HSP70 proteins are constitutively expressed and strongly upregulated upon heat stress, indicating their importance in all compartments for housekeeping functions and in maintaining protein homeostasis under stress (Table 3). Several studies have shed light onto these functions and in the following they will be discussed compartment-wise for the HSP70 members including their cochaperones.

*Cytosolic HSP70A* – In addition to its localization in the cell body, HSP70A was found in the ciliary proteome (Pazour et al. 2005) and detected via immunofluorescence with a discontinuous, punctuate pattern in the cilium. The highest HSP70A concentration was observed at the ciliary tip (Bloch and Johnson 1995; Shapiro et al. 2005) where axoneme assembly primarily occurs (Johnson and Rosenbaum 1992), implicating HSP70A in ciliogenesis. HSP70A was also found associated with the central pair C1b projection, where it might act as a conformational switch for central pair regulation of ciliary motility (Mitchell et al. 2005). The only JDP in cilia, RSP16, is located in a different complex, the T-shaped radial spoke (Yang et al. 2005). RSP16 is a type II J-domain protein with a G/F-rich region and a DnaJ C-terminal domain for peptide binding and dimerization. While *Chlamydomonas* RSP16 harbors an HPD motif in its J domain, this motif is degenerated in RSP16 orthologs from other organisms. Accordingly, RSP16 was proposed to act independently of an HSP70 partner by accompanying its client radial spoke precursor when traveling to the ciliary tip, where it aids in precursor folding to a mature configuration and remains part of the radial spoke to maintain its structural rigidity (Yang et al. 2008; Zhu et al. 2019).

In a mutagenesis screen for *Chlamydomonas* mutants resistant to the microtubule-binding and the destabilizing agent amiprophosphomethyl (APM), several APM-resistant mutants were obtained with increased microtubule stability (James et al. 1988). It turned out that the *APM1* and *APM2* gene products are DNJ1 and HSP70A, respectively (Silflow et al. 2011). The mutations affect DNJ1 protein abundance, or residues involved in substrate binding by DNJ1 or HSP70A. It was proposed that a client protein, whose functionality depends on folding assistance by HSP70A and DNJ1, promotes dynamic instability of microtubules (Silflow et al. 2011). The mutations appear to compromise the chaperoning activity of the HSP70A/DNJ1 couple just enough to confer resistance to APM while retaining sufficient chaperoning power to enable other housekeeping functions and to maintain protein homeostasis. This would explain why one allele of *apm1* and all *apm2* alleles showed a growth defect at 33°C and why crosses combining *apm1* and *apm2* alleles are lethal (James et al. 1988; Silflow et al. 2011): both situations might create intolerable further challenges to the chaperoning capacity of HSP70A/DNJ1. One *apm1* allele also showed a growth defect at 15°C (Silflow et al. 2011). Lower temperatures might also create a challenge to cellular chaperoning power as implied by the upregulation of several *HSP70* and *HSP90* genes in *Chlamydomonas* cells in the cold (7°C), including *HSP70A* (Maikova et al. 2016).

A specialized function of HSP70A has been reported in *Volvox*, where HSP70A cooperates with the JDP GlsA in mediating asymmetric cell divisions in embryonic cells (Cheng et al. 2005). Asymmetric cell divisions in *Volvox* determine the fate of embryonic cells in development: cells larger than 8 µm develop into immortal gonidia, whereas cells smaller than 8 µm differentiate into mortal somatic cells (Kirk et al. 1993). In the *glsA* mutant (*gonidialless*), asymmetric cell division is abolished, and all embryonic cells differentiate into somatic cells. GlsA is equally distributed in all blastomeres until the 16-cell embryo, as is the case for HSP70A. In 32-, 64-, and 128-cell stages, however, HSP70A is more abundant in the anterior region of the embryo where asymmetrically dividing cells are located. That GlsA functionality requires an HSP70 partner was demonstrated by its interaction with HSP70A and the finding that a variant with a mutated HPD motif in the J domain could not complement the *glsA* mutant (Miller and Kirk 1999; Cheng et al. 2005).

GlsA contains two SANT domains in addition to the J domain, which are known to mediate the interaction of chromatin modifiers with histones (Miller and Kirk 1999; Cheng et al. 2005). Presumably via the SANT domains, HSP70A and GlSsA both co-localize with histones during interphase. This finding suggested that HSP70A-GlsA complexes might modify chromatin in such a way that a gene product required to bring about a shift in the division plane is produced (Cheng et al. 2005). Interestingly, the *Volvox glsA* mutant could be complemented with a *Chlamydomonas* ortholog of GlsA, *GARI*, that is 70% identical to GlsA (Cheng et al. 2003).

*Chlamydomonas* HSP70A was found to interact with heat shock factor 1 (HSF1) (Schulz-Raffelt et al. 2007). Its possible role in the regulation of the cytosolic unfolded protein response is discussed in the section on UPRs (see below).

Nothing is known yet on specific functions of the putative HSP70A cochaperones HSP70E, BAG6 and HSPBP1 except for possible activities as NEFs. However, as protein levels of all of them increased drastically upon heat stress (Mühlhaus et al. 2011; Hemme et al. 2014) (Table 3), they might play a role in regulating HSP70A activity during protein (re) folding.

*Chloroplast HSP70B* – The so far best-studied HSP70 in *Chlamydomonas* is the stromal HSP70B protein. A small fraction of HSP70B associates with chloroplast membranes under ambient conditions (Schroda et al. 2001b). In cells treated with H<sub>2</sub>O<sub>2</sub> this fraction can amount to one third of the total HSP70B pool (Theis et al. 2020). The major interaction partner of HSP70B is its GrpE-type NEF CGE1 (Schroda et al. 2001b; Willmund et al. 2007). Like its bacterial counterpart GrpE (Figure 2), CGE1 forms dimers. However, while dimerization in GrpE is realized by the four-helix bundle domain, it is mediated by a coiled-coil interaction of the extended N-terminal  $\alpha$ -helices in CGE1.

The biochemical characterization of HSP70B was initially hampered by the apparent non-functionality of the *E. coli*-produced protein which, unlike HSP70B purified from *Chlamydomonas*, could not interact with CGE1 (Willmund et al. 2007). A similar observation was made for yeast mitochondrial Hsp70s, which even aggregated if produced in *E. coli* – unless co-expressed with the mitochondrial HSP70 escort protein Hep1 (Sichting et al. 2005). And indeed, co-expression of HSP70B with a chloroplast-targeted homolog of Hep1, termed HEP2, gave rise to functional HSP70B (Willmund et al. 2008b). As observed for mitochondrial HSP70 and Hep1, the addition of HEP2 to inactive HSP70B could not activate HSP70B, suggesting that the HEPs act during *de novo* folding of their HSP70 partner (Willmund et al. 2008b; Blamowska et al. 2012). This might be due to different folding paths taken by HSP70s following *de novo* synthesis at the ribosome and during import into the organelle. Alternatively, the dependence of organellar HSP70 folding on HEPs might have evolved to avoid activation of the organellar HSP70s in the cytosol prior to import into the organelle; this would suggest that HEP2, which does not have access to proteins in the cytosol, would work on the unfolded HSP70B as it enters the chloroplast through the TIC-TOC system. While HEPs targeted to mitochondria and chloroplasts are highly conserved in eukaryotes, they do not exist in (cyano)bacteria and must have evolved after the endosymbiotic event.

The functionality of HSP70B, produced recombinantly in the presence of HEP2, eventually allowed its biochemical characterization in comparison with *E. coli* DnaK (Veyel et al. 2014). The steady-state ATPase activity of HSP70B had a higher V<sub>max</sub> (0.65

compared to 0.03–0.045 pmol of ATP hydrolysed/min per pmol of protein) and  $K_m$  value for ATP (118  $\mu$ M compared to 3–20  $\mu$ M) than DnaK (Zmijewski et al. 2004; Veyel et al. 2014). However, ATPase activities were comparable in the presence of the proper JDP (DnaJ for DnaK and CDJ1 for HSP70B). HSP70B alone prevented the aggregation of denatured malate dehydrogenase, indicating a function as a holdase (Veyel et al. 2014). Moreover, HSP70B supported the folding of denatured luciferase to the native state, but only in the presence of its co-chaperones CGE1 and CDJ1. HSP70B assisted substrate refolding best when the cochaperones were supplied at ratios close to those found *in vivo* (HSP70B:CDJ1:CGE1 = 6.7:5.9:1) (Liu et al. 2007; Willmund et al. 2008a; Veyel et al. 2014). HSP70B-CDJ1-CGE1 had a ~6-fold higher refolding yield than DnaK-DnaJ-GrpE, probably because luciferase was a better substrate for the former. While the chloroplast cochaperones generally supported folding activity of DnaK and *vice versa*, the ability to support luciferase refolding was ~10-fold lower with the respective heterologous JDP, and ~2-fold lower with the respective heterologous NEF. These findings suggest that the cochaperones have co-evolved with their respective HSP70 partner, most likely as an adaptation to the different spectrum of substrate proteins (Veyel et al. 2014). Nevertheless, CGE1 and CDJ1 fully complemented *E. coli* *grpE* and *dnaJ* mutants, respectively (Willmund et al. 2007; Willmund et al. 2008a). Roles of HSP70B as a holdase and foldase *in vivo* was implied by its identification in HSP22E/F aggregates formed after heat shock (Rütgers et al. 2017a). CDJ1 was found to be upregulated upon depletion of the plastidic ClpP protease and to partition into insoluble cell fractions (Ramundo et al. 2014).

Temperature-dependent alternative splicing of the first intron in *CGE1* was found to give rise to two CGE1 protein isoforms, termed CGE1a and CGE1b (Schroda et al. 2001b). CGE1b contains two additional amino acids, valine and glutamine, close to the N-terminus in the unstructured domain. The ratio of CGE1b to CGE1a increased upon heat stress and CGE1b was shown to have a slightly higher affinity for HSP70B (Willmund et al. 2007). The additional valine/glutamine residues are predicted to increase the affinity of the unstructured N-terminus of CGE1b with HSP70B's SBD $\beta$  (Figure 2). Therefore, CGE1b might more efficiently occupy HSP70B's substrate binding pocket than CGE1a to prevent rebinding of released substrate (Rosenzweig et al. 2019). As no difference was observed between CGE1a and CGE1b regarding their efficiency to support the refolding of denatured luciferase by HSP70B (Veyel et al. 2014), such an effect might occur only with some substrates.

HSP70B was found to interact with the VIPP1 protein via the type III JDP CDJ2 (Liu et al. 2005). CDJ2 is mainly localized to the chloroplast stroma and in its C-terminus contains conserved motifs predicted to mediate coiled-coil interactions. Presumably, via these motifs CDJ2 interacts with VIPP1. VIPP1 is a member of the ancient ESCRT-III membrane-remodelling superfamily. In cyanobacteria, VIPP1 forms large basket-like assemblies with five to seven rungs each consisting of 11 to 18 subunits (Gupta et al. 2021; Liu et al. 2021). Inside of the basket, N-terminal amphipathic helices from each monomer align to form large hydrophobic columns, enabling the basket to bind to membranes and to encapsulate a vesicle-like bud. Certain point mutations in the amphipathic helix led to the formation of long rods rather than baskets. Thus, binding of the amphipathic helix to lipids may influence how VIPP1 oligomeric assemblies form, tuning the equilibrium between baskets and rods (Gupta et al. 2021). *Chlamydomonas* VIPP1 was found to predominantly form rods *in vitro*, which were able to suck in liposomes into their lumen if the liposomes

contained 5% phosphatidyl inositol phosphate (Theis et al. 2019a). The expression of VIPP1 fused C-terminally with mCherry in *Chlamydomonas* allowed localizing VIPP1 within chloroplasts, where VIPP1 was found in long tubules engulfing membranes and in short rods forming connections between the inner envelope and thylakoids (Gupta et al. 2021). These connections can explain how lipids produced at the inner envelope get into thylakoids and, thus, why *Arabidopsis* chloroplasts lacking VIPP1 are devoid of thylakoids (Zhang et al. 2012). *Chlamydomonas* expressing VIPP1 to 25% of wild-type levels and *Synechocystis* expressing VIPP1 variants with impaired ability to bind membranes have aberrant membrane structures in regions where multiple thylakoids converge and exhibit severe thylakoid swelling in high light (Nordhues et al. 2012; Gupta et al. 2021). These phenotypes might also be related to a reduced number of connections between thylakoid membranes.

Some findings suggest that VIPP1 may have functions in addition to membrane tubulation: first, VIPP1 improved protein export via the bacterial and thylakoidal TAT pathways (DeLisa et al. 2004; Lo and Theg 2012). Second, in an *in vitro* reconstituted system to study the cotranslational insertion of the D1 protein into thylakoid membranes, VIPP1 stimulated the formation of a D1 insertion intermediate and was found complexed with cpSecY, Alb3 and cpFtsY (Walter et al. 2015). Accordingly, *Chlamydomonas alb3.2* knock-down mutants have elevated levels of VIPP1, HSP70B, and CDJ2 (Göhre et al. 2006). These results suggest an involvement of VIPP1/HSP70B/CDJ2 in processes related to membrane protein sorting, possibly by organizing membrane nanodomains (Theis and Schroda 2016).

The HSP70B-CDJ2-CGE1 chaperone system was found to catalyze the ATP-dependent assembly of VIPP1 monomers/dimers into large assemblies and their disassembly to monomers/dimers *in vitro* (Liu et al. 2007). Moreover, the chaperones formed complexes with VIPP1 (dis)assembly intermediates (~670 kDa) in ATP-replete cells extracts, whereas they interacted with large (>>670 kDa) and small (<230 kDa) VIPP1 assembly states in ATP-depleted cell extracts. Finally, very large VIPP1 oligomers in cell extracts were partially disassembled by the addition of ATP and essentially completely disassembled by the addition of ATP and purified chaperones. Hence, CDJ2 appears to be a specialized J-domain protein that recruits HSP70B-CGE1 to VIPP1 for the dynamic remodeling of its assembly state.

One of the earliest investigations of chloroplast HSP70B revealed that its gene is induced by light (von Gromoff et al. 1989), resulting in an approximately two-fold increase in HSP70B protein levels (Drzymalla et al. 1996). This finding suggested a possible role for this chaperone in processes that help the cell to cope with photodamage. Accordingly, cells overexpressing HSP70B exhibited less severe damage to photosystem II and recovered photosystem II activity faster after photoinhibition, compared to wild-type cells. The opposite effect – more severe damage and slower recovery – was observed for cells underexpressing HSP70B (Schroda et al. 1999). It was hypothesized that HSP70B might facilitate a coordinated exchange of damaged D1 protein by *de novo*-synthesized D1 protein (Schroda et al. 2001a). In support of this hypothesis, HSP70B in the green alga *Dunaliella salina* was found to be part of a ~320 kDa complex containing photodamaged D1, D2, and CP47 proteins (Yokthongwattana et al. 2001). Alternatively, HSP70B-CDJ2 might play an indirect role in PSII repair by facilitating the cotranslational insertion of D1 via VIPP1 (Walter et al. 2015; Theis and Schroda 2016).

Like CDJ2, the CDJ3-5 proteins are type III JDPs and have evolved after the endosymbiotic event. They are weakly expressed and contain bacterial-type ferredoxin domains in addition to the J domain (Dorn et al. 2010). Phylogenetically, CDJ3 and 4 belong to a different clade than CDJ5 (Petitjean et al. 2012). CDJ3 and CDJ4 could be expressed recombinantly and were found to contain redox-active 4Fe-4S clusters (Dorn et al. 2010; Auerbach et al. 2017). The expression of the *CDJ3* and *CDJ4* genes declined upon heat stress, but *CDJ3* gene expression was strongly induced after shifting cells from dark to light, indicating that the proteins do not play a role in protein folding. Accordingly, CDJ3/4 were ineffective in promoting folding but stimulated HSP70B's ATPase activity (Veyel et al. 2014). Both CDJ3/4 interacted with HSP70B in the ATP state and CDJ3 was found in complexes with apparent molecular masses of 550–2800 kDa, which appeared to contain RNA (Dorn et al. 2010). It was speculated that the CDJ3–5 proteins might represent redox switches that act by recruiting HSP70B for the reorganization of regulatory protein complexes.

*Mitochondrial HSP70C* – Although the *HSP70C* gene was found long ago to be induced by heat stress and light (von Gromoff et al. 1989), there are yet no dedicated functional analyses on the mitochondrial HSP70 system in *Chlamydomonas*. Nevertheless, the presence of genes encoding homologs of the escort protein HEP1, the NEF MGE1 and the type I JDP MDJ1 (Table 3) suggests that HSP70C depends on HEP1 for its own folding and with MGE1 and MDJ1 facilitates the folding of mitochondrial proteins, just as in yeast (Rowley et al. 1994; Blamowska et al. 2012).

*ER-resident BIP1 and BIP2* – Although both BIP1 and BIP2 were detected in proteomic analyses, BIP1 appears to be expressed at higher levels than BIP2 (Table 3). BIP1 accumulated strongly during long-term heat stress (Hemme et al. 2014). Moreover, the *BIP1* gene is strongly induced by light (Vasileuskaya et al. 2004). An antibody raised against plant BiP detected BIPs in *Chlamydomonas* throughout the cell by immunofluorescence, with a more intense signal in the region of basal bodies (Diaz-Troya et al. 2008). Inhibition of TOR signaling by rapamycin induced the phosphorylation of BIP at Thr residues in the peptide-binding domain, including Thr-520 (Diaz-Troya et al. 2011). BIP phosphorylation was induced also by feeding cells with cycloheximide, indicating that BIP phosphorylation was induced by the inhibition of protein synthesis. BIP phosphorylation was abolished under conditions requiring BIP chaperone activity, such as heat shock or tunicamycin treatment, which inhibits protein glycosylation in the ER. Tunicamycin treatment resulted in a modified cellular distribution of BIPs to a central region of the cell near the nucleus where ER and Golgi compartments likely localize. These findings suggest that phosphorylation occurs under conditions where BIP chaperoning power is barely needed, generating a pool of inactive BIP that can quickly be reactivated if needed (Crespo 2012). In support of this idea, BIP1 variants with Thr520Ala or Thr520Arg replacements were able to partially complement a conditional yeast BiP mutant, while a BIP1 variant with the phosphomimetic Thr520-Glu could not (Diaz-Troya et al. 2011).

The HSP110-type NEF HSP70G, which is likely to serve as a NEF for the BIPs in the ER, was found to be *N*-glycosylated at seven sites (Mathieu-Rivet et al. 2013). Interestingly, HSP70G was identified in total cell extracts, in the supernatant containing

secreted proteins, and in chloroplast fractions, pointing to its targeting also to cell compartments other than the ER (Terashima et al. 2010; Mathieu-Rivet et al. 2013). There is no information available on other potential BIP cochaperones.

## HSP90s

*General structure* – HSP90s consist of three highly conserved domains: the N-terminal domain (NTD), which mediates ATP binding; the middle domain (MD), which is important for ATP hydrolysis and the binding of substrates (or clients); and the carboxy-terminal domain (CTD), which is responsible for HSP90 dimerization (Ali et al. 2006). The functionally active form of Hsp90 is the dimer (Figure 3).

*Molecular mechanism underlying HSP90 function* – HSP90s stabilize proteins in late folding steps and can prevent partially unfolded proteins from further unfolding under stress conditions (Nathan et al. 1997). Under ambient conditions, HSP90s can facilitate the formation of an active conformation of a protein, which occurs for many kinases (Grammatikakis et al. 1999). Moreover, HSP90s can promote the binding of ligands to bound client proteins, which is required, for example, for hormone binding to steroid hormone receptors (Pratt and Toft 2003), or for the loading of siRNAs onto Argonaute proteins (Iwasaki et al. 2015). HSP90s can also facilitate the formation of multiprotein complexes, such as the kinetochore (Kitagawa et al. 1999).

To fulfill these functions, HSP90s undergo a reaction cycle that is driven by ATP hydrolysis (Schopf et al. 2017; Biebl and Buchner 2019). The cycle starts with the HSP90 dimer in a V-shaped, open conformation in the ATP-free state. ATP-binding to the NTDs is followed by the closure of “lids” within the NTDs and the transition into the intermediate state. Next, the NTDs interact, leading to the closed state 1. The closed state 2 is reached when also the MDs interact (Figure 3). In this state, the MDs contribute sequences that, with the NTDs, complete the ATPase domains to allow ATP hydrolysis. After ATP hydrolysis, the NTDs dissociate, ADP and inorganic phosphate are released and HSP90 returns to the open conformation. This cycle is slow, with  $k_{cat}$  values ranging between  $\sim 0.09$  and  $\sim 0.5 \text{ min}^{-1}$  for cytosolic, mitochondrial, and bacterial HSP90s (Panaretou et al. 1998; Felts et al. 2000; McLaughlin et al. 2002).

In cytosolic HSP90s, this cycle is regulated by specific cochaperones, whereas bacterial and organellar HSP90s do not appear to depend on such cochaperones (Schopf et al. 2017; Sima and Richter 2018; Biebl and Buchner 2019). At the beginning of the cycle, the HSC70/HSP90-organizing protein (HOP), possibly already complexed with HSP70 and bound substrate, binds to the open conformation of HSP90 and facilitates the transfer of client proteins from HSP70 to HSP90. In the case of kinases, their delivery to HSP90 is mediated by CDC37. Following ATP-binding, other cochaperones take over and replace HOP or CDC37. These include diverse peptidylprolyl isomerases (PPIases), AHA1, P23, the PP5 phosphatase and, depending on the client to be processed, many others. Here, AHA1 promotes the formation of the closed 1 state and accelerates the cycle, while P23 competes with AHA1, stabilizes the closed state 2 and regulates cycle progression by reducing the ATPase activity of HSP90. Following ATP hydrolysis, ADP, Pi, cochaperones and the activated client are released and HSP90 is back in the open conformation to start another cycle. HSP90 activity is also regulated by post-translational

modifications, including phosphorylation, acetylation or sumoylation. It is worth noting that ATP is bound in a unique, 'kinked' conformation by HSP90s that can be mimicked by geldanamycin and radicicol. This allows the use of these compounds as HSP90-specific inhibitors (Roe et al. 1999).

*Chlamydomonas HSP90 chaperone and cochaperone members* – *Chlamydomonas* encodes three HSP90s that are targeted to the cytosol (HSP90A), ER (HSP90B), and the chloroplast (HSP90C) (Schroda 2004) (Table 4). While the chloroplast localization of HSP90C was experimentally verified (Willmund and Schroda 2005), the localizations of HSP90A and HSP90B are based on the presence of the MEEVD and KDEL motifs at their C-termini, which are characteristic for HSP90s localized to cytosol and ER, respectively. *Arabidopsis* encodes seven HSP90s with four targeted to nucleus/cytosol, and one each to ER, chloroplasts, and mitochondria (Krishna and Gloor 2001). The HSP90 gene family has expanded even more in crop plants, with soybean encoding 15, rice 9, and maize 12 HSP90 members (Xu et al. 2012). Hence, *Chlamydomonas* harbors a minimal set of HSP90s and it is interesting that a mitochondrially targeted form is absent. Phylogenetic analysis revealed an interesting aspect concerning the evolution of organellar HSP90s: While mitochondrial HSP90s are closely related to bacterial HtpG, plastid HSP90s are more closely related to members localized in the ER. Thus, plastid HSP90 may not be derived from its cyanobacterial ancestor but rather from a gene duplication event of the ER HSP90 and subsequent acquisition of a plastid transit peptide (Emelyanov 2002).

Homologs of several cochaperones of cytosolic HSP90 are present in *Chlamydomonas* (Table 4). Many cochaperones bind to the C-terminal MEEVD motif of cytosolic HSP90s via tetratricopeptide repeat (TPR) domains (Young et al. 1998). Of the HSP90 cochaperone homologs identified in *Chlamydomonas*, these are HOP1, CCPP5, FKB62, CYN40, TPR2, CNS1, and CHIP1. HOP harbors three TPR domains and simultaneously binds the MEEVD motifs at the C-termini of HSP90 and HSP70 (Chen and Smith 1998), which are conserved in *Chlamydomonas* HSP90A and HSP70A. P23, AHA1, CDC37, and SGTA bind HSP90 via different domains (Schopf et al. 2017). Surprisingly, no CDC37 homologs were identified in *Chlamydomonas* or land plants (MacLean and Picard 2003). However, possible CDC37 homologs appear to be present in members of the Prasinophytes, diatoms, and brown algae. In yeast, cytosolic HSP90 is in large molar excess over its cochaperones (Biebl and Buchner 2019) and this is the case also in *Chlamydomonas* (Table 4).

*Functions of Chlamydomonas HSP90s* – The expression of all three *Chlamydomonas HSP90* genes was strongly induced under heat stress (Willmund and Schroda 2005; Schulz-Raffelt et al. 2007; Schmollinger et al. 2013; Traewachiwiphak et al. 2018). Expression of the *HSP90B* gene was increased also by protein folding stress in the ER induced by DTT feeding (Traewachiwiphak et al. 2018). In line with heat-induced transcript accumulation, all three *Chlamydomonas* HSP90 proteins increased strongly upon heat stress (Mühlhaus et al. 2011; Hemme et al. 2014). This was observed also for the homologs of cytosolic HSP90 cochaperones HOP1, CCPP23, AHA1, CCPP5, FKB62, CYN40, and SGTA1 (Table 4). Cytosolic HSP90A was already abundant under non-stress conditions (rank 85) and it became the second most abundant soluble protein after 24 h of heat stress. These data point to a prominent role of HSP90s in maintaining protein homeostasis in

*Chlamydomonas*. *Chlamydomonas* HSP90A was found to interact with heat shock factor 1 (HSF1) (Schmollinger et al. 2013). A possible role of HSP90A in the regulation of the cytosolic unfolded protein response is discussed in the section on UPRs (see below).

The so far best studied *Chlamydomonas* HSP90 is chloroplast HSP90C. HSP90C is localized mainly in the stroma and is associated to a lesser extent with chloroplast membranes (Willmund and Schroda 2005). HSP90C forms dimers and displays a low ATP hydrolysis rate ( $K_m = 48 \mu\text{M}$ ;  $k_{cat} = 0.71 \text{ min}^{-1}$ ), which is comparable with those of other HSP90s (Panaretou et al. 1998; Felts et al. 2000; Willmund and Schroda 2005). HSP90C's ATPase activity is sensitive to radicicol. Instead of the conserved C-terminal MEEVD motif serving as binding motif for cochaperones of cytosolic HSP90s, HSP90C, like all plastid HSP90s, harbors a distinct C-terminal DPW motif, which might potentially serve as recognition site for plastid cochaperones (Schmitz et al. 1996; Cao et al. 2003). However, no cochaperones have yet been identified for plastid HSP90s. Interestingly, like cytosolic HSP90s, *Chlamydomonas* HSP90C was found to form a multi-chaperone complex with stromal HSP70B, CDJ1 and CGE1, indicating an orthologous function in protein folding (Willmund et al. 2008a; Schroda and Mühlhaus 2009). HSP90C and HSP70B were both found to interact with the vesicle-inducing protein in plastids 1 (VIPP1) and postulated to play a role in the disassembly of VIPP1 oligomeric complexes (Heide et al. 2009; Feng et al. 2014). How the interaction between both chaperone systems is realized remains an open question, as purified recombinant HSP70B and HSP90C did not directly interact *in vitro* (Willmund and Schroda 2005).

## HSP100s

*General structure* – HSP100/Clp chaperones belong to the large family of AAA+ proteins (ATPases associated with various cellular activities) (Neuwald et al. 1999). The ~230 amino acid AAA+ module consists of an N-terminal  $\alpha/\beta$ -nucleotide-binding domain with the Walker A and B consensus and sensor 1 sequences, followed by a C-terminal  $\alpha$ -helical domain containing the sensor-2 sequence (Hanson and Whiteheart 2005). HSP100/Clp proteins are divided into two classes, with class II members containing one (ClpX, ClpY = HslU), and class I members containing two AAA+ modules in tandem (ClpA to E) (Schirmer et al. 1996). They all assemble into homohexameric rings with a central pore (Figure 4). ClpA, ClpC, ClpE and ClpX contain a conserved tripeptide [LIV]-G-[FL] in a loop that lies C-terminal of sensor 1 in the AAA+ module. This motif is crucial for binding to an associated protease like ClpP or HslV and is lacking in ClpB and ClpY family members (Kim et al. 2001). ClpB family members contain two additional domains: the N-terminal domain and the middle domain, which forms a coiled-coil structure that is inserted in the first AAA+ module (Mogk et al. 2015).

*Molecular mechanism underlying HSP100/Clp function* – HSP100/Clp chaperones use the energy from ATP hydrolysis to translocate protein substrates through their central pore (Mogk et al. 2015; Mogk et al. 2018). This threading activity can initiate at the N- or C-termini or at internal sites of substrate proteins such that entire peptide loops are translocated through the pore (Avellaneda et al. 2020). Translocation is mediated by mobile loops in the central pore (Figure 4). These contact the substrate via conserved aromatic residues. Driven by ATP hydrolysis, the loops move downwards along the translocation

channel. Axial staggering of the loops facilitates substrate handover and prevents substrate backsliding. *E. coli* ClpB exerts pulling forces of more than 50 pN at speeds of more than 500 residues per second in bursts of up to 28 residues (Avellaneda et al. 2020).

If the HSP100/Clp chaperone is associated with a protease (e.g. in ClpAP or ClpXP), its threading activity serves to feed polypeptide substrates into the proteolytic chamber for degradation. The threading activity of ClpB family members serves to disentangle single polypeptides from protein aggregates. For this, ClpB must be activated by several HSP70s at the same time, a condition that is fulfilled when multiple HSP70s engage in close vicinity with the surface of an aggregate (Mogk et al. 2018). The HSP70s are in the ADP-bound state with substrate bound. They interact with the middle domains of ClpB subunits, which inhibit ClpB's ATPase activity. Once activated via HSP70s, ClpB can recognize a hydrophobic stretch of the substrate in the aggregate and actively displace it from the aggregate and from HSP70 by applying pulling force. Once displaced to the opposite side of the ClpB hexameric ring, the substrate can fold to the native state by itself or aided by HSP70 and/or chaperonins.

*Chlamydomonas HSP100/Clp members* – Ten genes encode HSP100/Clp proteins in *Chlamydomonas*. One of them is of the ClpX-type, two of the ClpY/HslU-type, five of the ClpB-type, and one each of the ClpC- and ClpD-types (Table 5). As judged from the localization of their orthologs in other organisms, CLPX1, HSLU1, and HSLU2 are localized to mitochondria, CLPB1/HSP101 to the cytosol, and CLPB3, CLPB4, CLPC1, and CLPD1 to the chloroplast. CLPB2 and CLPB5 have not been detected in proteomics studies and lack EST support (Schroda and Vallon (2009); Table 5). Moreover, CLPB2 lacks a conserved DE sequence in the Walker B motif of the second AAA domain. Hence, it is questionable whether these proteins are made and are functional. The *CLPC* gene model is incomplete, but the protein has been detected in proteomics studies (Table 5).

*Functions of Chlamydomonas HSP100/CLPs* – There are no dedicated studies on HSP100/CLP proteins in *Chlamydomonas*, yet. CLPB1, CLPB3, and CLPB4 were found to accumulate rapidly and with similar kinetics during heat stress at 42°C, with a plateau reached already after 2 h at elevated temperatures (Mühlhaus et al. 2011). *CLPB3* gene expression increased upon depletion of chloroplast ClpP1 and supplementing cells with nickel ions or the chloroplast fatty acid synthesis inhibitor cerulenin (Ramundo et al. 2014; Blaby-Haas et al. 2016; Heredia-Martínez et al. 2018). The lack of synthesis of proteins of ~100 kD (presumably CLPBs) in *HSF1*-RNAi strains correlated with the inability of these strains to survive heat stress (Schulz-Raffelt et al. 2007). This is in line with a role of cytosolic and chloroplast CLPBs in conferring thermotolerance to land plants (Queitsch et al. 2000; Yang et al. 2006). Interestingly, compared to ambient conditions, levels of CLPB1 and CLPB3 were 22- and 5.7-fold higher after 3 h of heat stress, but only 3.1- and 2.5-fold higher after 24 h of heat stress (Hemme et al. 2014). Hence, during long-term heat stress, both proteins were actively degraded, which was the case only for 29 proteins among 688 found to change in abundance during heat stress. This active degradation of CLPB1 and CLPB3 might be related to the potential toxicity of excess disaggregation activity under conditions of protein homeostasis. Accordingly, the expression of constitutively active ClpB/Hsp104 variants under non-stress conditions was found to be highly toxic,

presumably because substrate threading occurs on native proteins in an uncontrolled fashion (Lipinska et al. 2013).

*Arabidopsis* ClpC, recombinantly produced in *E. coli*, was able to activate *E. coli* ClpP for the ATP-dependent degradation of a model substrate and therefore could functionally replace *E. coli* ClpA (Shanklin et al. 1995). ClpC precipitated from pea stroma was found to interact with ClpP only in the presence of ATP and this complex was proteolytically active (Halperin et al. 2001). In contrast, the isolation of large quantities of the ClpP complex from *Chlamydomonas* chloroplasts did not result in the co-purification of any AAA+ chaperone, but did co-purify with substantial amounts of the CPN20/23/11 cochaperonin complex (Wang et al. 2021). The latter was found to bind to the heptameric ClpP complex via the same mobile loops with which it binds to the chaperonin, thereby blocking the entry of substrates into the pore of the top ClpP ring. While *E. coli* ClpP did not show proteolytic activity on its own, the *Chlamydomonas* ClpP complex did; and this activity was inhibited by the binding of the co-chaperonin complex. These results imply that *Chlamydomonas* ClpP might not necessarily require an AAA+ chaperone for its activity and that protein folding and degradation are concomitantly regulated by the cochaperonin (Wang et al. 2021). However, since the ClpP complex from *Chlamydomonas* was isolated without ATP, an interaction of AAA+ chaperones CLPC and CLPD with the ClpP complex cannot be completely ruled out.

## ClpP proteases

*General structure of ClpPs* – Clp proteases are soluble ATP-dependent serine proteases of bacterial origin found in the chloroplast stroma and the mitochondrial matrix of eukaryotes. Clp proteases consist of a barrel-like ClpP core complex associated with assistant chaperones. The *E. coli* ClpP core complex is formed of two stacked heptameric rings, with one catalytic triad Ser-His-Asp in each subunit (Wang et al. 1997). This *E. coli* core complex associates with two hexameric rings of AAA+ chaperones (ClpA or ClpX), one on each side (Sauer and Baker 2011). In mitochondria, the ClpP core consists also of 14 identical subunits (de Sagarra et al. 1999). In chloroplasts, the ClpP core complex comprises ClpP subunits, ClpR subunits (homologous to ClpP but having lost at least one residue of the catalytic triad), and ClpT subunits (homologous to the N-terminal domain of AAA+ chaperones). The ClpT subunits are proposed to link and stabilize the two heptameric rings of the ClpP core (Kim et al. 2015).

*Molecular mechanism underlying ClpP function* – As discussed for HSP100s, ATP hydrolysis by AAA+ chaperones contributes to substrate unfolding and the threading of substrate into the central cavity of the proteolytic degradation chamber of the ClpP core complex. Substrate-bound structures of AAA+ proteins show an ATPase spiral encircling the translocating substrate along the central pore providing grip on the substrate, the sequential ATP hydrolysis via conformational changes powers substrate translocation (Puchades et al. 2020) (Figure 4).

*Chlamydomonas ClpP members* – Eleven genes encode *Chlamydomonas* ClpP/R/T proteins (Table 6). In *Chlamydomonas*, three P-type (ClpP1, P4 and P5, the first being chloroplast encoded), five R-type (CLPR1-4 and R6) and two T-type (CLPT3 and T4)

constitute the chloroplast ClpP complex (Majeran et al. 2005; Schroda and Vallon 2009). ClpP<sub>H</sub> is processed by unknown peptidases to generate an N-terminal ClpP<sub>N</sub> fragment, and two C-terminal ClpP<sub>C</sub> and ClpP<sub>C'</sub> fragments (with N-terminal sequences NYLD and YRK, respectively) which are part of the ClpP complex (Derrien et al. 2009; Derrien et al. 2012). The cryo-EM structure of the *Chlamydomonas* chloroplast ClpP core complex was resolved (Wang et al. 2021) (Figure 5A). Its top ring contains one CLPR6, three CLPP4, and three CLPP5 subunits, while its bottom ring is composed of one of each of the CLPR1-4 subunits and three ClpP<sub>C</sub> subunits. CLPT4 participates in connecting the two rings and CLPT3 might contribute in some unassigned density. Its top ring is capped by the CPN20/23/11 cochaperonin complex (not by Clp chaperones), as discussed at the end of the section on HSP100s. The *Chlamydomonas* mitochondrial Clp protease consists of a homo-tetradecameric CLPP2 core associated with a CLPX chaperone (Figure 5B). In contrast, *Arabidopsis* has three different X-type chaperones (CLPX1-CLPX3) (Petereit et al. 2020).

*Functions of Chlamydomonas ClpP complexes* – Unlike its *E. coli* ortholog, the chloroplast protease ClpP1 is essential for cell viability, based on the experimental failure to generate homoplasmic *clpP1* knock-out lines. In *Chlamydomonas*, attenuated expression of ClpP1 was achieved by replacing the AUG start codon of *ClpP1* with AUU, a less efficient initiation codon (Majeran et al. 2000). The accumulation of ClpP1 protein was reduced by 70% and led to delayed degradation of Rubisco and of the cytochrome *b<sub>6</sub>f* complex under nitrogen or sulfur starvation (Majeran et al. 2000; Wei et al. 2014; De Mia et al. 2019). In addition, ClpP levels control the accumulation of unassembled proteins of photosynthetic complexes, especially soluble proteins in the stroma including the Rubisco SSU in the absence of the LSU and unassembled CF1 $\beta$  (Majeran et al. 2019). The decrease of the chloroplast Clp complex in the *Arabidopsis clpR2-1* mutant results in an increase in abundance of chloroplast proteins involved in plastid protein quality control (Zybailov et al. 2009). Similarly, in *Chlamydomonas*, a selective gradual depletion of chloroplast ClpP (using a repressible system) activates nuclear genes involved in plastid autophagy and plastid protein quality control (Ramundo et al. 2014). The proteins whose abundance increases upon ClpP depletion could be ClpP protease substrates and/or could result from a plastid unfolded protein response (UPR), as reviewed below in the section on UPRs. Altogether, these results show that ClpP has essential roles in chloroplast biogenesis and maintenance.

The single gene for the mitochondrial Clp protease subunit CLPP2 is dispensable. It was shown in a *clpP2* knockout mutant that mitochondrial CLPP2 assists in the coordination and homeostasis of respiratory complexes in *Arabidopsis* (Petereit et al. 2020).

## FtsH proteases

*General structure of FtsHs* – FtsHs are membrane bound chaperones and proteases. These ATP-dependent zinc metalloproteases of bacterial origin are found in chloroplasts and mitochondria of eukaryotes. Nuclear-encoded FTSH proteins are synthesized as precursors in the cytosol, and their N-terminal target peptide is cleaved off after import into organelles by the stromal or the mitochondrial processing peptidase. FtsHs are membrane bound at

their N-terminus by at least one transmembrane helix. The FtsH membrane anchoring domain is followed by an ATPase domain (AAA+) with nucleotide binding consensus sequences Walker A, Walker B and Second Region of Homology (SRH). The Zn-binding protease domain is at the C-terminus and contains the consensus HEXXH motif. FtsHs assemble into hexameric rings with a central pore (Figure 6). The pore loop is in the ATPase domain between the Walker A and Walker B motifs. Most prokaryotes, like *E. coli*, encode only one FtsH and form homo-hexameric rings. Eukaryotes and *Synechocystis* sp. PCC 6803 encode numerous FtsH isoforms and form homo- or hetero-hexameric complexes (Sokolenko et al. 2002). In chloroplasts, FtsHs are localized in the inner envelope membrane, or in the thylakoid membrane, all with the ATPase and protease domains facing the stroma. In the inner membrane of the mitochondrial envelope, *m*-FtsHs have their ATPase and protease domains facing the matrix, while *i*-FtsHs are oriented oppositely with their ATPase and protease domains facing the intermembrane space.

*Molecular mechanism underlying FtsH function* – FtsH substrates are threaded through the central pore. The ATPase activity is required for pulling out substrate proteins from the membrane and entering them into the internal pore of the FtsH ring structure for proteolysis. As for HSP100/Clp chaperones, the translocation is mediated by domain movements in the central pore powered by a sequential ATP hydrolysis cycle with a spiral organization of the ATPase hexamer around the translocating protein substrate (Bieniossek et al. 2009; Puchades et al. 2020). The ATPase acts coordinately and drives substrate extraction from membranes and translocation of stable substrates when all the hexamer subunits are ATP-hydrolysis competent (Puchades et al. 2020). ATP-hydrolysis incompetent FTSH1 subunits inactivate thylakoid FTSH1/FTSH2 in the *Chlamydomonas* *ftsh1-1* mutant (Malnoe et al. 2014). In contrast, the protease activity is still efficient when part of the hexamer subunits are proteolytically inactive. For example, the protease activity of type B subunits is totally dispensable for *Arabidopsis* chloroplast development (Zhang et al. 2010). FtsHi and Ycf2 isoforms found in the chloroplast envelope have conserved the pulling motor ATPase domain but have lost the Zn-binding motif and the protease function.

*Chlamydomonas FtsH members* – 12 FTSH isomers are found in *Chlamydomonas* (Table 7): six nuclear genes encode proteolytically active FTSH isomers and five nuclear genes encode proteolytically inactive FTSHi genes. Moreover, the chloroplast-encoded AAA protein Ycf2 is a proteolytically inactive isoform of FtsH proposed to have evolved from an endosymbiotic cyanobacterial ancestor (Kikuchi et al. 2018). The identification of genes encoding homologous proteins has been limited by the quality of the *Chlamydomonas* genome sequence and the rapid evolution of some paralogs. The more complete recent genome revealed two additional FTSHi in *Chlamydomonas*. The complexity of the FtsH protein family is higher in *Arabidopsis*, with a total of 18 FTSH isomers (12 proteolytically active, 5 FTSHi, and Ycf2). Phylogenetic studies revealed the complexity and evolution of FtsH proteins (Supplemental Figure 1 of Malnoe et al. (2014); Shao et al. (2018)). FTSHi and FTSH12 have rapidly evolved and diverged. *Chlamydomonas* FTSH3 has been identified by proteomics in mitochondria (Atteia et al. 2009) and is phylogenetically close to the mitochondrial FtsH proteins of the *m*-FtsH type, At-FTSH3 and At-FTSH10 in *Arabidopsis*, and Sc-YTA10 and Sc-YTA12 in *Saccharomyces*. *Chlamydomonas* FTSH4 is phylogenetically close to mitochondrial FtsH proteins of the *i*-FtsH type, At-FTSH4 in

*Arabidopsis*, and Sc-YTA11 and Sc-YTA12 in *Saccharomyces*. *Chlamydomonas* FTSH1 and FTSH2 are located in the thylakoid membranes (Allmer et al. 2006) and form the *Chlamydomonas* thylakoid FtsH protease as FTSH1/2 hetero-hexamers (Malnoe et al. 2014; Wang et al. 2017). As in *Arabidopsis*, *Chlamydomonas* FTSH7/9, FTSH11, five FTSHis and Ycf2 are in the inner membrane of the chloroplast envelope (Terashima et al. 2010; Ramundo et al. 2020). FTSH9 (alias FTSH7) is phylogenetically close to FTSHi3 (alias FHL2). Other FTSHi isoforms group with At-FTSHi and At-FTSH12. At-FTSH12 was demonstrated to localize in the inner membrane of the chloroplast envelope with ATPase and protease domains facing the stroma (Mielke et al. 2021). *Chlamydomonas* FTSHi1-4 are named based on their closest relative in *Arabidopsis*, the fifth FTSHi is named FTSHi6 (and not FTSHi5) because it has no close relative in *Arabidopsis*. There is no close homolog of At-FTSHi5 or At-FTSH12 in *Chlamydomonas*.

*Functions of Chlamydomonas FtsH complexes* – Damage and repair of the D1 subunit of PSII in high light was first reported in *Chlamydomonas* (Ohad et al. 1984). The role of thylakoid FtsH (thyl-FtsH) in PSII repair upon photoinhibition is the focus of many studies. However, thyl-FtsH has a wider diversity of substrates, which have been revealed more recently. A genetic suppressor strategy enabled the isolation of *Chlamydomonas* thyl-FtsH mutants: *ftsh1-1* (R420C, lacks ATP hydrolysis) accumulates wild-type levels of inactive FTSH1/2 (Malnoe et al. 2014), and *ftsh1-2* (*FTSH1* promoter insertion mutant) accumulates little FTSH1/2 (Wang et al. 2017). Due to their concerted accumulation, most cytochrome *b<sub>6</sub>f* subunits are degraded when their assembly is compromised. The same holds for the Cytochrome *c* Biogenesis CCB2 and CCB4 proteins, which control *c'*-heme binding to cytochrome *b<sub>6</sub>* and are degraded when one of them is lacking. Using cytochrome *b<sub>6</sub>f* or CCB mutants, placed in a genetic context mutated for FtsH, it was shown that depletion of FtsH function resulted in the rescue of misassembled *b<sub>6</sub>f* and CCB proteins (Malnoe et al. 2011; Malnoe et al. 2014). Recently, FtsH protease inactivation was shown to allow accumulation of aberrant PSII in a *Chlamydomonas* mutant lacking the iron-containing rubredoxin RBD1, suggesting that RBD1 would promote proper D1 folding, possibly via non-heme iron delivery or reduction during PSII assembly (Calderon et al. 2022). The FtsH protease inactive context preserves cytochrome *b<sub>6</sub>f* complexes and biogenesis factors during nitrogen or sulfur starvation, which are degraded in the wild-type context (Malnoe et al. 2014; Wei et al. 2014; De Mia et al. 2019). Thyl-FtsH also controls the accumulation of the PSI antenna (Bujaldon et al. 2017) and is required for PSII recovery from photoinhibition (Malnoe et al. 2014). The accumulation of PSII D1 fragments in the *ftsh1-1* mutant suggests that, similar to what has been proposed for plant chloroplasts, there could be a joint action of Deg (endoproteolytic cuts) and FtsH (processive degradation) proteases for the degradation and repair of D1 upon photoinhibition of *Chlamydomonas* (Malnoe et al. 2014).

There is extensive thyl-FtsH dynamics upon low light to high light transition in *Chlamydomonas*, including increased proteolytic activation through a redox-controlled reduction of intermolecular disulfide bridges between FtsH subunits, and increased transcript and protein accumulation, despite a reduced thyl-FtsH protein half-life (Wang et al. 2017). The formation of photoinhibition-related energy dissipation  $q_i$  requires oxygen, while the loss of  $q_i$  relies on PSII proteolysis by FtsH in *Chlamydomonas* (Nawrocki et al. 2021). In *Arabidopsis*, the oxidative post-translational modifications of chloroplast

EXECUTER 1 (EX1) and EX2 proteins lead to their FtsH-dependent proteolysis, which appears to be essential for mediating singlet-oxygen triggered chloroplast-to-nucleus retrograde signaling (Dogra et al. 2021). Altogether, these results show that thyl-FtsH is a major housekeeping and regulatory protease.

Phosphorylation sites were identified in thylakoid FtsH proteases of *Chlamydomonas* and *Arabidopsis* (Supplementary Figure 10 in Wang et al. (2017)). FtsH phosphorylation was also reported in an antarctic *Chlamydomonas* strain (Szyszka-Mroz et al. 2015). In *Arabidopsis*, phosphorylation was suggested to affect FtsH complex formation or stability (Kato and Sakamoto 2019). In *Chlamydomonas*, thyl-FtsH is mainly found in ~1 MDa complexes, *i.e.* complexes that are larger than the 410-kDa FTSH1/2 hexamer (Wang et al. 2017). These complexes are active *in vivo* in wild-type and Strep-tagged FTSH1 strains, and isolated Strep-tagged FTSH1/2 complexes showed *in vitro* proteolytic activity using  $\beta$ -casein as substrate (Wang et al. 2017). These *Chlamydomonas* thyl-FtsH megacomplexes accumulate similarly in wild type grown in low light and grown in low light followed by two hours high light. In contrast, *Arabidopsis* thyl-FtsH proteins are mainly found in smaller complexes than functional hexamers and oligomerization was suggested to contribute in the regulation of FtsH activity (Kato and Sakamoto 2018). Most chloroplast proteins are encoded by nuclear genes and must cross the chloroplast envelope membranes via the translocon at the outer envelope membrane of chloroplasts (TOC) and at the inner membrane (TIC) to reach their proper destination inside the chloroplast. Elegant studies to purify and identify translocation machinery components (affinity-tag on machinery components or on preproteins under translocation) were performed in *Arabidopsis* (Kikuchi et al. 2018; Schreier et al. 2018) and more recently in *Chlamydomonas* (Ramundo et al. 2020). Ycf2/FTSHi complexes and FTSHi3-comprising complexes mediate protein import into the chloroplast; they serve as a motor that associates with TIC/Ycf1 for protein import into chloroplasts in *Arabidopsis* and *Chlamydomonas*. *Ycf1* and *ycf2* are chloroplast-encoded essential genes. *Arabidopsis ftshi* and *ftsh12* knock-out mutants are embryo lethal (except *ftshi3*), while knock-down mutants are pale green or variegated. There is no insertion mutant in FTSHi exons in the *Chlamydomonas* mutant library (<https://www.chlamylibrary.org/>). At-FTSH12 forms FtsH hetero-hexamers with Ycf2/FTSHi1/2/4/5 and its proteolytic activity is dispensable for protein import activity (Kikuchi et al. 2018). FTSHi3 forms another complex, presumably with its phylogenetically close homologs FTSH7/9.

There is no study dedicated to *Chlamydomonas* FTSH11. At-FTSH11 forms homo-hexamers in the chloroplast envelope inner membrane, with the bulk of the protease tentatively proposed to be exposed to the stroma (although there are no topology studies, this proposition is consistent with the detection in affinity purified FTSH11 complexes of many stromal interacting/trapped proteins). At-FTSH11 proteolytic activity is essential for thermotolerance and regulation at the level of the chloroplast import machinery (Adam et al. 2019).

## Deg proteases

*General structure of Degs* – Degradation of periplasmic proteins (Deg) proteases / high-temperature requirement A (HtrA) proteases are ATP-independent, Ser endopeptidases. They combine an N-terminal proteolytic domain containing the catalytic His-Asp-Ser triad,

usually with at least one C-terminal peptide-binding PDZ domain. They are soluble proteins that can associate peripherally with membranes. Most Degs form trimers that are stabilized by contacts between their protease domains. These trimers can form hexamers by stacking two trimers on top of each other which are stabilized by interactions between PDZ and protease domains, with the active sites sequestered inside the catalytic cage (Kley et al. 2011). The nucleus located *Arabidopsis* Deg9 displays a novel octameric structure consisting of two tetrameric rings that have distinct conformations (Ouyang et al. 2017).

*Molecular mechanism underlying Deg function* – Because the proteolytic sites are inside a cage, the substrates must enter through pores as unfolded proteins or extended polypeptide loops. Structural studies of their oligomeric architecture show that the chloroplast Deg proteins use structural changes, induced by both specific substrates and changes in pH, to regulate substrate access to the proteolytic chamber (Kley et al. 2011; Sun et al. 2012; Sun et al. 2013). This structural plasticity allows a rapid response to the presence of misfolded proteins.

*Chlamydomonas Deg members* – The *Chlamydomonas* and *Arabidopsis* genomes, respectively, encode fourteen and sixteen Deg proteins (Table 7) (Schuhmann and Adamska 2012). *Chlamydomonas* Deg proteins are named based on their closest relative in *Arabidopsis*. Deg proteins are of bacterial origin and localize in eukaryotes mainly to the organelles. Phylogenetic studies revealed the diversity and evolution of Deg proteins (Schroda and Vallon 2009). The minimal set of conserved Deg protease types found thus far in every plant consists of eight members, Deg1/2/5/7/8/9/10/15 (Schuhmann et al. 2012). The improved *Chlamydomonas* genome sequence enabled the identification of DEG9A, which is missing the beta-glycan hydrolase domain, DEG9C with a conserved catalytic triad, fourteen DEG genes (twelve with the active protease domain including DEG9A and DEG9C, plus two lacking the catalytic triad DEGO1 and DEGO2), and updated sequences/information on all of the *Chlamydomonas* Deg family members (Schuhmann et al. 2012). *Chlamydomonas* has 3 DEG1 and 3 DEG9 orthologs. While *Arabidopsis* DEG1 is in the thylakoid lumen, *Chlamydomonas* DEG1C is localized in the stroma and on the stromal side of the thylakoid membranes (Theis et al. 2019b). According to the localization of *Arabidopsis* orthologs, *Chlamydomonas* DEG1A, DEG1B, DEG5, and DEG8 would be in the thylakoid lumen, DEG2 and DEG7 in the stroma, the three DEG9s in the nucleus, DEG10 in the mitochondria, and DEG15 in the peroxisome. The number of PDZ domains associated with a DEG varies from no PDZ domain in DEG5 and DEG15 to three PDZ domains in DEG7. *Chlamydomonas* encodes DEGO1 and DEGO2 paralogs that lack the catalytic triad (inactive as peptidases) and have an expanded domain between the peptidase and PDZ domains, with a Gly-rich region that is rich in Arg residues in DEGO1 and in Glu/Asp residues in DEGO2, suggesting they may interact (Schroda and Vallon 2009).

#### *Functions of Chlamydomonas Degs*

According to what has been proposed for plant chloroplasts, there is a joint action of Deg (endoproteolytic cuts in soluble loops) and FtsH (processive degradation) proteases in the degradation and repair of thylakoid transmembrane D1 protein upon photoinhibition in *Chlamydomonas*. Indeed, the apparent molecular weight and epitope content of D1

fragments accumulating in the *ftsh1-1* mutant (Malnoe et al. 2014) match the predicted fragments that would be generated by luminal and stromal Deg cleavage sites, based on *Arabidopsis* studies (Kapri-Pardes et al. 2007; Kato and Sakamoto 2009; Sun et al. 2010; Kato et al. 2012). The thylakoid lumen acidifies in the light and this acidification triggers oligomerization of DEG1 into its active hexameric form, which allows activation of DEG1 when photosynthetic proteins are damaged by light (Kley et al. 2011). In *Arabidopsis*, DEG1 forms homohexamers whereas DEG5 and DEG8 form heterohexamers. DEG1 is more abundant and active than DEG5-DEG8, and the triple KO mutant *deg158* grows poorly, especially under harsh conditions, up-regulating proteins involved in protein homeostasis (Butenko et al. 2018). The only study dedicated to a *Chlamydomonas* Deg mutant, is the characterization of the *deg1C* mutant (Theis et al. 2019b). DEG1C exhibits a dynamic oligomerization, with high proteolytic activity against unfolded substrates that increases with temperature and pH. DEG1C accumulation increased upon nutrient, high light or heat stress conditions. DEG1C depletion triggers high light protection responses, even when the *deg1C* mutant was grown at low light intensities (as detailed in the section on UPRs).

*Chlamydomonas* has an ortholog of the *Arabidopsis* mitochondrial DEG10, probably the only mitochondrial Deg in *Chlamydomonas* since it does not have an ortholog to the other *Arabidopsis* mitochondrial Deg, DEG14 in *Arabidopsis* (HTRA1/HTRA2 in humans) (Schroda and Vallon 2009). The accumulation of *Chlamydomonas* DEG10 increased upon nitrogen deprivation (Park et al. 2015) while the *Arabidopsis* DEG10 accumulated during temperature stress. Depletion of *Arabidopsis* for DEG10 altered mitochondrial proteostasis at elevated temperature (Huber et al. 2019).

The DEG15 type has a C-terminal protease domain and no PDZ domain. *Arabidopsis* DEG15 changes substrate specificity from a general protease as a monomer, to a protease that specifically processes the N-terminal peroxisomal targeting signal 2 as a dimer; dimerization is mediated by Ca<sup>2+</sup>/calmodulin (Dolze et al. 2013). In *Arabidopsis*, the nuclear-localized DEG9 protease modulates cytokinin and light signaling by regulating the level of response regulator 4 (Chi et al. 2016). The subcellular location and possible roles in light signaling of the three DEG9 orthologs in *Chlamydomonas* remain to be determined.

## Regulation of unfolded protein responses (UPRs) in *Chlamydomonas*

*The heat shock response* – When organisms are exposed to temperatures between ~10-15°C above their optimal growth temperature, they trigger a so-called heat shock response (Lindquist 1986). A hallmark of the heat shock response is the upregulation of genes encoding heat shock proteins (HSPs), the most prominent among them are the molecular chaperones described above (Lindquist and Craig 1988; Mühlhaus et al. 2011). Based on massively increased expression of *HSP* genes, *Chlamydomonas* cells trigger a heat shock response when shifted from 25°C to temperatures above ~35°C, with shifts to temperatures above ~43°C being lethal (Schroda et al. 2015). The temperature threshold varies between different studies, probably because it depends on the physiological state of the cells prior to heat shock, the strain used, the HSP used as a marker, and the sensitivity of the assay employed. Accordingly, threshold temperatures determined for *Chlamydomonas* were

35°C (Zhang et al. 2021), 36°C (Kobayashi et al. 2014), 37°C (Rütgers et al. 2017b), and 39°C (Tanaka et al. 2000).

A shift to elevated temperatures likely causes accumulation of misfolded proteins to an extent that exceeds the chaperoning capacity of the cell (Figure 7), leading to the formation of protein aggregates (Balchin et al. 2016). Misfolded proteins can trigger the upregulation of *HSP* genes without a temperature change, as demonstrated by the direct injection of denatured proteins into *Xenopus* oocytes (Ananthan et al. 1986), or the feeding of mammalian or *Chlamydomonas* cells with the arginine analog canavanine (Hightower and White 1981; Schmollinger et al. 2013). Hence, this response can be considered as unfolded protein response (UPR), while heat has many more consequences for a cell than only the challenge of protein homeostasis. (Hemme et al. 2014; Schroda et al. 2015; Zhang et al. 2021).

*HSFs are key regulators of the cytosolic unfolded protein response* – In all eukaryotes, the upregulation of *HSP* genes under proteotoxic stress is mediated by heat shock transcription factors (HSFs). HSFs bind to heat shock elements (HSEs) in the promoters of the *HSP* genes, which are repeats of at least three 5-bp sequences 5'-nGAAn-3' arranged in alternating orientation (Gomez-Pastor et al. 2018) (Figure 7). *Chlamydomonas* encodes two HSFs termed HSF1 and HSF2 (Schulz-Raffelt et al. 2007). While yeast encodes only a single HSF, land plants encode multiple HSFs, with *Arabidopsis* having 21 and soybean 52 (Scharf et al. 2012). Unlike yeast HSF and like plant HsfAs, *Chlamydomonas* HSF1 levels increase during heat shock (Wiederrecht et al. 1988; Hubel and Schoffl 1994; Schulz-Raffelt et al. 2007). Moreover, unlike yeast HSF, *Chlamydomonas* HSF1 shares all sequence signatures typical of land plant class A HSFs, which are the master regulators of the plant heat shock response (Nover et al. 2001; Schulz-Raffelt et al. 2007; Scharf et al. 2012). Accordingly, *Chlamydomonas* HSF1 is the master regulator of the alga's heat shock response, as depletion of HSF1 led to reduced synthesis of the major HSPs upon heat shock and to cell death (Schulz-Raffelt et al. 2007; Schmollinger et al. 2010). *Chlamydomonas* HSF2 contains the conserved DNA-binding domain but lacks the sequence motifs specific for plant HSFs. HSF2 levels increase during heat stress, but the role HSF2 plays in the heat shock response is not clear (Schulz-Raffelt et al. 2007).

*Activation of HSFs* –As a first step toward gaining transcriptional competence, HSFs must form trimers. While yeast HSF and *Chlamydomonas* HSF1 are constitutively trimeric, mammalian HSF1 and plant HsfAs are monomeric under ambient conditions and must trimerize upon heat stress (Sorger and Nelson 1989; Lee et al. 1995; Schulz-Raffelt et al. 2007). In mammals, HSF1 trimerization is prevented by the binding of HSF1 monomers to HSP90 under non-stress conditions. Once HSP90 is attracted to unfolding proteins under stress, HSF1 monomers are released, allowing for trimer formation. Hence, HSP90 serves as negative regulator of HSF1 activity (Zou et al. 1998). *Chlamydomonas* HSP90A also appears to act as a negative regulator for HSF1 as the HSP90 inhibitors geldanamycin and radicicol triggered *HSP* gene expression under ambient conditions, and enhanced and prolonged *HSP* gene expression under heat stress (Schmollinger et al. 2013), as observed in other organisms (Ali et al. 1998; Zou et al. 1998; Yamada et al. 2007). However, *Chlamydomonas* HSF1 is a constitutive trimer that is found complexed with HSP90A and HSP70A at the same stoichiometry under ambient and heat stress conditions (Schulz-

Raffelt et al. 2007; Schmollinger et al. 2013). Therefore, it is possible that the chaperones play a role in HSF1 maturation or in keeping HSF1 in an activation-competent conformation. In this case, transcriptional activation of HSF1 after feeding HSP90 inhibitors might result from the accumulation and aggregation of misfolded HSP90A clients and the negative effect that HSP90A exerts on HSF1 activity would be an indirect one (Schroda et al. 2015).

Following trimerization, HSFs must be hyperphosphorylated to be competent for transcriptional activation of its target genes (Cotto et al. 1996) (Figure 7). Accordingly, hyperphosphorylation of *Chlamydomonas* HSF1 correlated with the accumulation of HSP transcripts during heat shock. Moreover, reduced phosphorylation of HSF1 after application of the protein kinase inhibitor staurosporine resulted in reduced accumulation of HSP gene transcripts (Schulz-Raffelt et al. 2007; Schmollinger et al. 2013). Like in land plants (Saidi et al. 2009), calcium plays an important role for activation of *Chlamydomonas* HSF1, as the calmodulin antagonist W7 severely impaired HSP accumulation under heat (Rütgers et al. 2017b) (Figure 7). In contrast to land plants, however, for *Chlamydomonas* the internal calcium stores appear to be most important since removal of extracellular calcium by EGTA or inhibition of plasma membrane calcium transporters did not affect accumulation of HSPs in response to elevated temperatures (Schmollinger et al. 2013; Rütgers et al. 2017b).

The mechanisms underlying the activation of stress kinases and the opening of calcium channels by heat stress are not clear. Several lines of evidence suggest that in plant cells this is achieved by increased membrane fluidity (Saidi et al. 2009; Saidi et al. 2010). However, because protein homeostasis must be a self-regulating process, it is not clear how the protein folding state of a cell would feedback on membrane fluidity. Accordingly, using *Chlamydomonas*, all evidence for this hypothesis could be attributed to problems in protein homeostasis (Rütgers et al. 2017b). Hence, the activation of stress kinases and the opening of calcium channels might be mediated directly by unfolded/aggregated proteins, e.g. by their attachment to membranes via exposed hydrophobic surfaces, resulting in the impairment of essential membrane functions; or indirectly by depletion of molecular chaperones, which upon binding to unfolded proteins/aggregates might release repressors of stress kinase(s) and/or calcium channels (Figure 7).

*Chlamydomonas* HSF1 does not only play a role in controlling HSP gene expression under heat shock conditions, but also regulates expression of at least the *HSP70A* and *HSP90A* genes under non-stress conditions. Accordingly, HSF1 occupies the *HSP70A* promoter also under ambient conditions (Lodha and Schroda 2005; Strenkert et al. 2011; Strenkert et al. 2013), and HSP90A accumulates to much lower levels under ambient conditions in cells depleted of HSF1 (Schmollinger et al. 2013). Moreover, levels of both chaperones increased 1.8-fold and more than 2.5-fold at 30°C and 35°C, respectively, compared with 25°C (Rütgers et al. 2017b). Apparently, HSF1 is gradually activated with temperature to control at least the levels of HSP70A and HSP90A. How this is achieved is unclear, although an interesting idea is that gradual HSF1 activation is elicited by H<sub>2</sub>O<sub>2</sub>. H<sub>2</sub>O<sub>2</sub> levels in the cytosol and nucleus have been shown to gradually increase with temperature in *Chlamydomonas* (Niemeyer et al. 2021), and H<sub>2</sub>O<sub>2</sub> is known to play a role in HSF1 activation in land plants (Volkov et al. 2006).

Even when cells are constantly exposed to heat, they inactivate HSF1 in a process termed attenuation. Attenuation only occurs when sufficient amounts of functional

chaperones (and proteases) have been synthesized to maintain protein homeostasis. Accordingly, attenuation did not occur when *Chlamydomonas* cells were fed with the cytosolic protein synthesis inhibitor cycloheximide or with the arginine analog canavanine before exposure to heat, and was slowed down when cells were administered with HSP90 inhibitors (Schmollinger et al. 2013). These data show how protein homeostasis feeds back on HSF1 activity (Figure 7).

*Compartment-specific unfolded protein responses* – Since genes encoding molecular chaperones targeted to mitochondria, ER, and the chloroplast contain HSEs in their promoters that bind HSF1 (Strenkert et al. 2011; Traewachiwiphak et al. 2018), it appears that the accumulation of unfolded proteins in the cytosol triggers expression of HSPs for all compartments (Figure 7). However, expression appears prioritized to cytosolic HSPs: when cytosolic protein synthesis was slowed down by high concentrations of DMSO, the heat-induced expression of genes encoding cytosolic HSPs was enhanced, whereas the expression of chloroplast-targeted HSPs was reduced (Rütgers et al. 2017b). While the reduced translation of cytosolic HSPs was compensated for by increased accumulation of their transcripts, both the translation and transcript accumulation of chloroplast-targeted chaperones were reduced. Hence, heat did not change the accumulation of cytosolic HSPs but strongly reduced chloroplast targeted HSP accumulation. It is not clear whether differences in the accumulation of transcripts encoding cytosolic and chloroplast HSPs are due to differences in transcript stability or transcription rates. Reduced transcription rates would imply a different affinity of HSF1 for promoters of genes encoding cytosolic and chloroplast HSPs. This was indeed observed: in heat-stressed cells with HSF1 levels reduced by RNAi/amiRNA, residual HSF1 was still found to bind to the *HSP70A* promoter (driving a cytosolic HSP) but not to the *HSP22F* promoter (driving a chloroplast HSP) (Strenkert et al. 2011). The preference of HSF1 for promoters of genes encoding cytosolic HSPs most likely is achieved by different promoter architectures. That is, by different numbers of HSEs (e.g., four in *HSP70A* versus one in *HSP22F*) and different degrees of HSE sequence degeneration (Lodha and Schroda 2005). Different chromatin pre-settings might also play a role, as reflected by the much higher levels of histone H3/4 acetylation associated with the *HSP70A* versus the *HSP22F* promoter (Strenkert et al. 2011).

In addition to supplying HSPs to various compartments through regulation by HSF1 and the cytosolic UPR, there is clear evidence for compartment-specific UPRs in *Chlamydomonas*. This holds for the ER, as feeding cells with the drugs tunicamycin and DTT, which induce ER-specific protein folding stress, resulted in the specific upregulation of genes encoding ER-localized chaperones, including calreticulin 2 (CAL2), J-domain protein PDI6, BIP1, and HSP90B (Perez-Martin et al. 2014; Traewachiwiphak et al. 2018; Yamaoka et al. 2019). As in other organisms, protein folding stress in the ER leads to the activation of inositol-requiring enzyme 1 (IRE1), which is a dual-function protein with kinase and RNase activity. Under ER stress, IRE1 dimerizes and then autophosphorylates, activating its RNase activity. In *Chlamydomonas*, active IRE1 catalyzes the splicing of the mRNA encoding the bZIP1 transcription factor. While bZIP1 arising from the unspliced transcript contains a transmembrane domain and is targeted to the ER membrane, bZIP1 arising from the spliced mRNA lacks the transmembrane domain and is targeted to the nucleus, where it drives the transcription of genes encoding proteins that help the cells cope with ER stress (Yamaoka et al. 2019) (Figure 7).

The first indications for a feedback of chloroplast protein homeostasis on nuclear gene expression in *Chlamydomonas* came from the finding that the heat-induced accumulation of HSPs targeted to all cellular compartments was deregulated in cells expressing the 5'UTR of the gene encoding chloroplast HSP70B in antisense orientation. (Schmollinger et al. 2013). This effect could be explained by the triggering of a (mild) heat shock response when levels of chloroplast HSP70B fall below a certain threshold. Cells having elicited such a stress response might be desensitized and therefore cannot fully respond to a sudden heat shock (note that *Chlamydomonas* cells need to recover for ~5 h from heat stress until they have regained competence for another full heat shock response (Schroda et al. 2000)). The picture became clearer by the analysis of responses in cells inducibly depleted of the chloroplast-encoded ClpP1 protein (Ramundo et al. 2014): among several other responses, these cells strongly upregulated expression of genes encoding chloroplast chaperones HSP70B, HSP22C, HSP22E/F, CLPB3 and chloroplast proteases DEG1C and FTSH2. To a lesser extent, genes encoding cytosolic chaperones HSP22A and CLPB1 as well as mitochondrial HSP70C were also upregulated, potentially explaining the desensitizing for heat of cells expressing the *HSP70B* antisense construct.

Remarkably, however, depletion of ClpP1 also led to the strong upregulation of VIPP1 and ALB3.2, two proteins involved in thylakoid biogenesis, as well as of VIPP2 (Göhre et al. 2006; Ramundo et al. 2014). VIPP1 is constitutively expressed and upregulated under various stress conditions including high light, H<sub>2</sub>O<sub>2</sub>, the inhibition of chloroplast fatty acid synthesis, the depletion of chloroplast proteases ClpP1 and DEG1C or the depletion of thylakoid membrane protein transport components ALB3.2 and SECA. VIPP2 is present at low levels under ambient conditions and strongly induced by the same stresses (Göhre et al. 2006; Nordhues et al. 2012; Ramundo et al. 2014; Heredia-Martínez et al. 2018; Perlaza et al. 2019; Theis et al. 2019b; Theis et al. 2020). Supplementing cells with NiCl also led to the upregulation of HSP22C, HSP22E/F, CLPB3, DEG1C, and VIPP2 (Blaby-Haas et al. 2016). This points to a specific disturbance of chloroplast protein homeostasis by nickel ions.

VIPP1 and VIPP2 are unlikely to act as molecular chaperones in protein folding. Rather, their N-terminal 24 amino acids form an amphipathic  $\alpha$ -helix (AHa) that mediates membrane binding upon oligomerization of the proteins (Otters et al. 2013; Jovanovic et al. 2014; McDonald et al. 2015; McDonald et al. 2017; Gupta et al. 2021). The major determinant for membrane binding is the extent of stored curvature elastic (SCE) stress, and a minor determinant is the presence of anionic lipids. SCE stress in membranes occurs *inter alia* upon the accumulation of misfolded or misassembled membrane proteins (McDonald et al. 2015). Hence, the VIPPs might sense SCE stress in chloroplast membranes induced by misfolded or misassembled membrane proteins and participate in recruiting molecular chaperones and proteases to cope with these proteins and to alleviate SCE stress (Theis et al. 2020). Accordingly, VIPP2 formed common membrane associated complexes with VIPP1, HSP22E/F, and HSP70B in cells exposed to H<sub>2</sub>O<sub>2</sub>. The non-polar face of VIPP2's AHa is much more hydrophobic than that of VIPP1, potentially explaining why upon H<sub>2</sub>O<sub>2</sub> exposure much more VIPP2 became associated with chloroplast membranes than VIPP1. A role for VIPP2 as a sensor for SCE stress in a retrograde signaling cascade is indicated by the finding that the induction of *HSP22E/F* gene expression was impaired in the *vipp2* mutant (Theis et al. 2020) (Figure 7). Another important component of this “unfolded chloroplast membrane protein response” is MARS1

(for mutant affecting retrograde signaling 1) (Perlaza et al. 2019). MARS1 is a cytosolic kinase and mutants lacking MARS1 do not induce the expression of a specific set of genes including those encoding chloroplast chaperones, proteases, and VIPP2 upon depletion of ClpP1 or exposure of the cells to high light (Figure 7). In contrast, cells expressing a constitutively active variant of MARS1 expressed this gene set constitutively and were more resistant to high light exposure or treatment with metronidazole, a drug known to lead to the production of H<sub>2</sub>O<sub>2</sub> in the light (Perlaza et al. 2019; Niemeyer et al. 2021). Accordingly, a mutant in an effector protein of this response, DEG1C, had increased levels of proteins involved in high light acclimation when grown at low light intensities (Theis et al. 2019b). These include proteins of the carbon concentrating mechanism, photorespiration or antioxidant defense, but also thylakoid biogenesis factors VIPP1 and ALB3.2 and the FTSH protease. Possibly, accumulating misfolded proteins in the *deg1c* mutant are “interpreted” as the result of high light damage, leading to the induction of a high light acclimation response.

## Conclusion

The simpler but closely related set of chaperones and proteases in *Chlamydomonas* compared to land plants, combined with genetic, transcriptomic, and proteomic approaches, has provided deep insights into the function and regulation of chaperone and protease systems in this model system. New tools such as mutant libraries, genome editing, and synthetic biology approaches will further advance research on proteotoxic responses in *Chlamydomonas* and their integration across compartments.

## Acknowledgements

This work was supported by the Deutsche Forschungsgemeinschaft (TRR 175 project C02 and SPP 1927) and by the ‘Initiative d'Excellence’ program from the French State (Grant ‘DYNAMO’, ANR-11-LABX-0011-01). Many thanks to Olivier Vallon for information from *Chlamydomonas* genome v6.

## Figures

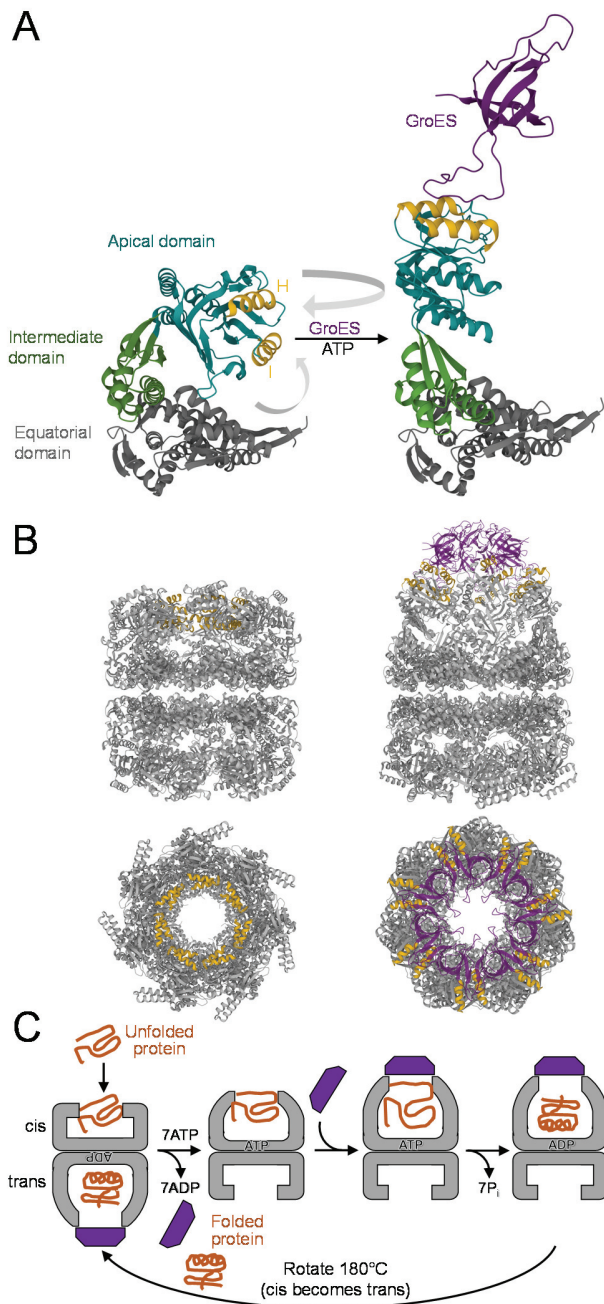


**Figure 1. Structure and functional cycle of group I chaperonins.**

(A) Structure of a ~60-kDa subunit of GroEL from *E. coli* in the nucleotide-free state (left, PDB ID: 1SS8) or after binding of ATP and cochaperonin GroES and ATP hydrolysis (right, PDB ID: 1PF9). Conformational changes turning away helices H and I (yellow) that form a hydrophobic cleft for substrate binding are indicated by grey arrows. Adopted from (Hayer-Hartl et al. 2016) using PDB-101. (B) Barrel-like structures formed by two rings of seven GroEL subunits each stacked back-to-back. The individual subunits shown in A were taken from the oligomeric structure. (C) Functional cycle of group I chaperonins. See text for details.

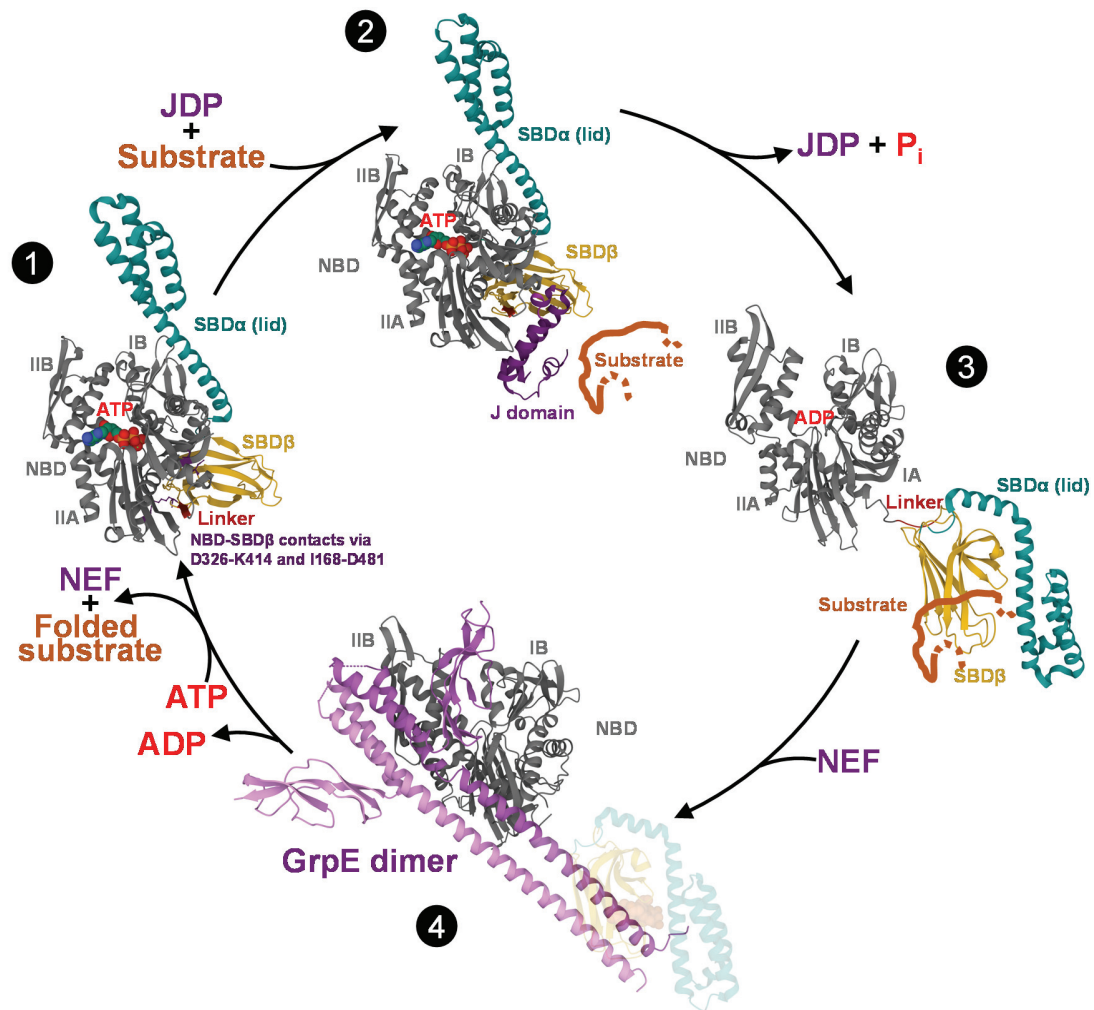


**Figure 2.** Functional cycle of bacterial and organellar Hsp70 systems. Structures shown are from *E. coli* DnaK and cochaperones. The nucleotide-binding domain (NBD) with its two lobes consisting of subdomains IA, IB, IIA, and IIB is shown in grey. The substrate binding domain (SBD) consists of SBDβ harboring the substrate binding pocket (yellow) and SBDα forming a lid (turquoise). Both are connected to the NBD via a hydrophobic linker (red). (1) (PDB ID: 4B9Q) In the ATP-bound state, the NBD lobes assume a conformation that opens a crevice at the bottom on the NBD into which the linker binds. This allows clamping of SBDβ to the NBD via two contact sites (purple) and locking of its lobes in a conformation preventing ATP hydrolysis. (2) (PDB ID: 5NRO) The delivery of a substrate (orange) to the SBDβ via a J-domain protein (JDP) (J-domain in purple, HPD motif in pink) results in the release of the clamp between SBD and NBD, rendering the NBD competent for ATP hydrolysis. (3) (PDB ID: 2KHO) Upon ATP hydrolysis, the lid closes over the bound substrate, and NBD and SBD are only loosely connected via the linker that has left the crevice. (4) (PDB ID: 1DKG) The dimeric nucleotide exchange factor (NEF) GrpE binds to the ADP-bound state of the NBD, inserting the β-sheet domain of one of the monomers to drive a wedge into the NBD. This induces a tilt of lobe IIB that results in an opening of the nucleotide binding cleft to allow ADP release. The rebinding of ATP converts Hsp70 back to the low affinity state for substrates and results in the release of substrate and NEF. The long, paired α-helices protruding towards the SBD (faded; PDB ID: 4EZW) harbor motifs at their N-termini that might prevent the rebinding of released substrate. Adopted from (Rosenzweig et al. 2019) using PDB-101.

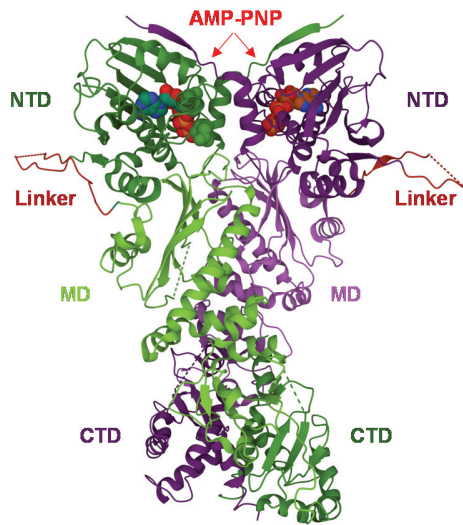


**Figure 3.** Structure of the yeast Hsp90 dimer representing the ATP-bound closed state 2. The N-terminal domain (NTD; dark green or dark purple) is connected via a charged linker (red; truncated and indicated by dashed lines) to the middle domain (MD; light green or light purple). CTD – C-terminal domain (PDB ID: 2CG9). The C-terminal MEEVD motif is disordered and not shown. Adopted from (Ali et al. 2006) using PDB-101.

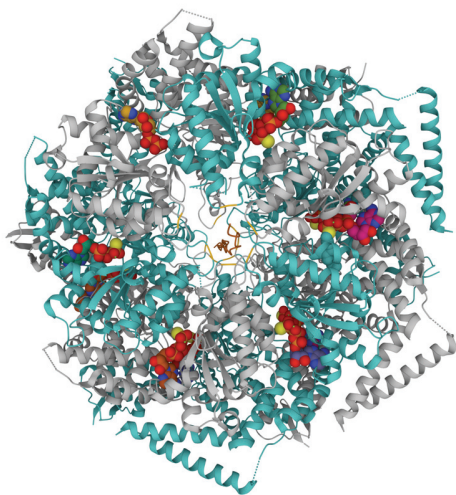


**Figure 4.** Structure of the homohexameric ClpB disaggregase from *E. coli* engaged on casein as substrate. Shown is a top view with the six ClpB protomers (alternating between grey and teal) forming a closed ring with a helical arrangement of two stacked AAA tiers (PDB ID: 6QS7, (Deville et al. 2019)). Each AAA domain extends a flexible pore loop arranged to form a spiral staircase around the translocation channel. The pore loops bear a tyrosine residue (yellow), which interacts with the backbone of the threading casein polypeptide (orange). Bound nucleotides (ATP $\gamma$ S) are shown with space-filling representation, unresolved regions as dashed lines. Drawn with PDB-101.

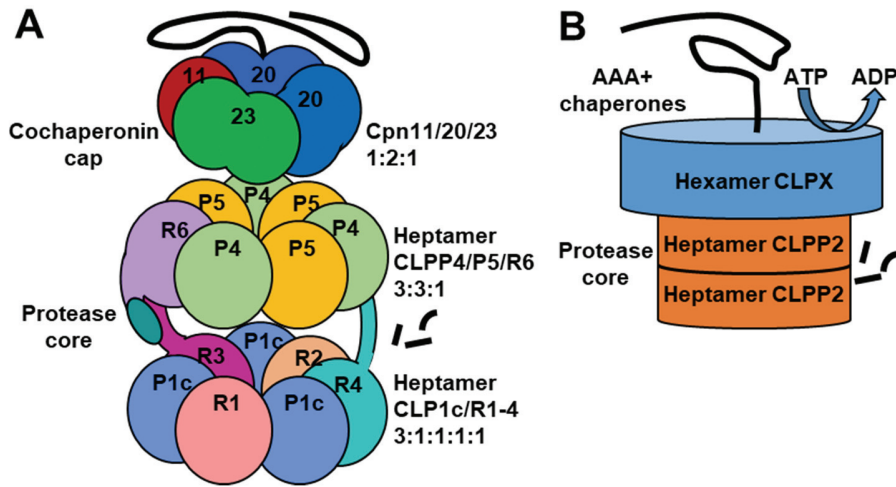


**Figure 5. Clp proteases in *Chlamydomonas* organelles.**

(A) Schematic view based on the cryo-EM structure of the chloroplast ClpP complex from *Chlamydomonas* (Wang et al. 2021). The chloroplast protease core is formed by two hetero-heptameric rings capped by seven cochaperonin domains (Cpn11 has one, while Cpn20 and Cpn23 each have two cochaperonin domains in tandem). (B) Simplified model of the mitochondrial Clp protease with two CLPP2 heptameric rings of the protease core associated with an hexameric ring of AAA+ chaperones CLPX (van Wijk 2015).

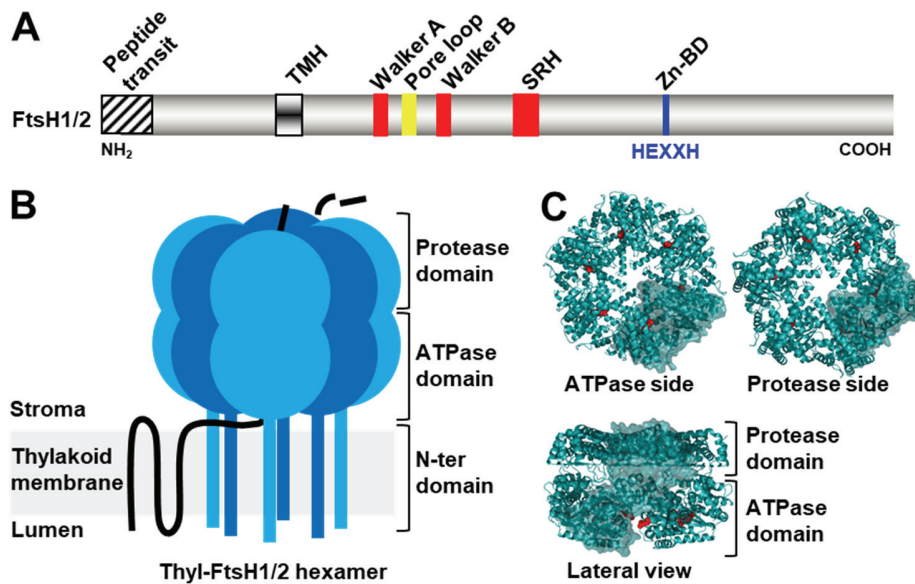


**Figure 6. FtsH protease.**

(A) Linear diagram of the domain organization of the *Chlamydomonas* FtsH1/2 subunits with N-ter transit peptide, trans-membrane helix (TMH), ATPase (in red) Walker A and B motifs, pore loop (in yellow), second region of homology (SRH) containing Arg residues required for ATP hydrolysis (one of which is substituted by Cys in *ftsH1-1* mutant), and Zn-binding domain (Zn-BD) with HEXXH motif (in blue). (B) Schematic representation of the FtsH1/2 hexameric complex in the thylakoid membrane. (C) Structure of *Thermotoga* FtsH hexamer lacking the transmembrane domain and ATP (PBD: 3KDS). SRH Arg (in red) indicates ATPase site at the intersubunit interface.

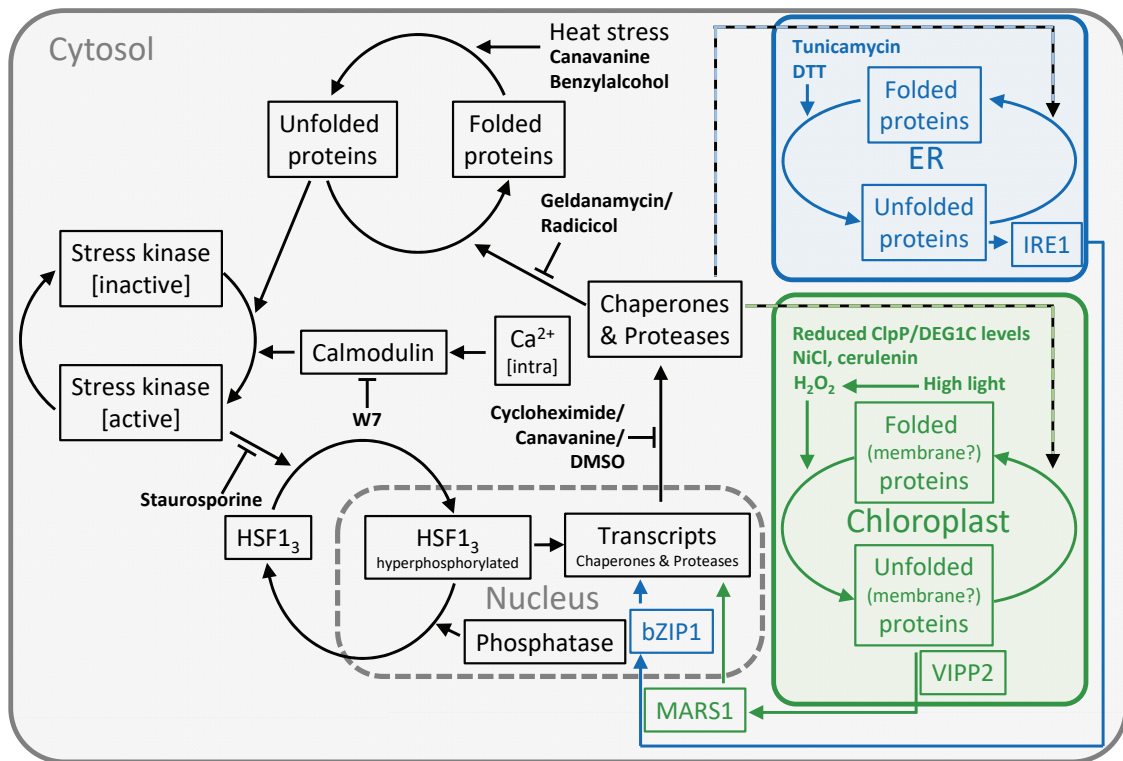


**Figure 7.** Model for unfolded protein responses (UPRs) in *Chlamydomonas*. Heat stress (or supplementing cells with canavanine or benzyl alcohol) leads to the accumulation of unfolded proteins in the cytosol which, by an unknown mechanism likely to involve molecular chaperones, activate stress kinase(s). The activation of stress kinase(s) requires calmodulin and calcium from intracellular stores. Active stress kinase(s) hyperphosphorylate constitutive HSF1 trimers – a process that is partially inhibited by staurosporine. Hyperphosphorylated HSF1 is transcriptionally competent and generates transcripts encoding molecular chaperones and proteases, whose translation into functional proteins is inhibited/slowed down by cycloheximide, canavanine, or DMSO. Increased levels of molecular chaperones and proteases targeted to the cytosol and to cellular compartments restore the cell’s protein folding equilibrium – a process that is slowed down when HSP90s are inactivated by geldanamycin or radicicol. Attenuation of the cytosolic UPR is realized when stress kinase activation ceases after the protein folding equilibrium is restored, and HSF1 might be dephosphorylated by a yet hypothetical, constitutively active phosphatase. Unfolded proteins accumulating in the ER trigger a compartment-specific response by activating the RNase IRE1 that splices the mRNA encoding the bZIP1 transcription factor. This leads to the synthesis of bZIP1 without a transmembrane domain, which allows its accumulation in the nucleus to drive the expression of genes that help restore ER protein homeostasis. High light exposure, H<sub>2</sub>O<sub>2</sub>, nickel ions, chloroplast fatty acid synthase inhibitor cerulenin, or the depletion of chloroplast chaperones ClpP1 or DEG1C results in the accumulation of unfolded/misassembled proteins in or at chloroplast membranes, causing lipid packing stress. The latter is sensed by VIPP proteins to trigger a retrograde signaling cascade involving the MARS1 kinase. This “unfolded chloroplast membrane protein” response results in the upregulation of molecular chaperones and proteases, as well as of other proteins involved in high light acclimation. Symbols in black, blue and green depict UPRs in cytosol, ER, and chloroplast, respectively. A mathematical model for the cytosolic UPR based on the model presented here has been developed recently (Magni et al. 2018).

Table 1. Small heat shock proteins.

Name	Accession Phytozome v5.5/NCBI <sup>a</sup>	Introns <sup>b</sup>	Localization <sup>c</sup>	ORF (aa)	kD (pre)	Detected by MS <sup>d</sup>	References for dedicated studies
HSP22A	Cre07.g318800/ XP_001701015	2	cyt (4)	157	16.7	Yes nd/7	(Grimm et al. 1989; Eisenberg-Domovich et al. 1994)
HSP22B	( <i>Cre07.g318850</i> )/ XP_001700830	1	cyt (5)	183	20.0	Yes	-
HSP22C	Cre03.g145787/ XP_001695717	1	cp (5)	291	30.0	Yes	-
HSP22D	Cre01.g020575/ XP_001689955	0	cp (2)	178	18.6	Yes	-
HSP22E	Cre14.g617450/ XP_001689821	1	cp (e)	241	25.2	Yes 973/280	(Rütgers et al. 2017a; Perlaza et al. 2019; Theis et al. 2020)
HSP22F	Cre14.g617400/ ( <i>XP_001690281</i> )	1	cp (e)	241	25.1	Yes	(Rütgers et al. 2017a; Perlaza et al. 2019; Theis et al. 2020)
HSP22G	Cre13.g572350/ XP_001693742	3	mt (4)	362	36.7	No	-
HSP22H	Cre07.g318600 ( <i>XP_001700827</i> )	4	cyt (3)	233	23.9	No	-

<sup>a</sup>Protein sequence wrong at italicized accessions in parenthesis.

<sup>b</sup>Introns within coding region.

<sup>c</sup>According to TargetP prediction (Emanuelsson et al. 2000); reliability class is given in parenthesis, the lower the value, the higher the reliability of the prediction. e – experimental proof.

<sup>d</sup>Mass spectrometry (MS) detection in at least one of these large-scale studies (Mühlhaus et al. 2011; Hemme et al. 2014; Ramundo et al. 2014; Park et al. 2015; Rütgers et al. 2017a). If quantified in Schroda et al. (2015), the rank among 1207 soluble proteins before/after 24 h heat stress is given.

ORF – open reading frame, aa – amino acids, pre – precursor, cyt – cytosol, cp – chloroplast, mt – mitochondria, nd – not detected.

Table 2. Chaperonins and cochaperonins.

Name	Accession Phytozome v5.5/NCBI <sup>a</sup>	Introns <sup>b</sup>	Localization <sup>c</sup>	ORF (aa)	Mat (aa)	kD (mat)	Detected by MS <sup>d</sup>	References for dedicated studies
CPN60A	( <i>Cre04.g231222</i> )/ XP_001703692	17	cp	580	547	58.1	Yes	(Balczun et al. 2006; Bai et al. 2015; Guo et al. 2015; Zhang et al. 2016a; Zhang et al. 2016b)
CPN60B1	Cre17.g741450/ ( <i>XP_001701113</i> )	16	cp	581	551	59	Yes 468/172	(Bai et al. 2015; Guo et al. 2015; Zhang et al. 2016a; Zhang et al. 2016b)
CPN60B2	Cre07.g339150/ XP_001692504	15	cp	577	546	58.5	Yes 157/17	(Bai et al. 2015; Guo et al. 2015; Zhang et al. 2016a; Zhang et al. 2016b)
CPN60C	Cre06.g309100/ ( <i>XP_001691353</i> )	14	mt	571	543	57.4	Yes 223/55	-
CPN23	Cre12.g505850/ XP_001690823	4	cp	238	212	23	Yes 279/42	(Tsai et al. 2012; Guo et al. 2015; Zhang et al. 2016b; Zhao et al. 2019)
CPN20	Cre08.g358562/ ( <i>XP_001703710</i> )	6	cp	216	194	20.5	Yes	(Tsai et al. 2012; Guo et al. 2015; Zhang et al. 2016a; Zhang et al. 2016b; Zhao et al. 2019)
CPN11	Cre16.g673729/ XP_001695900	4	cp	128	101	10.8	Yes	(Tsai et al. 2012; Guo et al. 2015; Zhang et al. 2016b; Zhao et al. 2019)
CPN10	Cre03.g178450/ XP_001703259	2	mt	99	93	10	Yes 189/24	-
CCT1	Cre10.g439100/ XP_001690556	11	cyt	551		59.3	Yes 645/479	-
CCT2	( <i>Cre09.g416750</i> )/ XP_001696757	13	cyt	528		57.0	Yes 769/554	-
CCT3	Cre10.g443250/ XP_001690337	11	cyt	555		60.8	Yes 561/347	-
CCT4	Cre05.g234639/ ( <i>XP_001700677</i> )	13	cyt	526		57.1	Yes	-
CCT5	Cre03.g156750/ XP_001697528	11	cyt	536		59	Yes 519/435	-
CCT6	Cre09.g397200/ ( <i>XP_001694510</i> )	10	cyt	547		59.8	Yes 515/426	-
CCT7	Cre01.g026550/ ( <i>XP_001690009</i> )	12	cyt	567		61.4	Yes 813/538	-
CCT8	Cre03.g168450/ XP_001703339	10	cyt	544		57.5	Yes 382/284	-

<sup>a</sup>Protein sequence wrong at italicized accessions in parenthesis.

<sup>b</sup>Introns within coding region.

<sup>c</sup>According to localization of *Arabidopsis* orthologs.

<sup>d</sup>Mass spectrometry (MS) detection in at least one of these large-scale studies (Atteia et al. 2009; Terashima et al. 2010; Mühlhaus et al. 2011; Valledor et al. 2013; Hemme et al. 2014; Ramundo et al. 2014; Park et al. 2015; Perez-Perez et al. 2017). If quantified in Schroda et al. (2015), the rank among 1207 soluble proteins before/after 24 h heat stress is given.

ORF – open reading frame, mat – mature protein, aa – amino acids, cyt – cytosol, cp – chloroplast, mt – mitochondria.

Table 3. HSP70s and selected auxiliary factors.

Name	Accession Phytozome v5.5/NCBI <sup>a</sup>	Introns <sup>b</sup>	Localization <sup>c</sup>	ORF (aa)	Mat (aa)	kD (mat)	Detected by MS <sup>d</sup>	References for dedicated studies
HSP70A	Cre08.g372100/ XP_001701326	6	cyt (e)	651		71.2	Yes 60/11	(Bloch and Johnson 1995; Shapiro et al. 2005; Schulz-Raffelt et al. 2007; Silflow et al. 2011; Schmollinger et al. 2013; Rütgers et al. 2017b)
HSP70B	Cre06.g250100/ XP_001696432	5	cp (e)	679	639	67.9	Yes 114/19	(Drzymalla et al. 1996; Schroda et al. 1999; Schroda et al. 2001b; Liu et al. 2005; Liu et al. 2007; Willmund et al. 2007; Michelet et al. 2008; Willmund et al. 2008a; Willmund et al. 2008b; Heide et al. 2009; Dorn et al. 2010; Veyel et al. 2014; Theis et al. 2020)
HSP70C	Cre09.g393200/ (XP_001694468)	18	mt (e)	663	632	67.6	Yes 263/124	-
BIP1	Cre02.g080700/ XP_001701685	7	ER (e)	656	632	70	Yes 200/87	(Diaz-Troya et al. 2008; Diaz-Troya et al. 2011)
BIP2	(Cre02.g080600/ XP_001701884)	9	ER	662	638	70.3	Yes	-
HSP70D	Cre12.g535700/ (XP_001692887)	11	cp/mt	578	541?	57?	No	-
HSP70E	(Cre16.g677000/ XP_001695858)	19	cyt	803		87.1	Yes 227/78	-
HSP70F	(Cre09.g412880/ XP_001696713)	?	cp/mt	?	?	?	No	-
HSP70G	Cre10.g439900/ (XP_001690543)	17	ER	1124	1104	119	Yes 748/361	(Mathieu-Rivet et al. 2013)
BAG6	Cre03.g152750/ (XP_001697564)	2	cyt	935		94.3	Yes	-
HSPBP1 alias MOT53	Cre09.g397512/ XP_001701310	8	cyt	448		45.2	Yes 1132/614	-
CGE1a	Cre07.g341600.t2/ Q945T2	7	cp (e)	258	219	23.8	Yes	(Schroda et al. 2001b; Liu et al. 2007; Willmund et al. 2007; Willmund et al. 2008a; Veyel et al. 2014)
CGE1b	Cre07.g341600.t1/ Q945T1	7	cp (e)	260	221	24.0	Yes 231/34	(Schroda et al. 2001b; Liu et al. 2007; Willmund et al. 2007; Willmund et al. 2008a; Veyel et al. 2014)
CGE2	(Cre14.g632000/ XP_001692653)	?	cp?	?	?	?	No	-
MGE1	Cre08.g370450/ XP_001701310	5	mt	264	220	23.5	Yes 509/520	-
HEP1	(Cre07.g334851/ XP_001700157) BM003684	2	mt	166	110	12	No	(Willmund et al. 2008b)
HEP2	Cre17.g707950/ XP_001691699	3	cp (e)	205	135	14.9	No	(Willmund et al. 2008b; Veyel et al. 2014)
DNJ1	Cre17.g701500/ (XP_001691598)	6	cyt	450		48.3	Yes 300/148	(Willmund et al. 2008a; Silflow et al. 2011)
MDJ1	Cre12.g560700/ (XP_001703128)	5	mt	535	489	48.7	No	(Willmund et al. 2008a)
CDJ1	Cre12.g507650/ XP_001690840	6	cp (e)	418	374	40.3	Yes 905/477	(Willmund et al. 2008a)
CDJ2	(Cre07.g316050/ XP_001700988)	6	cp (e)	374	262	26.8	No	(Liu et al. 2005; Liu et al. 2007)
CDJ3	(Cre01.g009900/ XP_001700257) GQ421467	6	cp (e)	393	352	38.3	No	(Dorn et al. 2010; Veyel et al. 2014; Auerbach et al. 2017)
CDJ4	(Cre02.g104500/ XP_001699768) GQ421468	8	cp (e)	382	306	33.1	No	(Dorn et al. 2010; Veyel et al. 2014; Auerbach et al. 2017)

CDJ5	<i>(Cre07.g320350)/ XP_001700843</i>	7	cp	383	333	37.6	No	(Dorn et al. 2010)
CDJ6	<i>(Cre02.g108800/ XP_001699952)</i>	?	cp?	?	?	?	No	-

<sup>a</sup> Protein sequence wrong at italicized accessions in parenthesis.

<sup>b</sup> introns within coding region.

<sup>c</sup> according to localization of orthologs; (e) determined experimentally.

<sup>d</sup> Mass spectrometry (MS) detection in at least one of these large-scale studies (Pazour et al. 2005; Atteia et al. 2009; Terashima et al. 2010; Mühlhaus et al. 2011; Mathieu-Rivet et al. 2013; Valledor et al. 2013; Hemme et al. 2014; Ramundo et al. 2014; Park et al. 2015; Perez-Perez et al. 2017). If quantified in Schroda et al. (2015), the rank among 1207 soluble proteins before/after 24 h heat stress is given.

ORF – open reading frame, mat – mature protein, aa – amino acids, cyt – nucleo-cytoplasm, cp – chloroplast, mt – mitochondrial.

Table 4. HSP90s and cochaperones.

Name	Accession Phytozome v5.5/NCBI <sup>a</sup>	Introns <sup>b</sup>	Localization <sup>c</sup>	ORF (aa)	Mat (aa)	kD (mat)	Detected by MS <sup>d</sup>	References for dedicated studies
HSP90A	Cre09.g386750/ XP_001695264	7	cyt	705		80.7	Yes 85/2	(Schulz-Raffelt et al. 2007; Schmollinger et al. 2013; Rütgers et al. 2017b)
HSP90B	Cre02.g080650/ (XP_001701885)	12	ER	819	795	90.6	Yes 285/95	(Traewachiwiphak et al. 2018)
HSP90C	Cre12.g514850/ XP_001702984	9	cp (e)	810	739	82.4	Yes 290/52	(Willmund and Schroda 2005; Willmund et al. 2008a; Heide et al. 2009)
HOP1	Cre03.g189950/ (XP_001691869)	12	cyt	577		63.9	Yes 454/99	-
CCPP23	Cre07.g341550/ XP_001692527	1	cyt	215		23	Yes 326/188	-
AHA1	Cre03.g199300/ (XP_001693239)	7	cyt	355		38.5	Yes 918/226	-
CCPP5 alias PPP29	Cre07.g326800/ XP_001690473	13	cyt	507		56.5	Yes 887/643	-
TPR2 alias DNJ8	Cre01.g032500/ (XP_001689602)	13	cyt	496		55.6	Yes	-
FKB62 alias ROF1	Cre09.g398067/ (XP_001694809)	16	cyt	603		65.1	Yes 838/36	-
CYN40 alias CYP40	Cre01.g047700/ XP_001690215	11	cyt	377		40.2	Yes 782/185	-
CHIP1	Cre11.g479650/ (XP_001697382)	7	cyt	267		29.7	No	-
SGTA1	Cre12.g513600/ (XP_001702976)	7	cyt	396		42.8	Yes 996/450	-
CNS1 alias TTC4	Cre08.g375650	7	cyt	388		42.8	Yes	-

<sup>a</sup> Protein sequence wrong at italicized accessions in parenthesis.

<sup>b</sup> Introns within coding region.

<sup>c</sup> According to localization of orthologs in *Arabidopsis*, yeast, and humans; (e) determined experimentally.

<sup>d</sup> Mass spectrometry (MS) detection in at least one of these large-scale studies (Atteia et al. 2009; Heide et al. 2009; Terashima et al. 2010; Mühlhaus et al. 2011; Valledor et al. 2013; Hemme et al. 2014; Ramundo et al. 2014; Park et al. 2015; Perez-Perez et al. 2017). If quantified in Schroda et al. (2015), the rank among 1207 soluble proteins before/after 24 h heat stress is given.

ORF – open reading frame, aa – amino acids, mat – mature, cyt – cytosol, cp – chloroplast.

Table 5. ORFs encoding Clp/Hsp100 proteins.

Name	Accession Phytozome v5.5/NCBI <sup>a</sup>	Scaffold in v1.0 <sup>b</sup>	Introns <sup>c</sup>	Localization <sup>d</sup>	ORF (aa)	Mat <sup>e</sup> (aa)	kD (mat)	Detected by MS <sup>f</sup>
CLPX1	Cre16.g663350/ <i>(XP_001697962)</i>	273	15	mt	585	554	59.7	Yes
HSLU1	<i>(Cre12.g510900)/</i> XP_001691057		11	mt	559	477	52.5	No
HSLU2	Cre02.g147850/ <i>(XP_001695024)</i>		10	mt	696	?	?	Yes
CLPB1 alias HSP101	Cre11.g467644/ XP_001698806	785	4	cyt	925	925	100.8	Yes 1142/101
CLPB2	<i>(Cre02.g091400/ XP_001701975)</i>	839	?	?	?	?	?	No
CLPB3	<i>(Cre02.g090850)/</i> XP_001701777	1344 & 3660	11	cp	1040	925	100.7	Yes 649/118
CLPB4	<i>(Cre11.g467575/ XP_001701404)</i>	2086	24?	?	927?	?	?	Yes
CLPB5	<i>(Cre12.g533351/ XP_001693009)</i>	1646	21?	?	1053?	?	?	No
CLPC1	<i>Cre02.g143307</i>	1573	?	cp	?	?	?	Yes
CLPD1	Cre10.g465550/ <i>(XP_001698633)</i>	977	19	cp	1033	961	102.8	Yes 715/746

<sup>a</sup> Protein sequence wrong at italicized accessions in parenthesis.

<sup>b</sup> Scaffolds in version 1.0 of the *Chlamydomonas* genome encoding Clp/HSP100 proteins (Schroda 2004).

<sup>c</sup> Introns within coding region.

<sup>d</sup> According to localization of orthologs.

<sup>e</sup> Determined with TargetP.

<sup>f</sup> Mass spectrometry (MS) detection in these studies (Terashima et al. 2010; Mühlhaus et al. 2011; Valledor et al. 2013; Hemme et al. 2014; Mettler et al. 2014; Ramundo et al. 2014; Perez-Perez et al. 2017). If quantified in Schroda et al. (2015), the rank among 1207 soluble proteins before/after 24 h heat stress is given.

ORF – open reading frame, mat – mature protein, aa – amino acids, cyt – cytosol, cp – chloroplast, mt – mitochondria.

Table 6. ORFs encoding ClpP core proteins.

Name	Accession Phytozome v5.6/NCBI <sup>a</sup>	Introns <sup>b</sup>	Localization <sup>c</sup>	ORF (aa) <sup>d</sup>	Mat (aa)	kD (mat)	kD (pre)	Detected by MS <sup>e</sup>	References for dedicated studies
ClpP <sub>H</sub>	cp encoded /NP_958364	0	cp (e)	524	523	59		Yes 642/583	(Majeran et al. 2000; Majeran et al. 2005; Derrien et al. 2012; Ramundo et al. 2014; Majeran et al. 2019; Wang et al. 2021)
ClpP <sub>C</sub>		0	cp (e)	524	208	23		Yes	(Derrien et al. 2012; Wang et al. 2021)
ClpP <sub>C'</sub>		0	cp (e)	524	192	21		Yes	(Derrien et al. 2012; Wang et al. 2021)
ClpP <sub>N</sub>		0	cp (e)	524		20		Yes	(Derrien et al. 2012; Wang et al. 2021)
CLPP2	Cre12.g521450 v6 ( <i>Cre12.g521450</i> )	7	mt	231 (185+15)			25	No	
CLPP4	Cre12.g500950	4	cp (e)	345	296	33		Yes 445/875	(Derrien et al. 2012; Wang et al. 2021)
CLPP5	Cre12.g486100	4	cp (e)	256			28	Yes 481/500	(Wang et al. 2021)
CLPR1	Cre14.g619100	7	cp (e)	411	246	28		Yes 795/724	(Derrien et al. 2012; Wang et al. 2021)
CLPR2	Cre16.g682900	7	cp (e)	282			32	Yes 919/1008	(Wang et al. 2021)
CLPR3	Cre07.g331500	12	cp (e)	415			47	Yes	(Wang et al. 2021)
CLPR4	Cre03.g204350	8	cp (e)	286+ 17	251	28		Yes	(Derrien et al. 2012; Wang et al. 2021)
CLPR6	Cre06.g229650	8	cp (e)	283			31	Yes 581/636	(Wang et al. 2021)
CLPT3	Cre10.g417550	6	cp (e)	303			31	Yes	(Wang et al. 2021)
CLPT4	Cre03.g144667	0	cp (e)	244	178	20		Yes	(Derrien et al. 2012; Wang et al. 2021)

<sup>a</sup> Protein sequence wrong at italicized accessions in parenthesis.

<sup>b</sup> Introns within coding region.

<sup>c</sup> According to localization of orthologs in *Arabidopsis*; (e) determined experimentally.

<sup>d</sup> CDS extension to upstream in-frame ATG at CDS + extension.

<sup>e</sup> Mass spectrometry (MS) detection in at least one of these large-scale studies (Derrien et al. 2012; Hemme et al. 2014; Park et al. 2015; Ramundo et al. 2020). If quantified in Schroda et al. (2015), the rank among 1207 soluble proteins before/after 24 h heat stress is given.

ORF – open reading frame, aa – amino acids, mat – mature, cp – chloroplast, mt – mitochondria.

Table 7. ORFs encoding FTSH proteins.

Name	Accession Phytozome v5.6/ Genbank or NCBI <sup>a</sup>	Introns <sup>b</sup>	Localization <sup>c</sup>	ORF (aa) <sup>d</sup>	Mat (aa)	kD (mat)	kD (pre)	Detected by MS <sup>e</sup>	References for dedicated studies
FTSH1	Cre12.g485800/ XP_001690889	5	cp ti (e)	727	646	69		Yes	(Malnoe et al. 2011; Malnoe et al. 2014; Wei et al. 2014; Bujaldon et al. 2017; Wang et al. 2017; De Mia et al. 2019)
FTSH2	Cre17.g720050/ XP_001697103	9	cp ti (e)	689	619	67		Yes	(Malnoe et al. 2014; Wang et al. 2017)
FTSH3	Cre01.g019850/ PNW88220	14	mt m- AAA <sup>b</sup> (e)	911			96	Yes	
FTSH4	Cre13.g568400/ PNW73682	15	mt i- AAA <sup>b</sup>	702			74	Yes	
FTSH9 alias FTSH7	Cre02.g078966/ PNW86257	13	cp ie	981			101	No	
FtsH11	Cre14.g625625/ PNW73269	19	cp ie	1199			121	No	
FTSHi1 alias Ctap1	Cre17.g739752 v6 ( <i>Cre17.g739752</i> )	25 19	cp ie (e)	982 780			108	Yes	(Ramundo et al. 2020)
FTSHi2	Cre04.g800432 v6 ( <i>Cre04.g217800</i> )	31 12	cp ie	1024 446			109	No	
FTSHi3 alias FHL2	Cre09.g393950/ PNW78515	13	cp ie	560			58	No	
FTSHi4 alias FHL1	Cre03.g201100/ PNW85891	25	cp ie (e)	1178			128	Yes	(Ramundo et al. 2020)
FTSHi6 alias FHL3	Cre07.g352350/ PNW81353	20	cp ie (e)	1058 +54			120	Yes	(Ramundo et al. 2020)
Ycf2 alias ORF2971	cp encoded Q32065 (uniprot)/AAB5800	0	cp ie (e)	2971	2971	342		Yes	(Ramundo et al. 2020)

<sup>a</sup>Protein sequence wrong at italicized accessions in parenthesis.

<sup>b</sup>Introns within coding region.

<sup>c</sup>According to localization of orthologs in *Arabidopsis*; (e) determined experimentally.

<sup>d</sup>CDS extension to upstream in-frame ATG at CDS + extension.

<sup>e</sup>Mass spectrometry (MS) detection in at least one of these large-scale studies (Allmer et al. 2006; Atteia et al. 2009; Terashima et al. 2010; Hemme et al. 2014; Ramundo et al. 2014; Park et al. 2015; Ramundo et al. 2020).

ORF – open reading frame, aa – amino acids, mat – mature protein, pre – precursor, cp – chloroplast, ie – inner envelope, ti – integral membrane thylakoid protein, mt – mitochondria.

Table 8. ORFs encoding DEG proteins.

Name	Accession Phytozome v5.6 <sup>a</sup>	Introns <sup>b</sup>	Localization <sup>c</sup>	ORF (aa)	kD (pre)	Detected by MS <sup>d</sup>	PDZs <sup>e</sup>	References for dedicated studies
DEG1A alias DEG1	Cre02.g088400	10	cp tl	432+98	55	Yes	1	
DEG1B alias DEG12	Cre14.g630550	10	cp tl	824	79	No	1	
DEG1C alias DEG13	Cre12.g498500	11	cp (e)	462+54	64	Yes 1133/730	1	(Theis et al. 2019b)
DEG2	Cre02.g092000	11	cp	643+75	76	No	2	
DEG5	Cre02.g110600	5	cp tl	269+87	36	No	0	
DEG7	Cre03.g180650	18	cp	1108	119	Yes	3	
DEG8	Cre01.g028350	12	cp tl	436	44	Yes	1	
DEG9A alias DEG4	Cre03.g200655 v6 ( <i>Cre03.g200655</i> )	11 23	nu	694 <i>1424</i>	72	No	2	
DEG9B alias DEG9	Cre14.g617600	15	nu	619	66	No	2	
DEG9C alias DEG6	Cre13.g579901	16	nu	680	71	No	2	
DEG10	Cre01.g013300	12	mt	739+72	84	Yes	1	
DEG15	Cre12.g548200	4	pe	1249	123	No	0	
DEGO1	Cre03.g203730	10	?	789	78	No	2	
DEGO2	Cre06.g293516	15	?	1199+3	118	No	2	

<sup>a</sup> Protein sequence wrong at italicized accessions in parenthesis.

<sup>b</sup> Introns within coding region.

<sup>c</sup> According to localization of orthologs in *Arabidopsis*; determined experimentally (e).

<sup>d</sup> Mass spectrometry (MS) detection in at least one of these large-scale studies (Terashima et al. 2010; Hemme et al. 2014; Ramundo et al. 2014; Park et al. 2015). If quantified in Schroda et al. (2015), the rank among 1207 soluble proteins before/after 24 h heat stress is given.

<sup>e</sup> Number of PDZ domains within the Deg protein, as predicted by Pfam and considering an E-value smaller than 0.01  
ORF – open reading frame, aa – amino acids, pre – precursor, cp – chloroplast, tl – thylakoid lumen, mt – mitochondria.

## Chapter References

- Adam Z (2015). Plastid intramembrane proteolysis. *Biochimica et Biophysica Acta* 1847: 910-914.
- Adam Z, Aviv-Sharon E, Keren-Paz A, Naveh L, Rozenberg M, Savidor A, Chen J (2019). The chloroplast envelope protease FTSH11 - interaction with CPN60 and identification of potential substrates. *Front Plant Sci* 10: 428.
- Ali A, Bharadwaj S, O'Carroll R, Ovsenek N (1998). HSP90 interacts with and regulates the activity of heat shock factor 1 in *Xenopus* oocytes. *Molecular and Cellular Biology* 18: 4949-4960.
- Ali MM, Roe SM, Vaughan CK, Meyer P, Panaretou B, Piper PW, Prodromou C, Pearl LH (2006). Crystal structure of an Hsp90-nucleotide-p23/Sba1 closed chaperone complex. *Nature* 440: 1013-1017.
- Allmer J, Naumann B, Markert C, Zhang M, Hippler M (2006). Mass spectrometric genomic data mining: Novel insights into bioenergetic pathways in *Chlamydomonas reinhardtii*. *Proteomics* 6: 6207-6220.
- Ananthan J, Goldberg AL, Voellmy R (1986). Abnormal proteins serve as eukaryotic stress signals and trigger the activation of heat shock genes. *Science* 232: 522-524.

- Atteia A, Adrait A, Brugiere S, Tardif M, van Lis R, Deusch O, Dagan T, Kuhn L, Gontero B, Martin W, Garin J, Joyard J, Rolland N (2009). A proteomic survey of *Chlamydomonas reinhardtii* mitochondria sheds new light on the metabolic plasticity of the organelle and on the nature of the alpha-proteobacterial mitochondrial ancestor. *Molecular Biology and Evolution* 26: 1533-1548.
- Auerbach H, Kalienkova V, Schroda M, Schünemann V (2017). Mössbauer spectroscopy of the chloroplast-targeted DnaJ-like proteins CDJ3 and CDJ4. *Hyperfine Interactions* 238: 86.
- Avellaneda MJ, Franke KB, Sunderlikova V, Bukau B, Mogk A, Tans SJ (2020). Processive extrusion of polypeptide loops by a Hsp100 disaggregase. *Nature* 578: 317-320.
- Bai C, Guo P, Zhao Q, Lv Z, Zhang S, Gao F, Gao L, Wang Y, Tian Z, Wang J, Yang F, Liu C (2015). Protomer roles in chloroplast chaperonin assembly and function. *Molecular Plant* 8: 1478-1492.
- Balchin D, Hayer-Hartl M, Hartl FU (2016). *In vivo* aspects of protein folding and quality control. *Science* 353: aac4354.
- Balczun C, Bunse A, Schwarz C, Piotrowski M, Kuck U (2006). Chloroplast heat shock protein Cpn60 from *Chlamydomonas reinhardtii* exhibits a novel function as a group II intron-specific RNA-binding protein. *FEBS Letters* 580: 4527-4532.
- Ballinger CA, Connell P, Wu Y, Hu Z, Thompson LJ, Yin LY, Patterson C (1999). Identification of CHIP, a novel tetratricopeptide repeat-containing protein that interacts with heat shock proteins and negatively regulates chaperone functions. *Molecular and Cellular Biology* 19: 4535-4545.
- Barraclough R, Ellis RJ (1980). Protein synthesis in chloroplasts. IX. Assembly of newly-synthesized large subunits into ribulose biphosphate carboxylase in isolated intact pea chloroplasts. *Biochimica et Biophysica Acta* 608: 19-31.
- Biebl MM, Buchner J (2019). Structure, function, and regulation of the Hsp90 machinery. *Cold Spring Harbor Perspectives in Biology* 11.
- Bieniossek C, Niederhauser B, Baumann UM (2009). The crystal structure of apo-FtsH reveals domain movements necessary for substrate unfolding and translocation. *Proceedings of the National Academy of Sciences of the United States of America* 106: 21579-21584.
- Blaby-Haas CE, Castruita M, Fitz-Gibbon ST, Kropat J, Merchant SS (2016). Ni induces the CRR1-dependent regulon revealing overlap and distinction between hypoxia and Cu deficiency responses in *Chlamydomonas reinhardtii*. *Metallomics* 8: 679-691.
- Blaby IK, Blaby-Haas CE, Perez-Perez ME, Schmollinger S, Fitz-Gibbon S, Lemaire SD, Merchant SS (2015). Genome-wide analysis on *Chlamydomonas reinhardtii* reveals the impact of hydrogen peroxide on protein stress responses and overlap with other stress transcriptomes. *Plant Journal* 84: 974-988.
- Blamowska M, Neupert W, Hell K (2012). Biogenesis of the mitochondrial Hsp70 chaperone. *Journal of Cell Biology* 199: 125-135.
- Bloch MA, Johnson KA (1995). Identification of a molecular chaperone in the eukaryotic flagellum and its localization to the site of microtubule assembly. *Journal of Cell Science* 108 ( Pt 11): 3541-3545.

- Bolognesi B, Kumita JR, Barros TP, Esbjorner EK, Luheshi LM, Crowther DC, Wilson MR, Dobson CM, Favrin G, Yerbury JJ (2010). ANS binding reveals common features of cytotoxic amyloid species. *ACS Chemical Biology* 5: 735-740.
- Bracher A, Verghese J (2015). The nucleotide exchange factors of Hsp70 molecular chaperones. *Front Mol Biosci* 2: 10.
- Bujaldon S, Kodama N, Rappaport F, Subramanyam R, de Vitry C, Takahashi Y, Wollman FA (2017). Functional accumulation of antenna proteins in chlorophyll b-less mutants of *Chlamydomonas reinhardtii*. *Molecular Plant* 10: 115-130.
- Butenko Y, Lin A, Naveh L, Kupervaser M, Levin Y, Reich Z, Adam Z (2018). Differential roles of the thylakoid lumenal Deg protease homologs in chloroplast proteostasis. *Plant Physiology* 178: 1065-1080.
- Calderon RH, de Vitry C, Wollman F-A, Niyogi KK (2022). FtsH protease inactivation allows accumulation of aberrant photosystem II in a *Chlamydomonas rubredoxin* mutant. *bioRxiv*: 2022.2002.2024.481860.
- Cannon WB (1929). Organization for physiological homeostasis. *Physiological Reviews* 9: 399-431.
- Cao D, Froehlich JE, Zhang H, Cheng CL (2003). The chlorate-resistant and photomorphogenesis-defective mutant *cr88* encodes a chloroplast-targeted HSP90. *Plant Journal* 33: 107-118.
- Cashikar AG, Duennwald M, Lindquist SL (2005). A chaperone pathway in protein disaggregation - Hsp26 alters the nature of protein aggregates to facilitate reactivation by Hsp104. *Journal of Biological Chemistry* 280: 23869-23875.
- Cheetham ME, Caplan AJ (1998). Structure, function and evolution of DnaJ: conservation and adaptation of chaperone function. *Cell Stress and Chaperones* 3: 28-36.
- Chen S, Smith DF (1998). Hop as an adaptor in the heat shock protein 70 (Hsp70) and hsp90 chaperone machinery. *Journal of Biological Chemistry* 273: 35194-35200.
- Cheng Q, Fowler R, Tam LW, Edwards L, Miller SM (2003). The role of GlsA in the evolution of asymmetric cell division in the green alga *Volvox carteri*. *Development Genes and Evolution* 213: 328-335.
- Cheng Q, Pappas V, Hallmann A, Miller SM (2005). Hsp70A and GlsA interact as partner chaperones to regulate asymmetric division in *Volvox*. *Developmental Biology* 286: 537-548.
- Chi W, Li J, He B, Chai X, Xu X, Sun X, Jiang J, Feng P, Zuo J, Lin R, Rochaix JD, Zhang L (2016). DEG9, a serine protease, modulates cytokinin and light signaling by regulating the level of ARABIDOPSIS RESPONSE REGULATOR 4. *Proceedings of the National Academy of Sciences of the United States of America* 113: E3568-3576.
- Chiu CC, Chen LJ, Su PH, Li HM (2013). Evolution of chloroplast J proteins. *PLoS One* 8: e70384.
- Cotto JJ, Kline M, Morimoto RI (1996). Activation of heat shock factor 1 DNA binding precedes stress-induced serine phosphorylation. Evidence for a multistep pathway of regulation. *Journal of Biological Chemistry* 271: 3355-3358.
- Craig EA (2018). Hsp70 at the membrane: driving protein translocation. *BMC Biology* 16: 11.
- Crespo JL (2012). BiP links TOR signaling to ER stress in *Chlamydomonas*. *Plant Signal Behav* 7: 273-275.

- De Mia M, Lemaire SD, Choquet Y, Wollman FA (2019). Nitric oxide remodels the photosynthetic apparatus upon S-starvation in *Chlamydomonas reinhardtii*. *Plant Physiology* 179: 718-731.
- de Sagarra MR, Mayo I, Marco S, Rodriguez-Vilarino S, Oliva J, Carrascosa JL, Casta n JG (1999). Mitochondrial localization and oligomeric structure of HClpP, the human homologue of *E. coli* ClpP. *Journal of Molecular Biology* 292: 819-825.
- DeLisa MP, Lee P, Palmer T, Georgiou G (2004). Phage shock protein PspA of *Escherichia coli* relieves saturation of protein export via the Tat pathway. *Journal of Bacteriology* 186: 366-373.
- Derrien B, Majeran W, Effantin G, Ebenezer J, Friso G, van Wijk KJ, Steven AC, Maurizi MR, Vallon O (2012). The purification of the *Chlamydomonas reinhardtii* chloroplast ClpP complex: additional subunits and structural features. *Plant Molecular Biology* 80: 189-202.
- Derrien B, Majeran W, Wollman FA, Vallon O (2009). Multistep processing of an insertion sequence in an essential subunit of the chloroplast ClpP complex. *Journal of Biological Chemistry* 284: 15408-15415.
- Deville C, Franke K, Mogk A, Bukau B, Saibil HR (2019). Two-Step Activation Mechanism of the ClpB Disaggregase for Sequential Substrate Threading by the Main ATPase Motor. *Cell Rep* 27: 3433-3446.e3434.
- Diaz-Troya S, Florencio FJ, Crespo JL (2008). Target of rapamycin and LST8 proteins associate with membranes from the endoplasmic reticulum in the unicellular green alga *Chlamydomonas reinhardtii*. *Eukaryot Cell* 7: 212-222.
- Diaz-Troya S, Perez-Perez ME, Perez-Martin M, Moes S, Jenoe P, Florencio FJ, Crespo JL (2011). Inhibition of protein synthesis by TOR inactivation revealed a conserved regulatory mechanism of the BiP chaperone in *Chlamydomonas*. *Plant Physiology*.
- Dogra V, Singh RM, Li M, Li M, Singh S, Kim C (2021). EXECUTER2 modulates the EXECUTER1 signalosome through its singlet oxygen-dependent oxidation. *Molecular Plant*.
- Dolze E, Chigri F, Howing T, Hierl G, Isono E, Vothknecht UC, Gietl C (2013). Calmodulin-like protein AtCML3 mediates dimerization of peroxisomal processing protease AtDEG15 and contributes to normal peroxisome metabolism. *Plant Molecular Biology* 83: 607-624.
- Dorn KV, Willmund F, Schwarz C, Henselmann C, Pohl T, Hess B, Veyel D, Usadel B, Friedrich T, Nickelsen J, Schroda M (2010). Chloroplast DnaJ-like proteins 3 and 4 (CDJ3/4) from *Chlamydomonas reinhardtii* contain redox-active Fe-S clusters and interact with stromal HSP70B. *Biochemical Journal* 427: 205-215.
- Drzymalla C, Schroda M, Beck CF (1996). Light-inducible gene HSP70B encodes a chloroplast-localized heat shock protein in *Chlamydomonas reinhardtii*. *Plant Molecular Biology* 31: 1185-1194.
- Eisenberg-Domovich Y, Klopstech K, Ohad I (1994). Reversible membrane association of heat-shock protein 22 in *Chlamydomonas reinhardtii* during heat shock and recovery. *European Journal of Biochemistry* 222: 1041-1046.
- Emanuelsson O, Nielsen H, Brunak S, von Heijne G (2000). Predicting subcellular localization of proteins based on their N-terminal amino acid sequence. *Journal of Molecular Biology* 300: 1005-1016.

- Emelyanov VV (2002). Phylogenetic relationships of organellar Hsp90 homologs reveal fundamental differences to organellar Hsp70 and Hsp60 evolution. *Gene* 299: 125-133.
- Felts SJ, Owen BA, Nguyen P, Trepel J, Donner DB, Toft DO (2000). The hsp90-related protein TRAP1 is a mitochondrial protein with distinct functional properties. *Journal of Biological Chemistry* 275: 3305-3312.
- Feng J, Fan P, Jiang P, Lv S, Chen X, Li Y (2014). Chloroplast-targeted Hsp90 plays essential roles in plastid development and embryogenesis in *Arabidopsis* possibly linking with VIPP1. *Physiol Plant* 150: 292-307.
- Fischer BB, Krieger-Liszkay A, Eggen RIL (2005). Oxidative stress induced by the photosensitizers neutral red (type I) or rose bengal (type II) in the light causes different molecular responses in *Chlamydomonas reinhardtii*. *Plant Science* 168: 747-759.
- Fleckenstein T, Kastenmuller A, Stein ML, Peters C, Daake M, Krause M, Weinfurter D, Haslbeck M, Weinkauff S, Groll M, Buchner J (2015). The chaperone activity of the developmental small heat shock protein Sip1 is regulated by pH-dependent conformational changes. *Molecular Cell* 58: 1067-1078.
- Gestaut D, Limatola A, Joachimiak L, Frydman J (2019). The ATP-powered gymnastics of TRiC/CCT: an asymmetric protein folding machine with a symmetric origin story. *Current Opinion in Structural Biology* 55: 50-58.
- Göhre V, Ossenbuhl F, Crevecoeur M, Eichacker LA, Rochaix JD (2006). One of two alb3 proteins is essential for the assembly of the photosystems and for cell survival in *Chlamydomonas*. *Plant Cell* 18: 1454-1466.
- Gomez-Pastor R, Burchfiel ET, Thiele DJ (2018). Regulation of heat shock transcription factors and their roles in physiology and disease. *Nature Reviews: Molecular Cell Biology* 19: 4-19.
- Grammatikakis N, Lin JH, Grammatikakis A, Tsihchlis PN, Cochran BH (1999). p50(cdc37) acting in concert with Hsp90 is required for Raf-1 function. *Molecular and Cellular Biology* 19: 1661-1672.
- Grantham J (2020). The molecular chaperone CCT/TRiC: an essential component of proteostasis and a potential modulator of protein aggregation. *Front Genet* 11.
- Grimm B, Ish-Shalom D, Even D, Glaczinski H, Ottersbach P, Ohad I, Kloppstech K (1989). The nuclear-coded chloroplast 22-kDa heat-shock protein of *Chlamydomonas*. Evidence for translocation into the organelle without a processing step. *European Journal of Biochemistry* 182: 539-546.
- Guo P, Jiang S, Bai C, Zhang W, Zhao Q, Liu C (2015). Asymmetric functional interaction between chaperonin and its plastidic cofactors. *FEBS J* 282: 3959-3970.
- Gupta TK, Klumpe S, Gries K, Heinz S, Wietrzynski W, Ohnishi N, Niemeyer J, Spaniol B, Schaffer M, Rast A, Ostermeier M, Strauss M, Plitzko JM, Baumeister W, Rudack T, Sakamoto W, Nickelsen J, Schuller JM, Schroda M, Engel BD (2021). Structural basis for VIPP1 oligomerization and maintenance of thylakoid membrane integrity. *Cell* 184: 3643-3659 e3623.
- Halperin T, Ostersetzer O, Adam Z (2001). ATP-dependent association between subunits of Clp protease in pea chloroplasts. *Planta* 213: 614-619.
- Han W, Christen P (2003). Mechanism of the targeting action of DnaJ in the DnaK molecular chaperone system. *Journal of Biological Chemistry* 278: 19038-19043.

- Hanson PI, Whiteheart SW (2005). AAA+ proteins: have engine, will work. *Nature Reviews: Molecular Cell Biology* 6: 519-529.
- Harrison CJ, Hayer-Hartl M, Di Liberto M, Hartl F, Kuriyan J (1997). Crystal structure of the nucleotide exchange factor GrpE bound to the ATPase domain of the molecular chaperone DnaK. *Science* 276: 431-435.
- Haslbeck M, Vierling E (2015). A first line of stress defense: small heat shock proteins and their function in protein homeostasis. *Journal of Molecular Biology* 427: 1537-1548.
- Haslberger T, Weibezahn J, Zahn R, Lee S, Tsai FT, Bukau B, Mogk A (2007). M domains couple the ClpB threading motor with the DnaK chaperone activity. *Molecular Cell* 25: 247-260.
- Hayer-Hartl M, Bracher A, Hartl FU (2016). The GroEL-GroES chaperonin machine: a nano-cage for protein folding. *Trends in Biochemical Sciences* 41: 62-76.
- Heide H, Nordhues A, Drepper F, Nick S, Schulz-Raffelt M, Haehnel W, Schroda M (2009). Application of quantitative immunoprecipitation combined with knockdown and cross-linking to *Chlamydomonas* reveals the presence of vesicle-inducing protein in plastids 1 in a common complex with chloroplast HSP90C. *Proteomics* 9: 3079-3089.
- Hemme D, Veyel D, Mühlhaus T, Sommer F, Juppner J, Unger AK, Sandmann M, Fehrle I, Schönfelder S, Steup M, Geimer S, Kopka J, Giavalisco P, Schroda M (2014). Systems-wide analysis of acclimation responses to long-term heat stress and recovery in the photosynthetic model organism *Chlamydomonas reinhardtii*. *Plant Cell* 26: 4270-4297.
- Heredia-Martínez LG, Andrés-Garrido A, Martínez-Force E, Pérez-Pérez ME, Crespo JL (2018). Chloroplast damage induced by the inhibition of fatty acid synthesis triggers autophagy in *Chlamydomonas*. *Plant Physiology* 178: 1112-1129.
- Hightower LE, White FP (1981). Cellular responses to stress: comparison of a family of 71--73-kilodalton proteins rapidly synthesized in rat tissue slices and canavanine-treated cells in culture. *Journal of Cellular Physiology* 108: 261-275.
- Hill JE, Hemmingsen SM (2001). *Arabidopsis thaliana* type I and II chaperonins. *Cell Stress and Chaperones* 6: 190-200.
- Horwich AL, Fenton WA, Chapman E, Farr GW (2007). Two families of chaperonin: physiology and mechanism. *Annual Review of Cell and Developmental Biology* 23: 115-145.
- Hubel A, Schoffl F (1994). *Arabidopsis* heat shock factor: isolation and characterization of the gene and the recombinant protein. *Plant Molecular Biology* 26: 353-362.
- Huber CV, Jakobs BD, Mishra LS, Niedermaier S, Stift M, Winter G, Adamska I, Funk C, Huesgen PF, Funck D (2019). DEG10 contributes to mitochondrial proteostasis, root growth, and seed yield in *Arabidopsis*. *J Exp Bot* 70: 5423-5436.
- Iwasaki S, Sasaki HM, Sakaguchi Y, Suzuki T, Tadakuma H, Tomari Y (2015). Defining fundamental steps in the assembly of the *Drosophila* RNAi enzyme complex. *Nature* 521: 533-536.
- James SW, Ranum LP, Silflow CD, Lefebvre PA (1988). Mutants resistant to anti-microtubule herbicides map to a locus on the uni linkage group in *Chlamydomonas reinhardtii*. *Genetics* 118: 141-147.

- Johnson KA, Rosenbaum JL (1992). Polarity of flagellar assembly in *Chlamydomonas*. *Journal of Cell Biology* 119: 1605-1611.
- Jovanovic G, Mehta P, McDonald C, Davidson AC, Uzdevinys P, Ying L, Buck M (2014). The N-terminal amphipathic helices determine regulatory and effector functions of phage shock protein A (PspA) in *Escherichia coli*. *Journal of Molecular Biology* 426: 1498-1511.
- Kabbage M, Dickman MB (2008). The BAG proteins: a ubiquitous family of chaperone regulators. *Cellular and Molecular Life Sciences* 65: 1390-1402.
- Kapri-Pardes E, Naveh L, Adam Z (2007). The thylakoid lumen protease Deg1 is involved in the repair of photosystem II from photoinhibition in *Arabidopsis*. *Plant Cell* 19: 1039-1047.
- Kato Y, Sakamoto W (2009). Protein quality control in chloroplasts: a current model of D1 protein degradation in the photosystem II repair cycle. *Journal of Biochemistry* 146: 463-469.
- (2018). FtsH Protease in the Thylakoid Membrane: Physiological Functions and the Regulation of Protease Activity. *Front Plant Sci* 9: 855.
  - (2019). Phosphorylation of the chloroplastic metalloprotease FtsH in *Arabidopsis* characterized by phos-tag SDS-PAGE. *Front Plant Sci* 10: 1080.
- Kato Y, Sun X, Zhang L, Sakamoto W (2012). Cooperative D1 degradation in the photosystem II repair mediated by chloroplastic proteases in *Arabidopsis*. *Plant Physiology* 159: 1428-1439.
- Ke X, Zou W, Ren Y, Wang Z, Li J, Wu X, Zhao J (2017). Functional divergence of chloroplast Cpn60alpha subunits during *Arabidopsis* embryo development. *PLoS Genet* 13: e1007036.
- Kelley WL (1998). The J-domain family and the recruitment of chaperone power. *Trends in Biochemical Sciences* 23: 222-227.
- Kikuchi S, Asakura Y, Imai M, Nakahira Y, Kotani Y, Hashiguchi Y, Nakai Y, Takafuji K, Bedard J, Hirabayashi-Ishioka Y, Mori H, Shiina T, Nakai M (2018). A Ycf2-FtsHi heteromeric AAA-ATPase complex is required for chloroplast protein import. *Plant Cell* 30: 2677-2703.
- Kim J, Kimber MS, Nishimura K, Friso G, Schultz L, Ponnala L, van Wijk KJ (2015). Structures, functions, and interactions of ClpT1 and ClpT2 in the Clp protease system of *Arabidopsis* chloroplasts. *Plant Cell* 27: 1477-1496.
- Kim KK, Kim R, Kim SH (1998). Crystal structure of a small heat-shock protein. *Nature* 394: 595-599.
- Kim YI, Levchenko I, Fraczkowska K, Woodruff RV, Sauer RT, Baker TA (2001). Molecular determinants of complex formation between Clp/Hsp100 ATPases and the ClpP peptidase. *Nature Structural Biology* 8: 230-233.
- Kirk MM, Ransick A, McRae SE, Kirk DL (1993). The relationship between cell size and cell fate in *Volvox carteri*. *Journal of Cell Biology* 123: 191-208.
- Kitagawa K, Skowrya D, Elledge SJ, Harper JW, Hieter P (1999). SGT1 encodes an essential component of the yeast kinetochore assembly pathway and a novel subunit of the SCF ubiquitin ligase complex. *Molecular Cell* 4: 21-33.
- Kityk R, Vogel M, Schlecht R, Bukau B, Mayer MP (2015). Pathways of allosteric regulation in Hsp70 chaperones. *Nat Commun* 6: 8308.

- Kley J, Schmidt B, Boyanov B, Stolt-Bergner PC, Kirk R, Ehrmann M, Knopf RR, Naveh L, Adam Z, Clausen T (2011). Structural adaptation of the plant protease Deg1 to repair photosystem II during light exposure. *Nature Structural & Molecular Biology* 18: 728-731.
- Kobayashi Y, Harada N, Nishimura Y, Saito T, Nakamura M, Fujiwara T, Kuroiwa T, Misumi O (2014). Algae sense exact temperatures: small heat shock proteins are expressed at the survival threshold temperature in *Cyanidioschyzon merolae* and *Chlamydomonas reinhardtii*. *Genome Biology and Evolution* 6: 2731-2740.
- Krishna P, Gloor G (2001). The Hsp90 family of proteins in *Arabidopsis thaliana*. *Cell Stress and Chaperones* 6: 238-246.
- Langer T, Lu C, Echols H, Flanagan J, Hayer MK, Hartl FU (1992). Successive action of DnaK, DnaJ and GroEL along the pathway of chaperone-mediated protein folding. *Nature* 356: 683-689.
- Lee JH, Hubel A, Schoffl F (1995). Derepression of the activity of genetically engineered heat shock factor causes constitutive synthesis of heat shock proteins and increased thermotolerance in transgenic *Arabidopsis*. *Plant Journal* 8: 603-612.
- Liberek K, Marszałek J, Ang D, Georgopoulos C, Zylicz M (1991). *Escherichia coli* DnaJ and GrpE heat shock proteins jointly stimulate ATPase activity of DnaK. *Proceedings of the National Academy of Sciences of the United States of America* 88: 2874-2878.
- Lin BL, Wang JS, Liu HC, Chen RW, Meyer Y, Barakat A, Delseny M (2001). Genomic analysis of the Hsp70 superfamily in *Arabidopsis thaliana*. *Cell Stress and Chaperones* 6: 201-208.
- Lindquist S (1986). The heat-shock response. *Annual Review of Biochemistry* 55: 1151-1191.
- Lindquist S, Craig EA (1988). The heat-shock proteins. *Annual Review of Genetics* 22: 631-677.
- Lipinska N, Zietkiewicz S, Sobczak A, Jurczyk A, Potocki W, Morawiec E, Wawrzycka A, Gumowski K, Slusarz M, Rodziejewicz-Motowidło S, Chrusciel E, Liberek K (2013). Disruption of ionic interactions between the nucleotide binding domain 1 (NBD1) and middle (M) domain in Hsp100 disaggregase unleashes toxic hyperactivity and partial independence from Hsp70. *Journal of Biological Chemistry* 288: 2857-2869.
- Liu C, Willmund F, Golecki JR, Cacace S, Hess B, Markert C, Schroda M (2007). The chloroplast HSP70B-CDJ2-CGE1 chaperones catalyse assembly and disassembly of VIPP1 oligomers in *Chlamydomonas*. *Plant Journal* 50: 265-277.
- Liu C, Willmund F, Whitelegge JP, Hawat S, Knapp B, Lodha M, Schroda M (2005). J-domain protein CDJ2 and HSP70B are a plastidic chaperone pair that interacts with vesicle-inducing protein in plastids 1. *Molecular Biology of the Cell* 16: 1165-1177.
- Liu J, Tassinari M, Souza DP, Naskar S, Noel JK, Bohuszewicz O, Buck M, Williams TA, Baum B, Low HH (2021). Bacterial Vipp1 and PspA are members of the ancient ESCRT-III membrane-remodeling superfamily. *Cell* 184: 3660-3673 e3618.
- Lo SM, Theg SM (2012). Role of vesicle-inducing protein in plastids 1 in cpTat transport at the thylakoid. *Plant Journal* 71: 656-668.

- Lodha M, Schroda M (2005). Analysis of chromatin structure in the control regions of the *Chlamydomonas HSP70A* and *RBCS2* genes. *Plant Molecular Biology* 59: 501-513.
- Mackinder LCM, Chen C, Leib RD, Patena W, Blum SR, Rodman M, Ramundo S, Adams CM, Jonikas MC (2017). A spatial interactome reveals the protein organization of the algal CO<sub>2</sub>-concentrating mechanism. *Cell* 171: 133-147 e114.
- MacLean M, Picard D (2003). Cdc37 goes beyond Hsp90 and kinases. *Cell Stress and Chaperones* 8: 114-119.
- Magni S, Succurro A, Skupin A, Ebenhoh O (2018). Data-driven dynamical model indicates that the heat shock response in *Chlamydomonas reinhardtii* is tailored to handle natural temperature variation. *J R Soc Interface* 15.
- Maikova A, Zalutskaya Z, Lapina T, Ermilova E (2016). The HSP70 chaperone machines of *Chlamydomonas* are induced by cold stress. *Journal of Plant Physiology* 204: 85-91.
- Majeran W, Friso G, van Wijk KJ, Vallon O (2005). The chloroplast ClpP complex in *Chlamydomonas reinhardtii* contains an unusual high molecular mass subunit with a large apical domain. *FEBS J* 272: 5558-5571.
- Majeran W, Wollman FA, Vallon O (2000). Evidence for a role of ClpP in the degradation of the chloroplast cytochrome b(6)f complex. *Plant Cell* 12: 137-150.
- Majeran W, Wostrikoff K, Wollman FA, Vallon O (2019). Role of ClpP in the biogenesis and degradation of RuBisCO and ATP synthase in *Chlamydomonas reinhardtii*. *Plants (Basel)* 8.
- Malnoe A, Wang F, Girard-Bascou J, Wollman FA, de Vitry C (2014). Thylakoid FtsH protease contributes to photosystem II and cytochrome *b<sub>6</sub>f* remodeling in *Chlamydomonas reinhardtii* under stress conditions. *Plant Cell* 26: 373-390.
- Malnoe A, Wollman FA, de Vitry C, Rappaport F (2011). Photosynthetic growth despite a broken Q-cycle. *Nat Commun* 2: 301.
- Mathieu-Rivet E, Scholz M, Arias C, Dardelle F, Schulze S, Le Mauff F, Teo G, Hochmal AK, Blanco-Rivero A, Loutelier-Bourhis C, Kiefer-Meyer M-C, Fufezan C, Burel C, Lerouge P, Martinez F, Bardor M, Hippler M (2013). Exploring the N-glycosylation Pathway in *Chlamydomonas reinhardtii* unravels novel complex structures. *Molecular & Cellular Proteomics* 12: 3160-3183.
- Mayer MP, Bukau B (2005). Hsp70 chaperones: cellular functions and molecular mechanism. *Cellular and Molecular Life Sciences* 62: 670-684.
- McDonald C, Jovanovic G, Ces O, Buck M (2015). Membrane stored curvature elastic stress modulates recruitment of maintenance proteins PspA and Vipp1. *MBio* 6: e01188-01115.
- McDonald C, Jovanovic G, Wallace BA, Ces O, Buck M (2017). Structure and function of PspA and Vipp1 N-terminal peptides: Insights into the membrane stress sensing and mitigation. *Biochimica et Biophysica Acta* 1859: 28-39.
- McLaughlin SH, Smith HW, Jackson SE (2002). Stimulation of the weak ATPase activity of human hsp90 by a client protein. *Journal of Molecular Biology* 315: 787-798.
- Mettler T, Mühlhaus T, Hemme D, Schöttler MA, Rupprecht J, Idoine A, Veyel D, Pal SK, Yaneva-Roder L, Winck FV, Sommer F, Vosloh D, Seiwert B, Erban A, Burgos A, Arvidsson S, Schönfelder S, Arnold A, Gunther M, Krause U, Lohse M, Kopka J, Nikoloski Z, Mueller-Roeber B, Willmitzer L, Bock R, Schroda M, Stitt M (2014).

- Systems analysis of the response of photosynthesis, metabolism, and growth to an increase in irradiance in the photosynthetic model organism *Chlamydomonas reinhardtii*. *Plant Cell* 26: 2310-2350.
- Michelet L, Zaffagnini M, Vanacker H, Le Marechal P, Marchand C, Schroda M, Lemaire SD, Decottignies P (2008). *In vivo* targets of S-thiolation in *Chlamydomonas reinhardtii*. *Journal of Biological Chemistry* 283: 21571-21578.
- Mielke K, Wagner R, Mishra LS, Demir F, Perrar A, Huesgen PF, Funk C (2021). Abundance of metalloprotease FtsH12 modulates chloroplast development in *Arabidopsis thaliana*. *J Exp Bot* 72: 3455-3473.
- Miller SM, Kirk DL (1999). *glsA*, a *Volvox* gene required for asymmetric division and germ cell specification, encodes a chaperone-like protein. *Development* 126: 649-658.
- Mitchell BF, Pedersen LB, Feely M, Rosenbaum JL, Mitchell DR (2005). ATP production in *Chlamydomonas reinhardtii* flagella by glycolytic enzymes. *Molecular Biology of the Cell* 16: 4509-4518.
- Mogk A, Bukau B, Kampinga HH (2018). Cellular handling of protein aggregates by disaggregation machines. *Molecular Cell* 69: 214-226.
- Mogk A, Kummer E, Bukau B (2015). Cooperation of Hsp70 and Hsp100 chaperone machines in protein disaggregation. *Front Mol Biosci* 2: 22.
- Mogk A, Schlieker C, Friedrich KL, Schonfeld HJ, Vierling E, Bukau B (2003). Refolding of substrates bound to small Hsps relies on a disaggregation reaction mediated most efficiently by ClpB/DnaK. *Journal of Biological Chemistry* 278: 31033-31042.
- Momose T, Ohshima C, Maeda M, Endo T (2007). Structural basis of functional cooperation of Tim15/Zim17 with yeast mitochondrial Hsp70. *EMBO Rep* 8: 664-670.
- Moseley JL, Chang CW, Grossman AR (2006). Genome-based approaches to understanding phosphorus deprivation responses and PSR1 control in *Chlamydomonas reinhardtii*. *Eukaryot Cell* 5: 26-44.
- Mühlhaus T, Weiss J, Hemme D, Sommer F, Schroda M (2011). Quantitative shotgun proteomics using a uniform <sup>15</sup>N-labeled standard to monitor proteome dynamics in time course experiments reveals new insights into the heat stress response of *Chlamydomonas reinhardtii*. *Molecular & Cellular Proteomics* 10: M110 004739.
- Muranaka LS, Rutgers M, Bujaldon S, Heublein A, Geimer S, Wollman FA, Schroda M (2016). TEF30 interacts with photosystem II monomers and is involved in the repair of photodamaged photosystem II in *Chlamydomonas reinhardtii*. *Plant Physiology* 170: 821-840.
- Nathan DF, Vos MH, Lindquist S (1997). *In vivo* functions of the *Saccharomyces cerevisiae* Hsp90 chaperone. *Proceedings of the National Academy of Sciences of the United States of America* 94: 12949-12956.
- Nawrocki WJ, Liu X, Raber B, Hu C, de Vitry C, Bennett DIG, Croce R (2021). Molecular origins of induction and loss of photoinhibition-related energy dissipation qI. *Sci Adv* 7: eabj0055.
- Neuwald AF, Aravind L, Spouge JL, Koonin EV (1999). AAA+: A class of chaperone-like ATPases associated with the assembly, operation, and disassembly of protein complexes. *Genome Research* 9: 27-43.

- Niemeyer J, Scheuring D, Oestreicher J, Morgan B, Schroda M (2021). Real-time monitoring of subcellular H<sub>2</sub>O<sub>2</sub> distribution in *Chlamydomonas reinhardtii*. *Plant Cell* 33: 2935-2949.
- Nordhues A, Miller SM, Mühlhaus T, Schroda M (2010). New insights into the roles of molecular chaperones in *Chlamydomonas* and *Volvox*. *International Review of Cell and Molecular Biology* 285: 75-113.
- Nordhues A, Schöttler MA, Unger AK, Geimer S, Schönfelder S, Schmollinger S, Rütgers M, Finazzi G, Soppa B, Sommer F, Mühlhaus T, Roach T, Krieger-Liszkay A, Lokstein H, Crespo JL, Schroda M (2012). Evidence for a role of VIPP1 in the structural organization of the photosynthetic apparatus in *Chlamydomonas*. *Plant Cell* 24: 637-659.
- Nover L, Bharti K, Doring P, Mishra SK, Ganguli A, Scharf KD (2001). *Arabidopsis* and the heat stress transcription factor world: how many heat stress transcription factors do we need? *Cell Stress and Chaperones* 6: 177-189.
- Ohad I, Kyle DJ, Arntzen CJ (1984). Membrane protein damage and repair: removal and replacement of inactivated 32-kilodalton polypeptides in chloroplast membranes. *Journal of Cell Biology* 99: 481-485.
- Otters S, Braun P, Hubner J, Wanner G, Vothknecht UC, Chigri F (2013). The first alpha-helical domain of the vesicle-inducing protein in plastids 1 promotes oligomerization and lipid binding. *Planta* 237: 529-540.
- Ouyang M, Li X, Zhao S, Pu H, Shen J, Adam Z, Clausen T, Zhang L (2017). The crystal structure of Deg9 reveals a novel octameric-type HtrA protease. *Nat Plants* 3: 973-982.
- Panaretou B, Prodromou C, Roe SM, O'Brien R, Ladbury JE, Piper PW, Pearl LH (1998). ATP binding and hydrolysis are essential to the function of the Hsp90 molecular chaperone *in vivo*. *EMBO Journal* 17: 4829-4836.
- Park JJ, Wang H, Gargouri M, Deshpande RR, Skepper JN, Holguin FO, Juergens MT, Shachar-Hill Y, Hicks LM, Gang DR (2015). The response of *Chlamydomonas reinhardtii* to nitrogen deprivation: a systems biology analysis. *Plant Journal* 81: 611-624.
- Pazour GJ, Agrin N, Leszyk J, Witman GB (2005). Proteomic analysis of a eukaryotic cilium. *Journal of Cell Biology* 170: 103-113.
- Peng L, Fukao Y, Myouga F, Motohashi R, Shinozaki K, Shikanai T (2011). A chaperonin subunit with unique structures is essential for folding of a specific substrate. *PLoS Biology* 9: e1001040.
- Perez-Martin M, Perez-Perez ME, Lemaire SD, Crespo JL (2014). Oxidative stress contributes to autophagy induction in response to endoplasmic reticulum stress in *Chlamydomonas reinhardtii*. *Plant Physiology* 166: 997-1008.
- Perez-Perez ME, Mauries A, Maes A, Tourasse NJ, Hamon M, Lemaire SD, Marchand CH (2017). The deep thioredoxome in *Chlamydomonas reinhardtii*: new insights into redox regulation. *Molecular Plant* 10: 1107-1125.
- Perlaza K, Toutkoushian H, Boone M, Lam M, Iwai M, Jonikas MC, Walter P, Ramundo S (2019). The Mars1 kinase confers photoprotection through signaling in the chloroplast unfolded protein response. *Elife* 8.
- Petereit J, Duncan O, Murcha MW, Fenske R, Cincu E, Cahn J, Pruzinska A, Ivanova A, Kollipara L, Wortelkamp S, Sickmann A, Lee J, Lister R, Millar AH, Huang S

- (2020). Mitochondrial CLPP2 assists coordination and homeostasis of respiratory complexes. *Plant Physiology* 184: 148-164.
- Petitjean C, Moreira D, Lopez-Garcia P, Brochier-Armanet C (2012). Horizontal gene transfer of a chloroplast DnaJ-Fer protein to *Thaumarchaeota* and the evolutionary history of the DnaK chaperone system in *Archaea*. *BMC Evolutionary Biology* 12: 226.
- Pratt WB, Toft DO (2003). Regulation of signaling protein function and trafficking by the hsp90/hsp70-based chaperone machinery. *Experimental Biology and Medicine (Maywood, NJ)* 228: 111-133.
- Puchades C, Sandate CR, Lander GC (2020). The molecular principles governing the activity and functional diversity of AAA+ proteins. *Nature Reviews: Molecular Cell Biology* 21: 43-58.
- Queitsch C, Hong SW, Vierling E, Lindquist S (2000). Heat shock protein 101 plays a crucial role in thermotolerance in *Arabidopsis*. *Plant Cell* 12: 479-492.
- Ramundo S, Asakura Y, Salome PA, Strenkert D, Boone M, Mackinder LCM, Takafuji K, Dinc E, Rahire M, Crevecoeur M, Magneschi L, Schaad O, Hippler M, Jonikas MC, Merchant S, Nakai M, Rochaix JD, Walter P (2020). Coexpressed subunits of dual genetic origin define a conserved supercomplex mediating essential protein import into chloroplasts. *Proceedings of the National Academy of Sciences of the United States of America* 117: 32739-32749.
- Ramundo S, Casero D, Mühlhaus T, Hemme D, Sommer F, Crevecoeur M, Rahire M, Schroda M, Rusch J, Goodenough U, Pellegrini M, Perez-Perez ME, Crespo JL, Schaad O, Civic N, Rochaix JD (2014). Conditional depletion of the *Chlamydomonas* chloroplast ClpP protease activates nuclear genes involved in autophagy and plastid protein quality control. *Plant Cell* 26: 2201-2222.
- Roe SM, Prodromou C, O'Brien R, Ladbury JE, Piper PW, Pearl LH (1999). Structural basis for inhibition of the Hsp90 molecular chaperone by the antitumor antibiotics radicicol and geldanamycin. *Journal of Medicinal Chemistry* 42: 260-266.
- Rosenzweig R, Nillegoda NB, Mayer MP, Bukau B (2019). The Hsp70 chaperone network. *Nature Reviews: Molecular Cell Biology* 20: 665-680.
- Rowley N, Prip-Buus C, Westermann B, Brown C, Schwarz E, Barrell B, Neupert W (1994). Mdj1p, a novel chaperone of the DnaJ family, is involved in mitochondrial biogenesis and protein folding. *Cell* 77: 249-259.
- Rüdiger S, Germeroth L, Schneider-Mergener J, Bukau B (1997). Substrate specificity of the DnaK chaperone determined by screening cellulose-bound peptide libraries. *EMBO Journal* 16: 1501-1507.
- Rütgers M, Muranaka LS, Mühlhaus T, Sommer F, Thoms S, Schurig J, Willmund F, Schulz-Raffelt M, Schroda M (2017a). Substrates of the chloroplast small heat shock proteins 22E/F point to thermolability as a regulative switch for heat acclimation in *Chlamydomonas reinhardtii*. *Plant Molecular Biology* 95: 579-591.
- Rütgers M, Muranaka LS, Schulz-Raffelt M, Thoms S, Schurig J, Willmund F, Schroda M (2017b). Not changes in membrane fluidity but proteotoxic stress triggers heat shock protein expression in *Chlamydomonas reinhardtii*. *Plant, Cell & Environment* 40: 2987-3001.

- Saidi Y, Finka A, Muriset M, Bromberg Z, Weiss YG, Maathuis FJ, Goloubinoff P (2009). The heat shock response in moss plants is regulated by specific calcium-permeable channels in the plasma membrane. *Plant Cell* 21: 2829-2843.
- Saidi Y, Peter M, Finka A, Cicekli C, Vigh L, Goloubinoff P (2010). Membrane lipid composition affects plant heat sensing and modulates Ca(2+)-dependent heat shock response. *Plant Signal Behav* 5: 1530-1533.
- Santhanagopalan I, Degiacomi MT, Shepherd DA, Hochberg GKA, Benesch JLP, Vierling E (2018). It takes a dimer to tango: oligomeric small heat shock proteins dissociate to capture substrate. *Journal of Biological Chemistry* 293: 19511-19521.
- Sauer RT, Baker TA (2011). AAA+ proteases: ATP-fueled machines of protein destruction. *Annual Review of Biochemistry* 80: 587-612.
- Scharf KD, Berberich T, Ebersberger I, Nover L (2012). The plant heat stress transcription factor (Hsf) family: structure, function and evolution. *Biochimica et Biophysica Acta* 1819: 104-119.
- Scharf KD, Siddique M, Vierling E (2001). The expanding family of *Arabidopsis thaliana* small heat stress proteins and a new family of proteins containing alpha-crystallin domains (Acd proteins). *Cell Stress and Chaperones* 6: 225-237.
- Schirmer EC, Glover JR, Singer MA, Lindquist S (1996). HSP100/Clp proteins: a common mechanism explains diverse functions. *Trends in Biochemical Sciences* 21: 289-296.
- Schmitz G, Schmidt M, Feierabend J (1996). Characterization of a plastid-specific HSP90 homologue: identification of a cDNA sequence, phylogenetic descent and analysis of its mRNA and protein expression. *Plant Molecular Biology* 30: 479-492.
- Schmollinger S, Mühlhaus T, Boyle NR, Blaby IK, Casero D, Mettler T, Moseley JL, Kropat J, Sommer F, Strenkert D, Hemme D, Pellegrini M, Grossman AR, Stitt M, Schroda M, Merchant SS (2014). Nitrogen-sparing mechanisms in *Chlamydomonas* affect the transcriptome, the proteome, and photosynthetic metabolism. *Plant Cell* 26: 1410-1435.
- Schmollinger S, Schulz-Raffelt M, Strenkert D, Veyel D, Vallon O, Schroda M (2013). Dissecting the heat stress response in *Chlamydomonas* by pharmaceutical and RNAi approaches reveals conserved and novel aspects. *Molecular Plant* 6: 1795-1813.
- Schmollinger S, Strenkert D, Schroda M (2010). An inducible artificial microRNA system for *Chlamydomonas reinhardtii* confirms a key role for heat shock factor 1 in regulating thermotolerance. *Current Genetics* 56: 383-389.
- Schopf FH, Biebl MM, Buchner J (2017). The HSP90 chaperone machinery. *Nature Reviews: Molecular Cell Biology* 18: 345-360.
- Schreier TB, Clery A, Schlafli M, Galbier F, Stadler M, Demarsy E, Albertini D, Maier BA, Kessler F, Hortensteiner S, Zeeman SC, Kotting O (2018). Plastidial NAD-dependent malate dehydrogenase: a moonlighting protein involved in early chloroplast development through its interaction with an FtsH12-FtsHi protease complex. *Plant Cell* 30: 1745-1769.
- Schroda M (2004). The *Chlamydomonas* genome reveals its secrets: chaperone genes and the potential roles of their gene products in the chloroplast. *Photosynth Res* 82: 221-240.

- Schroda M, Blocker D, Beck CF (2000). The *HSP70A* promoter as a tool for the improved expression of transgenes in *Chlamydomonas*. *Plant Journal* 21: 121-131.
- Schroda M, Hemme D, Mühlhaus T (2015). The *Chlamydomonas* heat stress response. *Plant Journal* 82: 466-480.
- Schroda M, Kropat J, Oster U, Rudiger W, Vallon O, Wollman FA, Beck CF (2001a). Possible role for molecular chaperones in assembly and repair of photosystem II. *Biochemical Society Transactions* 29: 413-418.
- Schroda M, Mühlhaus T (2009). A 'foldosome' in the chloroplast? *Plant Signal Behav* 4: 301-303.
- Schroda M, Vallon O. 2009. *Chaperones and Proteases*. In: *The Chlamydomonas Sourcebook, Second Edition*. Elsevier / Academic Press, San Diego, CA.
- Schroda M, Vallon O, Whitelegge JP, Beck CF, Wollman FA (2001b). The chloroplastic GrpE homolog of *Chlamydomonas*: two isoforms generated by differential splicing. *Plant Cell* 13: 2823-2839.
- Schroda M, Vallon O, Wollman FA, Beck CF (1999). A chloroplast-targeted heat shock protein 70 (HSP70) contributes to the photoprotection and repair of photosystem II during and after photoinhibition. *Plant Cell* 11: 1165-1178.
- Schuhmann H, Adamska I (2012). Deg proteases and their role in protein quality control and processing in different subcellular compartments of the plant cell. *Physiol Plant* 145: 224-234.
- Schuhmann H, Huesgen PF, Adamska I (2012). The family of Deg/HtrA proteases in plants. *BMC Plant Biology* 12: 52.
- Schulz-Raffelt M, Lodha M, Schroda M (2007). Heat shock factor 1 is a key regulator of the stress response in *Chlamydomonas*. *Plant Journal* 52: 286-295.
- Shanklin J, DeWitt ND, Flanagan JM (1995). The stroma of higher plant plastids contain ClpP and ClpC, functional homologs of *Escherichia coli* ClpP and ClpA: an archetypal two-component ATP-dependent protease. *Plant Cell* 7: 1713-1722.
- Shao S, Cardona T, Nixon PJ (2018). Early emergence of the FtsH proteases involved in photosystem II repair. *Photosynthetica* 56: 163-177.
- Shapiro J, Ingram J, Johnson KA (2005). Characterization of a molecular chaperone present in the eukaryotic flagellum. *Eukaryot Cell* 4: 1591-1594.
- Sharma SK, Christen P, Goloubinoff P (2009). Disaggregating chaperones: an unfolding story. *Curr Protein Pept Sci* 10: 432-446.
- Sichting M, Mokranjac D, Azem A, Neupert W, Hell K (2005). Maintenance of structure and function of mitochondrial Hsp70 chaperones requires the chaperone Hep1. *EMBO Journal* 24: 1046-1056.
- Silflow CD, Sun X, Haas NA, Foley JW, Lefebvre PA (2011). The hsp70 and hsp40 chaperones influence microtubule stability in *Chlamydomonas*. *Genetics* 189: 1249-1260.
- Sima S, Richter K (2018). Regulation of the Hsp90 system. *Biochim Biophys Acta Mol Cell Res* 1865: 889-897.
- Sokolenko A, Pojidaeva E, Zinchenko V, Panichkin V, Glaser VM, Herrmann RG, Shestakov SV (2002). The gene complement for proteolysis in the cyanobacterium *Synechocystis* sp. PCC 6803 and *Arabidopsis thaliana* chloroplasts. *Current Genetics* 41: 291-310.

- Sorger PK, Nelson HC (1989). Trimerization of a yeast transcriptional activator via a coiled-coil motif. *Cell* 59: 807-813.
- Strenkert D, Schmollinger S, Schroda M (2013). Heat shock factor 1 counteracts epigenetic silencing of nuclear transgenes in *Chlamydomonas reinhardtii*. *Nucleic Acids Research* 41: 5273-5289.
- Strenkert D, Schmollinger S, Sommer F, Schulz-Raffelt M, Schroda M (2011). Transcription factor dependent chromatin remodeling at heat shock and copper responsive promoters in *Chlamydomonas reinhardtii*. *Plant Cell* 23: 2285-2301.
- Sun R, Fan H, Gao F, Lin Y, Zhang L, Gong W, Liu L (2012). Crystal structure of *Arabidopsis* Deg2 protein reveals an internal PDZ ligand locking the hexameric resting state. *Journal of Biological Chemistry* 287: 37564-37569.
- Sun W, Gao F, Fan H, Shan X, Sun R, Liu L, Gong W (2013). The structures of *Arabidopsis* Deg5 and Deg8 reveal new insights into HtrA proteases. *Acta Crystallographica Section D: Biological Crystallography* 69: 830-837.
- Sun X, Fu T, Chen N, Guo J, Ma J, Zou M, Lu C, Zhang L (2010). The stromal chloroplast Deg7 protease participates in the repair of photosystem II after photoinhibition in *Arabidopsis*. *Plant Physiology* 152: 1263-1273.
- Sung DY, Vierling E, Guy CL (2001). Comprehensive expression profile analysis of the *Arabidopsis* Hsp70 gene family. *Plant Physiology* 126: 789-800.
- Szyska-Mroz B, Pittock P, Ivanov AG, Lajoie G, Huner NP (2015). The antarctic psychrophile *Chlamydomonas* sp. UWO 241 preferentially phosphorylates a photosystem I-cytochrome b<sub>6</sub>/f supercomplex. *Plant Physiology* 169: 717-736.
- Tam S, Geller R, Spiess C, Frydman J (2006). The chaperonin TRiC controls polyglutamine aggregation and toxicity through subunit-specific interactions. *Nature Cell Biology* 8: 1155-1162.
- Tanaka Y, Nishiyama Y, Murata N (2000). Acclimation of the photosynthetic machinery to high temperature in *Chlamydomonas reinhardtii* requires synthesis de novo of proteins encoded by the nuclear and chloroplast genomes. *Plant Physiology* 124: 441-449.
- Terashima M, Specht M, Naumann B, Hippler M (2010). Characterizing the anaerobic response of *Chlamydomonas reinhardtii* by quantitative proteomics. *Molecular & Cellular Proteomics* 9: 1514-1532.
- Theis J, Gupta TK, Klingler J, Wan W, Albert S, Keller S, Engel BD, Schroda M (2019a). VIPP1 rods engulf membranes containing phosphatidylinositol phosphates. *Scientific Reports* 9: 8725.
- Theis J, Lang J, Spaniol B, Ferte S, Niemeyer J, Sommer F, Zimmer D, Venn B, Mehr SF, Muhlhaus T, Wollman FA, Schroda M (2019b). The *Chlamydomonas deg1c* mutant accumulates proteins involved in high light acclimation. *Plant Physiology* 181: 1480-1497.
- Theis J, Niemeyer J, Schmollinger S, Ries F, Rutgers M, Gupta TK, Sommer F, Muranaka LS, Venn B, Schulz-Raffelt M, Willmund F, Engel BD, Schroda M (2020). VIPP2 interacts with VIPP1 and HSP22E/F at chloroplast membranes and modulates a retrograde signal for HSP22E/F gene expression. *Plant, Cell & Environment* 43: 1212-1229.
- Theis J, Schroda M (2016). Revisiting the photosystem II repair cycle. *Plant Signal Behav* 11: e1218587.

- Thompson MD, Paavola CD, Lenvik TR, Gantt JS (1995). *Chlamydomonas* transcripts encoding three divergent plastid chaperonins are heat-inducible. *Plant Molecular Biology* 27: 1031-1035.
- Tomoyasu T, Ogura T, Tatsuta T, Bukau B (1998). Levels of DnaK and DnaJ provide tight control of heat shock gene expression and protein repair in *Escherichia coli*. *Molecular Microbiology* 30: 567-581.
- Traewachiwiphak S, Yokthongwattana C, Ves-Urai P, Charoensawan V, Yokthongwattana K (2018). Gene expression and promoter characterization of heat-shock protein 90B gene (*HSP90B*) in the model unicellular green alga *Chlamydomonas reinhardtii*. *Plant Science* 272: 107-116.
- Trösch R, Mühlhaus T, Schroda M, Willmund F (2015). ATP-dependent molecular chaperones in plastids--More complex than expected. *Biochimica et Biophysica Acta* 1847: 872-888.
- Tsai YC, Mueller-Cajar O, Saschenbrecker S, Hartl FU, Hayer-Hartl M (2012). Chaperonin cofactors, Cpn10 and Cpn20, of green algae and plants function as hetero-oligomeric ring complexes. *Journal of Biological Chemistry* 287: 20471-20481.
- Tsvetkova NM, Horvath I, Torok Z, Wolkers WF, Balogi Z, Shigapova N, Crowe LM, Tablin F, Vierling E, Crowe JH, Vigh L (2002). Small heat-shock proteins regulate membrane lipid polymorphism. *Proceedings of the National Academy of Sciences of the United States of America* 99: 13504-13509.
- Ungewickell E, Ungewickell H, Holstein SE, Lindner R, Prasad K, Barouch W, Martin B, Greene LE, Eisenberg E (1995). Role of auxilin in uncoating clathrin-coated vesicles. *Nature* 378: 632-635.
- Valledor L, Furuhashi T, Hanak AM, Weckwerth W (2013). Systemic cold stress adaptation of *Chlamydomonas reinhardtii*. *Molecular & Cellular Proteomics* 12: 2032-2047.
- van Montfort RL, Basha E, Friedrich KL, Slingsby C, Vierling E (2001). Crystal structure and assembly of a eukaryotic small heat shock protein. *Nature Structural Biology* 8: 1025-1030.
- van Wijk KJ (2015). Protein maturation and proteolysis in plant plastids, mitochondria, and peroxisomes. *Annual Review of Plant Biology* 66: 75-111.
- Vasileuskaya Z, Oster U, Beck CF (2004). Involvement of tetrapyrroles in inter-organellar signaling in plants and algae. *Photosynth Res* 82: 289-299.
- Veyel D, Sommer F, Muranaka LS, Rütgers M, Lemaire SD, Schroda M (2014). In vitro characterization of bacterial and chloroplast Hsp70 systems reveals an evolutionary optimization of the co-chaperones for their Hsp70 partner. *Biochemical Journal* 460: 13-24.
- Vitlin Gruber A, Nisemblat S, Azem A, Weiss C (2013). The complexity of chloroplast chaperonins. *Trends Plant Sci* 18: 688-694.
- Volkov RA, Panchuk, II, Mullineaux PM, Schoffl F (2006). Heat stress-induced H<sub>2</sub>O<sub>2</sub> is required for effective expression of heat shock genes in *Arabidopsis*. *Plant Molecular Biology* 61: 733-746.
- von Gromoff ED, Treier U, Beck CF (1989). Three light-inducible heat shock genes of *Chlamydomonas reinhardtii*. *Molecular and Cellular Biology* 9: 3911-3918.

- Walter B, Hristou A, Nowaczyk MM, Schunemann D (2015). *In vitro* reconstitution of co-translational D1 insertion reveals a role of the cpSec-Alb3 translocase and Vipp1 in photosystem II biogenesis. *Biochemical Journal* 468: 315-324.
- Wang F, Qi Y, Malnoe A, Choquet Y, Wollman FA, de Vitry C (2017). The high light response and redox control of thylakoid FtsH protease in *Chlamydomonas reinhardtii*. *Molecular Plant* 10: 99-114.
- Wang J, Hartling JA, Flanagan JM (1997). The structure of ClpP at 2.3 Å resolution suggests a model for ATP-dependent proteolysis. *Cell* 91: 447-456.
- Wang N, Wang Y, Zhao Q, Zhang X, Peng C, Zhang W, Liu Y, Vallon O, Schroda M, Cong Y, Liu C (2021). The cryo-EM structure of the chloroplast ClpP complex. *Nature Plants* 7: 1505-1515.
- Waters ER, Vierling E (2020). Plant small heat shock proteins - evolutionary and functional diversity. *New Phytol* 227: 24-37.
- Wei L, Derrien B, Gautier A, Houille-Vernes L, Boulouis A, Saint-Marcoux D, Malnoe A, Rappaport F, de Vitry C, Vallon O, Choquet Y, Wollman FA (2014). Nitric oxide-triggered remodeling of chloroplast bioenergetics and thylakoid proteins upon nitrogen starvation in *Chlamydomonas reinhardtii*. *Plant Cell* 26: 353-372.
- Weiss C, Bonshtien A, Farchi-Pisanty O, Vitlin A, Azem A (2009). Cpn20: siamese twins of the chaperonin world. *Plant Molecular Biology* 69: 227-238.
- Wiederrecht G, Seto D, Parker CS (1988). Isolation of the gene encoding the *S. cerevisiae* heat shock transcription factor. *Cell* 54: 841-853.
- Willmund F, Dorn KV, Schulz-Raffelt M, Schroda M (2008a). The chloroplast DnaJ homolog CDJ1 of *Chlamydomonas reinhardtii* is part of a multichaperone complex containing HSP70B, CGE1, and HSP90C. *Plant Physiology* 148: 2070-2082.
- Willmund F, Hinnenberger M, Nick S, Schulz-Raffelt M, Mühlhaus T, Schroda M (2008b). Assistance for a chaperone: *Chlamydomonas* HEP2 activates plastidic HSP70B for cochaperone binding. *Journal of Biological Chemistry* 283: 16363-16373.
- Willmund F, Mühlhaus T, Wojciechowska M, Schroda M (2007). The NH<sub>2</sub>-terminal domain of the chloroplast GrpE homolog CGE1 is required for dimerization and cochaperone function in vivo. *Journal of Biological Chemistry* 282: 11317-11328.
- Willmund F, Schroda M (2005). HEAT SHOCK PROTEIN 90C is a bona fide Hsp90 that interacts with plastidic HSP70B in *Chlamydomonas reinhardtii*. *Plant Physiology* 138: 2310-2322.
- Xu ZS, Li ZY, Chen Y, Chen M, Li LC, Ma YZ (2012). Heat shock protein 90 in plants: molecular mechanisms and roles in stress responses. *Int J Mol Sci* 13: 15706-15723.
- Yam AY, Xia Y, Lin HT, Burlingame A, Gerstein M, Frydman J (2008). Defining the TRiC/CCT interactome links chaperonin function to stabilization of newly made proteins with complex topologies. *Nature Structural & Molecular Biology* 15: 1255-1262.
- Yamada K, Fukao Y, Hayashi M, Fukazawa M, Suzuki I, Nishimura M (2007). Cytosolic HSP90 regulates the heat shock response that is responsible for heat acclimation in *Arabidopsis thaliana*. *Journal of Biological Chemistry* 282: 37794-37804.
- Yamaoka Y, Shin S, Choi BY, Kim H, Jang S, Kajikawa M, Yamano T, Kong F, Légeret B, Fukuzawa H, Li-Beisson Y, Lee Y (2019). The bZIP1 transcription factor regulates lipid remodeling and contributes to ER stress management in *Chlamydomonas reinhardtii*. *Plant Cell* 31: 1127-1140.

- Yang C, Compton MM, Yang P (2005). Dimeric novel HSP40 is incorporated into the radial spoke complex during the assembly process in flagella. *Molecular Biology of the Cell* 16: 637-648.
- Yang C, Owen HA, Yang P (2008). Dimeric heat shock protein 40 binds radial spokes for generating coupled power strokes and recovery strokes of 9 + 2 flagella. *Journal of Cell Biology* 180: 403-415.
- Yang JY, Sun Y, Sun AQ, Yi SY, Qin J, Li MH, Liu J (2006). The involvement of chloroplast HSP100/ClpB in the acquired thermotolerance in tomato. *Plant Molecular Biology* 62: 385-395.
- Yokthongwattana K, Chrost B, Behrman S, Casper-Lindley C, Melis A (2001). Photosystem II damage and repair cycle in the green alga *Dunaliella salina*: involvement of a chloroplast-localized HSP70. *Plant and Cell Physiology* 42: 1389-1397.
- Young JC, Obermann WM, Hartl FU (1998). Specific binding of tetratricopeptide repeat proteins to the C-terminal 12-kDa domain of hsp90. *Journal of Biological Chemistry* 273: 18007-18010.
- Zhang D, Kato Y, Zhang L, Fujimoto M, Tsutsumi N, Sodmergen, Sakamoto W (2010). The FtsH protease heterocomplex in *Arabidopsis*: dispensability of type-B protease activity for proper chloroplast development. *Plant Cell* 22: 3710-3725.
- Zhang L, Kato Y, Otters S, Vothknecht UC, Sakamoto W (2012). Essential role of VIPP1 in chloroplast envelope maintenance in *Arabidopsis*. *Plant Cell* 24: 3695-3707.
- Zhang N, Mattoon EM, McHargue W, Venn B, Zimmer D, Pecani K, Jeong J, Anderson CM, Chen C, Berry JC, Xia M, Tzeng S-C, Becker E, Pazouki L, Evans B, Cross F, Cheng J, Czymbek KJ, Schroda M, Mühlhaus T, Zhang R (2021). Systems-wide analysis revealed shared and unique responses to moderate and acute high temperatures in the green alga *Chlamydomonas reinhardtii*. *bioRxiv*: 2021.2008.2017.456552.
- Zhang S, Zhou H, Yu F, Bai C, Zhao Q, He J, Liu C (2016a). Structural insight into the cooperation of chloroplast chaperonin subunits. *BMC Biology* 14: 29.
- Zhang S, Zhou H, Yu F, Gao F, He J, Liu C (2016b). Functional partition of Cpn60 $\alpha$  and Cpn60 $\beta$  subunits in substrate recognition and cooperation with co-chaperonins. *Molecular Plant* 9: 1210-1213.
- Zhang Z, Shrager J, Jain M, Chang CW, Vallon O, Grossman AR (2004). Insights into the survival of *Chlamydomonas reinhardtii* during sulfur starvation based on microarray analysis of gene expression. *Eukaryot Cell* 3: 1331-1348.
- Zhao Q, Liu C (2017). Chloroplast chaperonin: an intricate protein folding machine for photosynthesis. *Front Mol Biosci* 4: 98.
- Zhao Q, Zhang X, Sommer F, Ta N, Wang N, Schroda M, Cong Y, Liu C (2019). Hetero-oligomeric CPN60 resembles highly symmetric group-I chaperonin structure revealed by Cryo-EM. *Plant Journal* 98: 798-812.
- Zhu X, Poghosyan E, Rezabkova L, Mehall B, Sakakibara H, Hirono M, Kamiya R, Ishikawa T, Yang P (2019). The roles of a flagellar HSP40 ensuring rhythmic beating. *Molecular Biology of the Cell* 30: 228-241.
- Zmijewski MA, Macario AJ, Lipinska B (2004). Functional similarities and differences of an archaeal Hsp70(DnaK) stress protein compared with its homologue from the bacterium *Escherichia coli*. *Journal of Molecular Biology* 336: 539-549.

- Zou J, Guo Y, Guettouche T, Smith DF, Voellmy R (1998). Repression of heat shock transcription factor HSF1 activation by HSP90 (HSP90 complex) that forms a stress-sensitive complex with HSF1. *Cell* 94: 471-480.
- Zou Y, Bozhkov PV (2021). Chlamydomonas proteases: classification, phylogeny, and molecular mechanisms. *J Exp Bot* 72: 7680-7693.
- Zybilov B, Friso G, Kim J, Rudella A, Rodriguez VR, Asakura Y, Sun Q, van Wijk KJ (2009). Large scale comparative proteomics of a chloroplast Clp protease mutant reveals folding stress, altered protein homeostasis, and feedback regulation of metabolism. *Molecular & Cellular Proteomics* 8: 1789-1810.